The role of 7SK noncoding RNA in development and function of motoneurons

Die Rolle der nichtkodierenden RNA 7SK bei der Entwicklung und Funktion von Motoneuronen

Doctoral thesis for a doctoral degree at the Graduate School of Life Sciences
Julius-Maximilians-Universität Würzburg,
Institut für Klinische Neurobiologie

Submitted by

Changhe Ji

Würzburg, 2020

Submitted on: ……..……..

Office stamp Members of the *Promotionskomitee*:

Chairperson: Prof. Dr. ……

Primary Supervisor: Prof. Dr. Michael Sendtner

Supervisor (Second): Dr. Michael Briese

Supervisor (Third): Prof. Dr. Utz Fischer

Date of Public Defence: ……..……

Date of Receipt of Certificates: ……

Affidavit

I hereby confirm that my thesis entitled “The role of 7SK noncoding RNA in development and function of motoneurons” is the result of my own work. I did not receive any help or support from commercial consultants. All sources and/or material applied are listed and specified in the thesis.

Furthermore, I confirm that this thesis has not yet been submitted as part of another examination process neither in identical nor in similar form.

Würzburg,
2020

Changhe Ji

Eidesstattliche Erklärung

Ich erkläre hiermit an Eides statt, dass ich die vorliegende Dissertation “Die Rolle der nichtkodierenden RNA 7SK bei der Entwicklung und Funktion von Motoneuronen” eigenständig, d.h. insbesondere ohne die Hilfe oder Unterstützung von kommerziellen Promotionsberatern, angefertigt habe. Ergänzend bestätige ich, dass ich keine anderen als die von mir angegebenen Quellen oder Hilfsmittel verwendet habe.

Ich erkläre außerdem, dass diese Dissertation weder in gleicher noch in ähnlicher Form bereits in einem Prüfungsverfahren vorgelegen hat.

Würzburg,
2020

Changhe Ji

ZUSAMMENFASSUNG

Bei Säugetieren wird ein großer Teil des Genoms als nicht-kodierende RNAs transkribiert. Es gibt immer mehr Hinweise darauf, dass nicht-kodierende RNAs eine wichtige Rolle sowohl für die normale Zellfunktion als auch bei Krankheitsprozessen wie Krebs oder Neurodegeneration spielen. Die Interpretation der Funktionen nicht-kodierender RNAs und der molekularen Mechanismen, über die sie wirken, ist eine der wichtigsten Herausforderungen, denen die RNA-Biologie heute gegenübersteht.

In meiner Promotionsarbeit habe ich die Rolle von 7SK, einer der am häufigsten vorkommenden nicht-kodierenden RNAs, bei der Entwicklung und Funktion von Motoneuronen untersucht. 7SK ist eine RNA, die aus 331 Nukleotiden besteht und deren Struktur bekannt ist. Sie wird von der RNA-Polymerase III transkribiert. Sie bildet vier Stem-Loop (SL)-Strukturen, die als Bindungsstellen für verschiedene Proteine dienen. LARP7 bindet an SL4 und schützt das 3'-Ende vor exonukleolytischem Abbau. SL1 dient als Bindungsstelle für HEXIM1, das den P-TEFb-Komplex rekrutiert, der aus CDK9 und Cyclin T1 besteht. P-TEFb hat eine stimulierende Rolle für die Transkription und wird durch Sequestrierung durch 7SK reguliert. In jüngerer Zeit wurde eine Reihe von heterogenen nukleären Ribonukleoproteinen (hnRNPs) als 7SK-Interaktoren identifiziert. Eines davon ist hnRNP R, von dem gezeigt wurde, dass es eine Rolle bei der Entwicklung von Motoneuronen spielt, indem es das Axonwachstum reguliert. Durch die Interaktion mit P-TEFb und RNA-bindenden Proteinen kann 7SK als Drehscheibe für die Rekrutierung und Freisetzung verschiedener Proteine betrachtet werden. Die Fragen, mit denen ich mich während meiner Doktorarbeit beschäftigt habe, lauten wie folgt: 1) Welche Region von 7SK interagiert mit hnRNP R, einem Hauptinteraktor von 7SK? 2) Welche Effekte treten in Motoneuronen auf, wenn die Bindung von hnRNP R an 7SK inhibiert wird? 3) Gibt es zusätzliche 7SK-bindende Proteine, die die Funktionen des 7SK RNPs regulieren?

Mit Hilfe von *in vitro* und *in vivo* Experimenten fand ich heraus, dass hnRNP R sowohl die SL1- als auch die SL3-Region von 7SK bindet, und dass P-TEFb nach der Deletion der SL1-Region nicht rekrutiert werden kann, aber in der Lage ist, an eine 7SK-Mutante mit Deletion von SL3 zu binden. Um die Frage zu beantworten, wie sich die 7SK-Mutationen auf Axonwachstum in primären Motoneuronen der Maus auswirken, führten wir Rettungsexperimente an Motoneuronen unter Verwendung lentiviraler Vektoren durch. Die Konstrukte wurden so konzipiert, dass sie 7SK-Deletionsmutanten durch den U6-Promotor der Maus exprimieren und gleichzeitig

eine 7SK-shRNA von einem H1-Promotor für die Depletion von endogenem 7SK transkribieren. Mit diesem System fanden wir heraus, dass 7SK-Mutanten, die Deletionen von SL1 oder SL3 beherbergen, den Axon-Wachstumsdefekt von 7SK-depletierten Motoneuronen nicht retten konnten, was darauf hindeutet, dass 7SK/hnRNP R-Komplexe für diesen Prozess von Bedeutung sind.

Um neue 7SK-Bindungsproteine zu identifizieren und ihre Funktionen zu untersuchen, führte ich Pulldown-Experimente durch, bei denen ich ein biotinyliertes RNA-Antisense-Oligonukleotid verwendete, das an die U17-C33-Region von 7SK bindet und dadurch Aufreinigung endogener 7SK-Komplexe erlaubt. Nach der Massenspektrometrie der gereinigten 7SK-Komplexe identifizierten wir eine Reihe neuer 7SK-Interaktoren. Einer davon ist der Smn-Komplex. Ein Mangel des Smn-Komplexes verursacht die Motoneuronerkrankung Spinale Muskelatrophie (SMA), die durch den Verlust der unteren Motoneuronen im Rückenmark gekennzeichnet ist. Es wurde bereits gezeigt, dass Smn mit hnRNP R interagiert. Dementsprechend fanden wir Smn als Teil des 7SK/hnRNP R-Komplexes. Diese Proteom-Daten deuten darauf hin, dass 7SK neben der Transkription möglicherweise auch in anderen Signalwegen wie der spliceosomalen snRNP Biogenese eine wichtige Rolle spielt.

SUMMARY

In mammals, a major fraction of the genome is transcribed as non-coding RNAs. An increasing amount of evidence has accumulated showing that non-coding RNAs play important roles both for normal cell function and in disease processes such as cancer or neurodegeneration. Interpreting the functions of non-coding RNAs and the molecular mechanisms through which they act is one of the most important challenges facing RNA biology today.

In my Ph.D. thesis, I have been investigating the role of 7SK, one of the most abundant non-coding RNAs, in the development and function of motoneurons. 7SK is a highly structured 331 nt RNA transcribed by RNA polymerase III. It forms four stem-loop (SL) structures that serve as binding sites for different proteins. Larp7 binds to SL4 and protects the 3' end from exonucleolytic degradation. SL1 serves as a binding site for HEXIM1, which recruits the pTEFb complex composed of CDK9 and cyclin T1. pTEFb has a stimulatory role for transcription and is regulated through sequestration by 7SK. More recently, a number of heterogeneous nuclear ribonucleoproteins (hnRNPs) have been identified as 7SK interactors. One of these is hnRNP R, which has been shown to have a role in motoneuron development by regulating axon growth. Taken together, 7SK's function involves interactions with RNA binding proteins, and different RNA binding proteins interact with different regions of 7SK, such that 7SK can be considered as a hub for recruitment and release of different proteins. The questions I have addressed during my Ph.D. are as follows: 1) which region of 7SK interacts with hnRNP R, a main interactor of 7SK? 2) What effects occur in motoneurons after the protein binding sites of 7SK are abolished? 3) Are there additional 7SK binding proteins that regulate the functions of the 7SK RNP?

Using *in vitro* and *in vivo* experiments, I found that hnRNP R binds both the SL1 and SL3 region of 7SK, and also that pTEFb cannot be recruited after deleting the SL1 region but is able to bind to a 7SK mutant with deletion of SL3. In order to answer the question of how the 7SK mutations affect axon outgrowth and elongation in mouse primary motoneurons, we proceeded to conduct rescue experiments in motoneurons by using lentiviral vectors. The constructs were designed to express 7SK deletion mutants under the mouse U6 promoter and at the same time to drive expression of a 7SK shRNA from an H1 promoter for the depletion of endogenous 7SK. Using this

system we found that 7SK mutants harboring deletions of either SL1 or SL3 could not rescue the axon growth defect of 7SK-depleted motoneurons suggesting that 7SK/hnRNP R complexes are integral for this process.

In order to identify novel 7SK binding proteins and investigate their functions, I proceeded to conduct pull-down experiments by using a biotinylated RNA antisense oligonucleotide that targets the U17-C33 region of 7SK thereby purifying endogenous 7SK complexes. Following mass spectrometry of purified 7SK complexes, we identified a number of novel 7SK interactors. Among these is the Smn complex. Deficiency of the Smn complex causes the motoneuron disease spinal muscular atrophy (SMA) characterized by loss of lower motoneurons in the spinal cord. Smn has previously been shown to interact with hnRNP R. Accordingly, we found Smn as part of 7SK/hnRNP R complexes. These proteomics data suggest that 7SK potentially plays important roles in different signaling pathways in addition to transcription.

1. Introduction

1.1. Structure of 7SK snRNA

7SK is an abundant (2x10^5-molecule-per-cell), long, noncoding nuclear RNA which contains 331 nucleotides and is also evolutionarily conserved in vertebrates. 7SK snRNA was first described in 1976. 15 years later, the human 7SK snRNA was structurally analyzed by Wassarman and Steitz [1] (**Figure 1**). 7SK forms four stem-loops (SL), and different loops associate with different proteins. The evolutionary conservation (**Figure 2**) and high abundance of the 7SK RNP suggest that it plays an important role in cell functions.

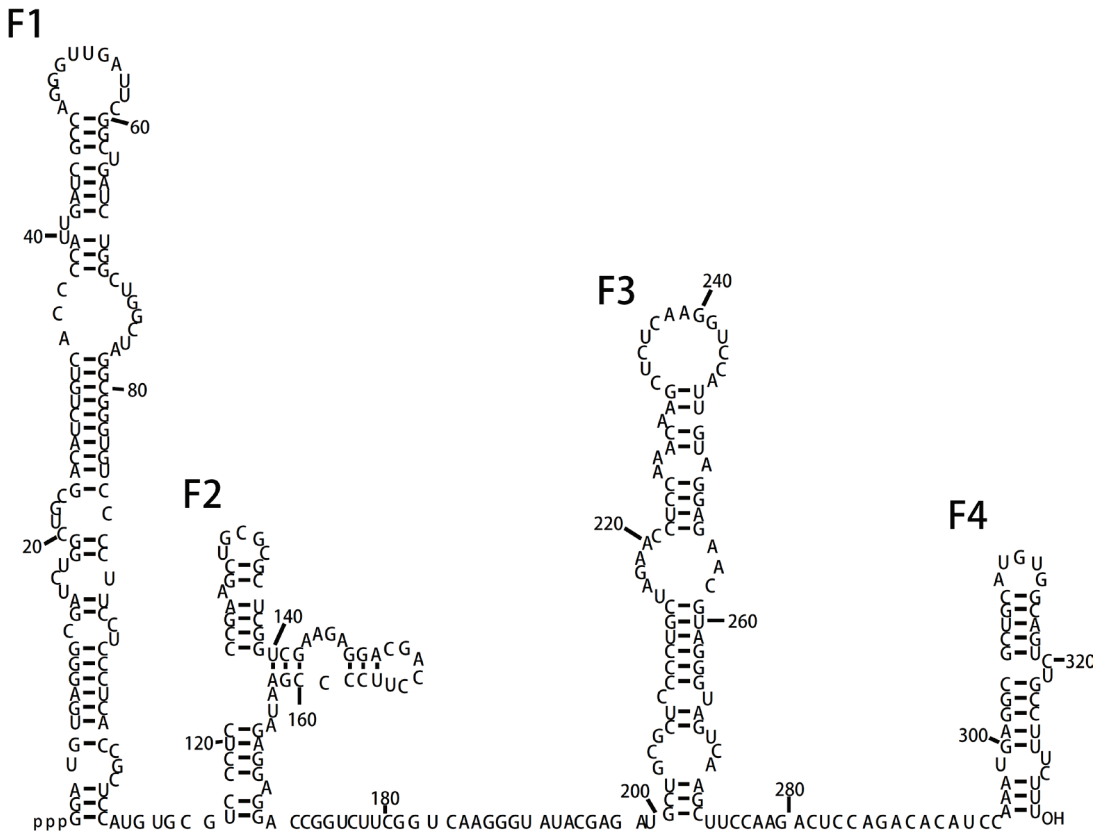

Figure 1: Structure of 7SK snRNA. The secondary structure of mouse 7SK snRNA has been adapted [1]. The F1-4 stem-loop structures of 7SK snRNA are indicated.

Figure 2: Alignment of vertebrate 7SK snRNA sequences. The sequences of human (GenBank accession number NR_001445), rat (K02909), lamprey (*Lampetra fluviatilis*) [2], chicken (AJ890101), zebra fish (AJ890102), *Tetraodon nigrovidis* (AJ890103), and *Fugu rubripes* (AJ890104) [3] were used for the alignment.

1.2. 7SK, MEPCE and LARP7 form a core 7SK snRNP complex

7SK acts as a hub, which can recruit different proteins to form different complexes. Two proteins, MEPCE and Larp7, have been identified as stable interactors of 7SK thereby forming the 7SK/MEPCE/Larp7 “core” snRNP [4].

7SK is stabilized at the 5' end by MEPCE, also called BCDIN3, which generates a monomethyl cap at the gamma-phosphate of the 5'-terminal guanosine triphosphate [5, 6]. The cap structure protects 7SK from degradation at the 5' end [7]. Accordingly, depletion of MEPCE decreases the steady-state levels of 7SK *in vivo* [5, 8]. Recently, one report found that *MEPCE* mutations associate with a neurodevelopmental disease [9]. Mutated MEPCE causes the disintegration of 7SK snRNP leading to P-TEFb release, thereby enhancing transcription through RNA Polymerase II activation. As a result, RNA polymerase II-dependent transcripts were upregulated including spliceosomal snRNAs like U1, U2 and U4. This suggests that MEPCE indirectly regulates spliceosomal snRNP biogenesis through regulating their transcription in a 7SK-dependent manner.

In 2008, La-related protein 7 (LARP7) was found to associate with and thereby stabilize 7SK snRNP [10-13]. LARP7 interacts with stem-loop 4 including the uridine-rich tail of 7SK RNA [14]. The LARP7 protein contains a La module at its N-terminus, followed by RNA recognition motif (RRM) 1 and RRM2, the latter located at the C-terminus. All three domains are needed for the stabilization of 7SK snRNA [10]. Interestingly, the C-terminus of LARP7 is often deleted in human tumors leading to destabilization of the 7SK complex and corresponding activation of P-TEFb followed by transcriptional induction of tumor-related genes [10]. Mutations in LARP7 were also identified in patients with facial dysmorphism, intellectual disability, and primordial dwarfism, the so-called Alazami syndrome [15-17]. In these patients loss of LARP7 leads to near-absent levels of 7SK. More recently, LARP7 has been found to guide certain box C/D small nucleolar RNAs (snoRNAs) to U6 spliceosomal snRNA, thereby facilitating 2'-O-methylation of U6 [18]. Thus, defects in multiple pathways might contribute to Alazami syndrome.

1.3. 7SK complexes function in transcriptional regulation

Within cells, 7SK is abundant in the nucleus where it regulates gene transcription. Whilst LARP7 and MEPCE are stably associated with 7SK, a number of proteins have been identified to interact directly or indirectly with 7SK in a transient manner (**Table 1**). These proteins often bind in a mutually exclusive manner such that 7SK subcomplexes of different composition co-exist in cells. For example, 7SK/HEXIM1/P-TEFb and 7SK/hnRNP complexes have been identified, and the balance between these complexes determines the cell's transcriptional activity [19]. Thus, 7SK functions as a hub bringing together different RNA binding proteins and secondary effectors to regulate their activity.

Table 1 Proteins interacting with 7SK snRNA [19, 20].

Complex	Component	Name	Size(KD)	Mode of action
Core	7SK snRNA	7SK small nuclear RNA	331nt	RNA platform of the complex
	LARP7	La-related protein 7	67	Binds 3' end and SL4 of 7SK to enable 7SK stability and binds P-TEFb to promote its incorporation into 7SK snRNP [14]
	MEPCE	Methylphosphate capping enzyme	74	Binds the basal part in SL1 of 7SK and caps 7SK at 5' end to enable 7SK stability [14]
P-TEFb	Cdk9	Cyclin dependent kinase 9	43/55	Catalytic subunit of P-TEFb that is inhibited by HEXIM1/2.
	CycT1	Cyclin T1	81	Regulatory subunit of P-TEFb that provides a binding surface for HEXIM1/2.
	CycT2a, 2b	Cyclin T2a, T2b	74/82	Regulatory subunit of P-TEFb that provides binding surface for HEXIM1/2.
hnRNPs	hnRNPA1	Heterogeneous nuclear ribonucleoprotein A1	38	Bind SL3 of 7SK to enable the release of P-TEFb and HEXIM1 from the canonical 7SK snRNP [12].
	hnRNPA2	Heterogeneous nuclear ribonucleoprotein A2	36	Bind SL3 of 7SK to enable the release of P-TEFb and HEXIM1 from the canonical 7SK snRNP.
	hnRNPQ1	Heterogeneous nuclear ribonucleoprotein Q1	62	Bind SL3 of 7SK to enable the release of P-TEFb and HEXIM1 from the canonical 7SK snRNP.
	hnRNPR	Heterogeneous nuclear ribonucleoprotein R	80	Bind SL3 of 7SK to enable the release of P-TEFb and HEXIM1 from the canonical 7SK snRNP.
DSIF	Spt4	Suppressor of Ty protein 4	16	Binds SL3 of 7SK and nascent RNA to trigger the release [21].
	Spt5	Suppressor of Ty protein 5	160	Binds SL3 of 7SK and nascent RNA to trigger the release [21].
others	H4R3me2	Histone H4 (di methyl R3)	11	Binds first half of 7SK to recruit 7SK snRNP to A-Pes [22].
	KAP1	Transcription intermediary factor 1-beta	89	Binds LARP7 to recruit 7SK snRNP to promoters [23]
	HMGA1	High mobility group protein HMG-I	12	Binds CTIP2 and SL2 of 7SK to recruit 7SK snRNP to promoters [24].
	PKC	Protein kinase C	77	Phosphorylates HEXIM1 Ser158 to prevent 7SK binding [25]
	ERK	Extracellular Signal-regulated Kinase	43	ERK-dependent kinase phosphorylates HEXIM1 Tyr271 and Tyr274 to prevent CycT1/P-TEFb binding [26].
	Akt	RAC-alpha serine/threonine-protein kinase	55	Phosphorylates HEXIM1 Ser270 and Thr278 to prevent CycT1/P-TEFb binding [27].
	PP2B+PP1a	Serine/threonine-protein phosphatase 2B+1a	3	PP1 dephosphorylates P-Thr186 in Cdk9 after PP2B remodels 7SK snRNP [28].
	Calpain2	Calpain-2 catalytic subunit	80	Cleaves MEPCE to destabilize core 7SK snRNP [29].
	tat	tat protein in HIV-1	10	Binds the distal part in SL1 of 7SK and CycT1 to dislodge HEXIM1;recruits PPM1G for P-Thr186 Cdk9dephosphorylation[30].
	tax	Human T-cell leukemia virus type I	40	Binds CycT1 to dislodge HEXIM1 [31].
	NF-KB	nuclear factor 'kappa-light-chain-enhancer' of activated B-cells	105	Recruits PPM1G for P-Thr186 Cdk9 dephosphorylation [30]
	SRSF2	Serine And Arginine Rich Splicing Factor 2	25	Binds SL3 of 7SK and nascent RNA to trigger the release [32].
	DDX21	DExD-Box Helicase 21	94	Binds SL3 of 7SK and changes the conformation of 7SK [33].
	JMJD6	Jumonji C-domain containing protein 6	47	Demethylates H4R3me2(s) and 7SK cap at A-Pes [22].
	RBM7	RNA Binding Motif Protein 7	31	RNA Binding Motif Protein 7 [34]

1.3.1. 7SK snRNA regulates P-TEFb and forms 7SK/HEXIM1/P-TEFb complex

In two seminal studies Yang et al. and Nguyen et al. showed that 7SK binds to HEXIM1 and thereby sequesters the kinase complex positive transcription elongation factor b (P-TEFb) composed of CDK9 and Cyclin T1 [35, 36]. P-TEFb stimulates transcription by phosphorylating the C-terminal domain of RNA polymerase II. Binding to 7SK inhibits P-TEFb activity. Therefore, 7SK acts as a negative regulator of transcription. Importantly, treatment of cells with transcriptional inhibitors such as Actinomycin D facilitates dissolution of the 7SK/P-TEFb complex representing a feedback loop through which the transcriptional output of a cell regulates itself. Beyond that, Prasanth et al. found 7SK associated with nuclear speckles or interchromatin granule clusters (IGCs) containing pre-mRNA processing factors [37]. They used a stably integrated in vivo reporter cell line system to show that knockdown of 7SK RNA results in increased expression of the reporter gene, accompanied by re-distribution of pre-mRNA processing factors from nuclear speckles to the gene locus.

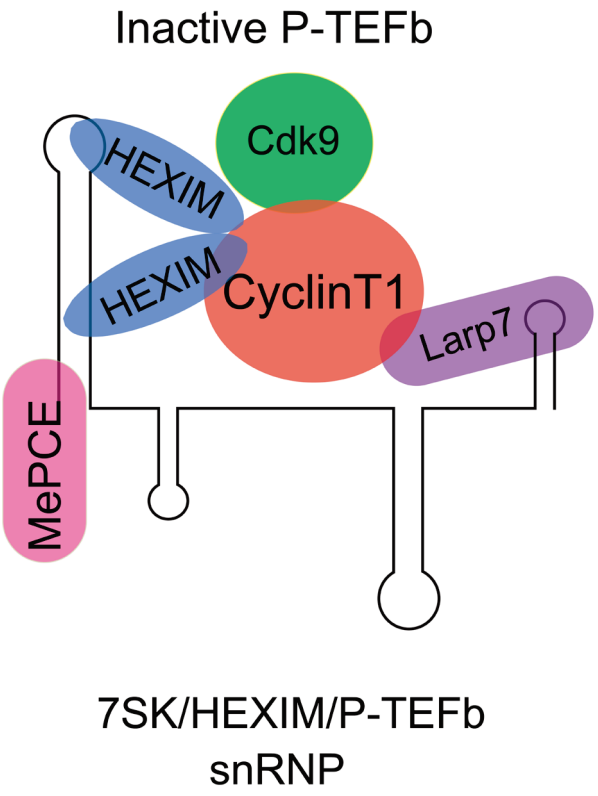

Figure 3: Model of 7SK/HEXIM/p-TEFb complex

Binding of P-TEFb to 7SK is mediated by HEXIM1, which interacts with SL1 (**Figure 3**) [38, 39]. The first report about HEXIM1 association with 7SK was published in 2003 by the Bensaude group [40]. They immunoprecipitated cyclin T1 and CDK9 from cells to identify protein interactors of the P-TEFb complex whose association was dependent on the transcription inhibitor Actinomycin D. They observed a 65-kDa protein co-immunoprecipitating with CDK9 and cyclin T1 that was identified as HEXIM1 by mass spectrometry. HEXIM1 binds to the Cdk9 catalytic site to inhibit P-TEFb activity [41]. The interaction between HEXIM1 and P-TEFb requires 7SK which, therefore, acts as a structural scaffold bringing these protein components together [38].

1.3.2. 7SK snRNA binds hnRNPs to form 7SK/hnRNP complexes

A central question regarding the regulatory role of 7SK in transcription is how P-TEFb is released from 7SK to become activated. In addition to HEXIM1 and the P-TEFb complex, a number of heterogeneous nuclear ribonucleoproteins (hnRNPs) have more recently been identified as interactors of 7SK [42]. Among these are the hnRNPs A1, A2/B1, Q and R (**Figure 4**). In transcriptionally active cells, hnRNPs bind to nascent RNA and contribute to multiple aspects of post-transcriptional RNA processing including alternative splicing, mRNA stabilization, transport and translational regulation [43].

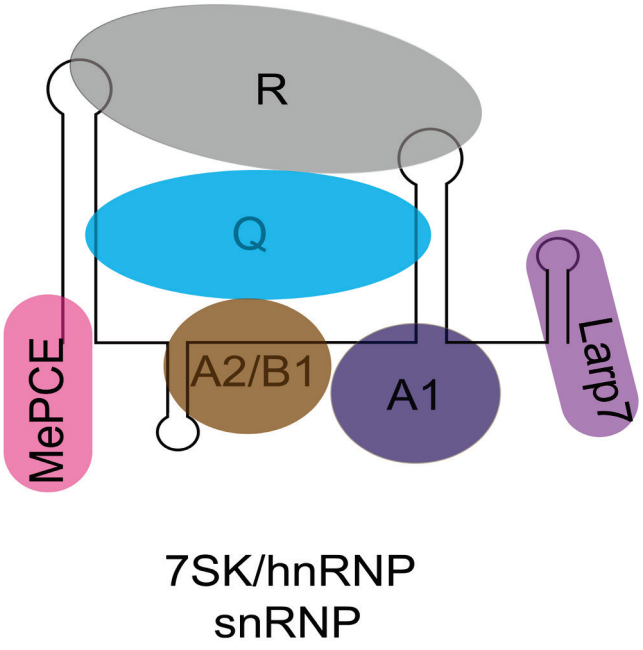

Figure 4: Model of 7SK/hnRNP complex

hnRNP A1

Heterogeneous nuclear ribonucleoprotein (hnRNP) A1 is a member of the hnRNP family, a group of related proteins known to associate with nascent mRNA [44-46]. hnRNP A1 is mostly located in the nucleus but can also shuttle between nucleus and cytoplasm [47].The nuclear localization of hnRNP A1 is mediated through its M9 sequence [48]. hnRNP A1 binds to exonic and intronic sequences [49, 50] and functions with other hnRNPs to control alternative splicing [51]. Beyond that, hnRNP A1 binds to AU-rich sequences along mRNAs to control their stability [52, 53].

Mutations in hnRNP A1 have been identified in patients with multisystem proteinopathy and ALS [54]. The mechanisms of pathogenicity of hnRNP A1 variants are not well studied. It has been shown that mutations in the C-terminal Gly-rich domain of hnRNP A1 that also encodes a Prion-like domain strengthen “steric zippers” already present in the wild-type protein, thereby increasing the aggregation propensity of hnRNP A1.

hnRNP A2/B1

hnRNP A2/B1 has two distinct isoforms, A2 (341 amino acids) and B1 (353 amino acids), both are transcribed from the *HNRNPA2B1* gene. Similar to hnRNP A1, hnRNP A2/B1 contains an M9 sequence and is primarily localized in the nucleus but

also shuttles to the cytoplasm [55, 56]. The putative functions of hnRNP A2/B1 include pre-mRNA splicing [57, 58], mRNA trafficking [59-61], and translational control [62]. hnRNP A2/B1 transports mRNAs to neuronal dendrites by binding to a 21-nucleotide A2 response element (A2RE) in target transcripts [60, 63, 64].

hnRNP R

Due to alternative splicing of exon 2, two hnRNP R isoforms are produced from the *HNRNPR* gene: a long isoform containing 632 amino acids and a short isoform containing 531 amino acids. Both isoforms harbor 3 RNA recognition motifs (RRMs), a nuclear localization signal and a Gln- and Asn-rich region which allows hnRNP R binding to other proteins. The only difference between the two isoforms is the presence of a 102 amino acid acidic N-terminus on the long isoform (**Figure 5**).

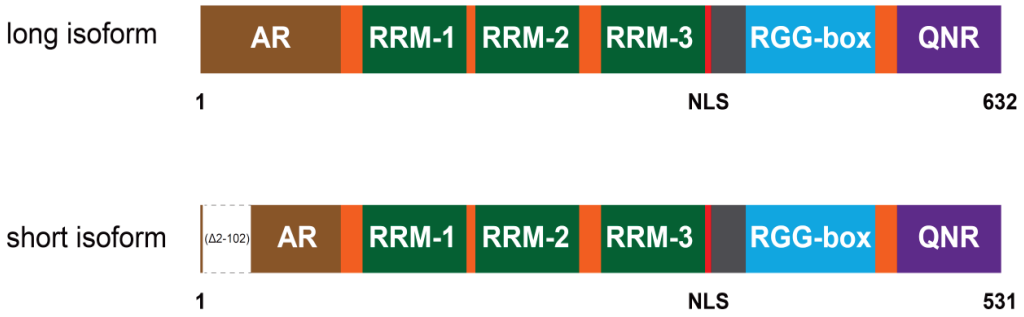

Figure 5: The schematic structure of hnRNP R long isoform and short isoform
Abbreviations: AR, an acidic region rich in glue and Asp; RRM, RNA recognition motif; NLS, nuclear localization signal;RGG-Box, RNA binding domain rich in Arg and Gly; QNR, Gln and Asn rich region

In mouse tissues, hnRNP R is abundant in the developing nervous system including motoneurons [65]. In the latter, hnRNP R is predominantly present in the nucleus but also localizes to the cytosol including axons and growth cones [66]. This finding suggests that hnRNP R exerts nuclear functions in post-transcriptional RNA processing, but also regulates axonal RNA transport. In agreement with this notion, knockdown of hnRNP R changes the levels of target transcripts both in the somatodendritic and the axonal compartment of motoneurons cultured in microfluidic chambers [67]. Depletion of hnRNP R in motoneurons reduces their axon length

indicating that hnRNP R plays a role in axon growth and possibly growth cone formation [68, 69]. Among RNA interactors, hnRNP R has been observed to bind to the 3'UTR of *β-actin* mRNA to control its axonal localization [69]. More recently, the RNA interactome of hnRNP R was investigated using individual nucleotide-resolution cross-linking and immunoprecipitation (iCLIP) [68]. In that study, to which the work presented in this thesis, has contributed to, 7SK was identified as the top interactor. Along 7SK, hnRNP R binding sites were identified in SL1 and SL3 regions.

hnRNP R interacts with a number of proteins implicated in motoneuron diseases such as Smn, the deficiency of which causes spinal muscular atrophy (SMA), and proteins associated with amyotrophic lateral sclerosis (ALS) such as TDP-43, FUS, MATR3, hnRNP A2B1, and hnRNP A1 [70-73]. The axonal localization of hnRNP R is reduced in Smn-deficient motoneurons,which might contribute to the axonal RNA transport defect observed upon Smn depletion [74, 75]. In the frontal cortex and hippocampus of patients with frontotemporal lobar degeneration (FTLD) hnRNP R was detected in FUS-positive cytoplasmic inclusions [76]. These data suggest that disruption of hnRNP R functions might contribute to the pathogenesis of neurodegenerative disorders. Recently, individuals with mutations in *HNRNPR* have been identified showing developmental defects including neurodevelopmental abnormalities of the brain [77].

1.3.3. 7SK snRNA balances 7SK/HEXIM1/P-TEFb and 7SK/hnRNPs complex

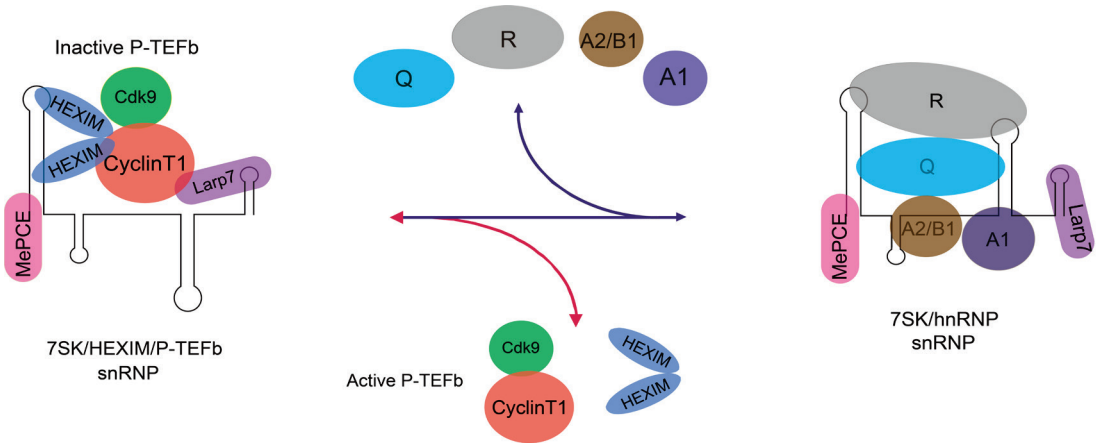

Figure 6: A model of how 7SK keeps the balance between 7SK/HEXIM1/P-TEFb and 7SK/hnRNP complexes

The identification of two separate and mutually exclusive 7SK complexes, 7SK/HEXIM1/P-TEFb and 7SK/hnRNP, has been reconciled in a model according to which the balance between these two complexes is tightly intertwined with the transcriptional output of a cell. In support of this model, transcriptional inhibition of RNA Polymerases II and III causes a shift in the balance between these two complexes that leads to P-TEFb release. Mechanistically, when transcription is inhibited by actinomycin D or DRB, for example, the amounts of nuclear hnRNP proteins associated with 7SK are increased due to reduced availability of nascent RNA [42, 78]. At the same time, the amount of P-TEFb bound to 7SK is decreased leading to more free P-TEFb. This dissociation of 7SK/HEXIM1/P-TEFb complexes upon DRB treatment was impaired following knockdown of hnRNP A1 and A2 [79]. Thus, 7SK/HEXIM1/P-TEFb and 7SK/hnRNP complexes are in a dynamic balance that can shift reversibly according to the transcriptional status of the cell. The level of free P-TEFb able to induce transcription is thereby indirectly controlled by the transcriptional output sensed by hnRNP proteins (**Figure 6**).

1.4. Cytosolic functions of 7SK

More recently, it has been suggested that 7SK also exerts functions in the cytoplasm. In mouse primary motoneurons, 7SK is abundant in the nucleus but also localizes to the cytoplasm including axons and growth cones [8, 9]. Using iCLIP to determine the RNA interactome of hnRNP R in motoneurons revealed ~3,500 RNA targets, predominantly with functions in synaptic transmission and axon guidance [9]. Among the RNA targets identified by iCLIP, the noncoding RNA 7SK was the top interactor of hnRNP R. In axons, 7SK localized in close proximity to hnRNP R, and depletion of hnRNP R reduced axonal 7SK. Furthermore, knockdown of 7SK led to defective axon growth that was accompanied by axonal transcriptome alterations similar to those caused by hnRNP R depletion. In addition, knockdown 7SK does not affect motoneuron survival. The function of 7SK in axon elongation was dependent on its interaction with hnRNP R but not with the P-TEFb complex involved in transcriptional regulation. These results propose a cytosolic role for 7SK as an essential interactor of hnRNP R. The composition and functions of these cytosolic 7SK complexes are unknown so far.

1.5. Aim of thesis

The central goal of this project was to characterize the interaction between hnRNP R and 7SK, and how this interaction modulates functional states in neuronal cells, in particular motoneurons. In addition, new complexes involving the 7SK RNA should be characterized on a molecular level, and how these complexes function in neuronal cells.

2. Materials

2.1. Animals

CD-1 mice were housed in the animal facilities of the Institute of Clinical Neurobiology at the University Hospital of Wuerzburg. Mice were kept under controlled conditions in a 12 h/12 h day/night cycle at 20–22 °C and 55–65% humidity with abundant supply of food and water. Experiments were performed strictly following the regulations on animal protection of the German federal law and of the Association for Assessment and Accreditation of Laboratory Animal Care, in agreement with and under control of the local veterinary authority.

2.2. Cell lines

HeLa was obtained from ATCC.

NSC-34 cells was obtained from Cedarlane.

2.3. Commercial kits

Name	Company	Number
DNA Rainbow Ladder, 100 - 3000 bp	GeneOn GmbH	307-105
GeneRuler 1 kb DNA Ladder	Thermo	SM0311
GeneRuler MLtra Low Range DNA Ladder	Thermo	SM1213
RiboRuler Low Range RNA Ladder,	Thermo	SM1831
PageRuler™ Prestained Protein Ladder	Thermo	26616
Turbofect	Thermo	R0531
Plasmid Miniprep kit	Macherey-Nagel	740.588.250
Plasmid midi Kit	Macherey-Nagel	740.410.100
Plasmid maxi Kit	Macherey-Nagel	740424.10
NucleoSpin RNA kit	Macherey-Nagel	740984.50
RNA Clean & Concentrator Kits	Zymo Research	R1017
QIAprep Spin Miniprep Kit	QIAGEN	27104
QIAquick Gel Extraction Kit	QIAGEN	28704
QIAquick PCR Purification Kit	QIAGEN	28104
Luminaris Color HiGreen qPCR Master Mix	Thermo	K0392
RevertAid First Strand cDNA Synthesis Kit	Thermo	K1622
CloneJET PCR Cloning Kit	Thermo	K1231
GlycoBlue™ Coprecipitant (15 mg/mL)	Invitrogen	AM9515
KAPA HiFi HotStart ReadyMix	ROCHE	KK2601
T7 RNA Polymerase (20 U/µL)	Thermo	EP0111
SimplyBlue™ SafeStain	Thermo	LC6060
Neurobasal™	Gibco	21103049
B-27	Gibco	17504044
GlutaMAX	Gibco	35050061
DMEM	Gibco	10566016
Fetal calf serum (FCS)	Linaris	ADI-NFCS-500
Phosphate gepufferte Saline (PBS)	Sigma	806552-500ML
Penicillin-Streptomycin (Pen/Strep)	Gibco	15140122
TrypLE	Gibco	12604021
Micro tube 1.5 mL l, PP	Sarstedt	72.706.400
Micro tube 2.0 mL, PP	Sarstedt	72.695.400
TC Flask T25,Standard	Sarstedt	83.3910.002
TC Flask T75,Standard	Sarstedt	83.3911.002
TC Flask T175,Standard	Sarstedt	83.3912.002

6 well plates	Greiner Bio-One	657.160
12 well plates	Greiner Bio-One	665.102
24 well plates	Greiner Bio-One	662.102
48 well plates	Greiner Bio-One	677.102
96 well plates	Greiner Bio-One	655.101
15 mL PP Test Tubes	Greiner Bio-One	188.261
50 mL PP Test Tubes	Greiner Bio-One	227.261
0.2 uM PVDF Western blotting membrane	GE	10.600.021

2.4. Chemicals

Name	Company	Number
TRIS base	Carl Roth GmbH	5429.2
Tris-HCl	Carl Roth GmbH	9090.3
Digitonin	Merck	300410-250MG
Tris-base	Carl Roth GmbH	2449.2
Sodium hydroxide	Sigma-Aldrich	06203-1KG
EDTA	Carl Roth GmbH	1408.3
TWEEN-20	Sigma-Aldrich	P1379-500ML
SDS	Sigma-Aldrich	L3771-500G
HEPES	Sigma-Aldrich	H3375-500G
Powdered milk	Carl Roth GmbH	T145.3
LE Agarose	Biozym	840004
Ampicillin	Sigma-Aldrich	A9518-25G

2.5. Buffers

2.5.1. General Solutions

SA RNP lysis buffer

Final concentration	Component
20 mM(pH 7.4)	Tris-HCl
150 mM	NaCl

1.5 mM	$MgCl_2$
0.5% (v/v)	NP40

Polysome lysis buffer

Final concentration	**Component**
10 mM (pH 7.0)	HEPES-KOH(pH7.0)
100 mM	KCl
5 mM	$MgCl_2$
0.5% (v/v)	NP40

10 x SDS-Running puffer

Final	**Component**
30 g	Tris base
144 g	glycine
10 g	SDS
1000 mL	Total

10 x Towbin transfer puffer

Final	**Component**
30 g	Tris base
144 g	glycine
1000 mL	Total

5x Laemmli Buffer

Final	**Component**
0.875 mL	1M Tris-HCl pH6.8
4.5 mL	Glycine
0.5 g	SDS
0.5 mL	0.25% Bromophenol blue (25mg in 10ml H_20)
1.25 mL	B-mercaptoethanol

10 mL	Total

10x TAE

Final	Component
48.4 g	Tris base
11.4 mL	20 mM pH 8,3 acetic acid
3.72 g	EDTA
1000 mL	Total

10x TBE buffer

Final	Component
107.78 g	Tris
7.44 g	EDTA-Na2-salt
55 g	Boric acid
1000 mL	Total

Buffers for mouse primary cell culture

Name	Component
Borate buffer	0.15 M boric acid pH 8.35
Depolarization buffer	30mM KCl, 0.8% NaCl, 2mM $CaCl_2$
Tris HCl	10mM, pH 9.5
Poly D-L-ornithine	1X diluted in borate buffer

2.5.2. Medium for bacteria and cell culture

Top 10 *E.coli* medium

4 g	LB Broth (Lennox)
(3 g)	(agar)
200 mL	de-iron water
1/1000	ampicillin (100 mg/mL)

HeLa and NSC34 medium

Standard medium	DMEM, 10% FCS, 1% Pen/Strep
Cryopreservation medium	DMEM, 50%FCS,10% (v/v)DMSO

Mouse primary motoneuron medium

Neurobasal with 1x Glutamax
2% Horse serum
1x B27 supplement
CNTF 5ng/ml

3. Methods

3.1. Primary mouse motoneuron culture

Spinal motoneurons were cultured protocol was previously established and used in Prof. Sendtner group. Briefly, lumbar spinal cord tissues from E12.5 CD-1 mouse embryos were dissected, and motoneurons were enriched via p75NTR antibody panning. Motoneurons were cultured in neurobasal medium (Gibco) supplemented with B27 (1:50; Gibco), 2% heat-inactivated horse serum (Linaris), 500 µM GlutaMAX (Invitrogen), and 5 ng/ml BDNF. The medium was replaced 24 h after plating and then every second day.

3.2. NSC-34 and HeLa cell culture

NSC-34 cells and HeLa cells were cultured at 37 °C and 5% CO_2 in high glucose DMEM (Gibco) supplemented with 10% fetal calf serum (Linaris), 2 mM GlutaMAX (Gibco) and 1% Penicillin-Streptomycin (Gibco) .Passage the cells when they are 80% confluent by following this protocol: sock off the medium, wash once with prewarmed PBS, then add 4 mL TrypLE and incubate 2 min in the incubator, then add 5 ml fresh medium, Spin down Cells at 0.2 RCF for 5 min. remove supernatant, add 1 mL medium and pipette up and down to dissociate the cells, then take 100 µL cells and put in the new flask for culturing.

For freezing the cells, 8 million cells for 1mL cryopreservation medium and keep in liquid nitrogen tank.

For thawing, take one tube of freezing cells from liquid nitrogen tank put on ice, then add in 37 °C water bar for 2 min. Then directly add the cells in the T-75 flask then add 10 mL prewarmed medium, put in the incubator for culturing.

3.3. Lentivirus-mediated 7SK rescue in HeLa cells

3.3.1. Cloning

Overlap PCR

Using overlap PCR, two DNA fragments with overlapping DNA regions can be joined. I used this method for fusing the cDNA encoding wild-type (**Figure 7**) or mutant (**Figures 8 and 9**) 7SK with the U6 promoter for subsequent cloning into the pSIH vector.

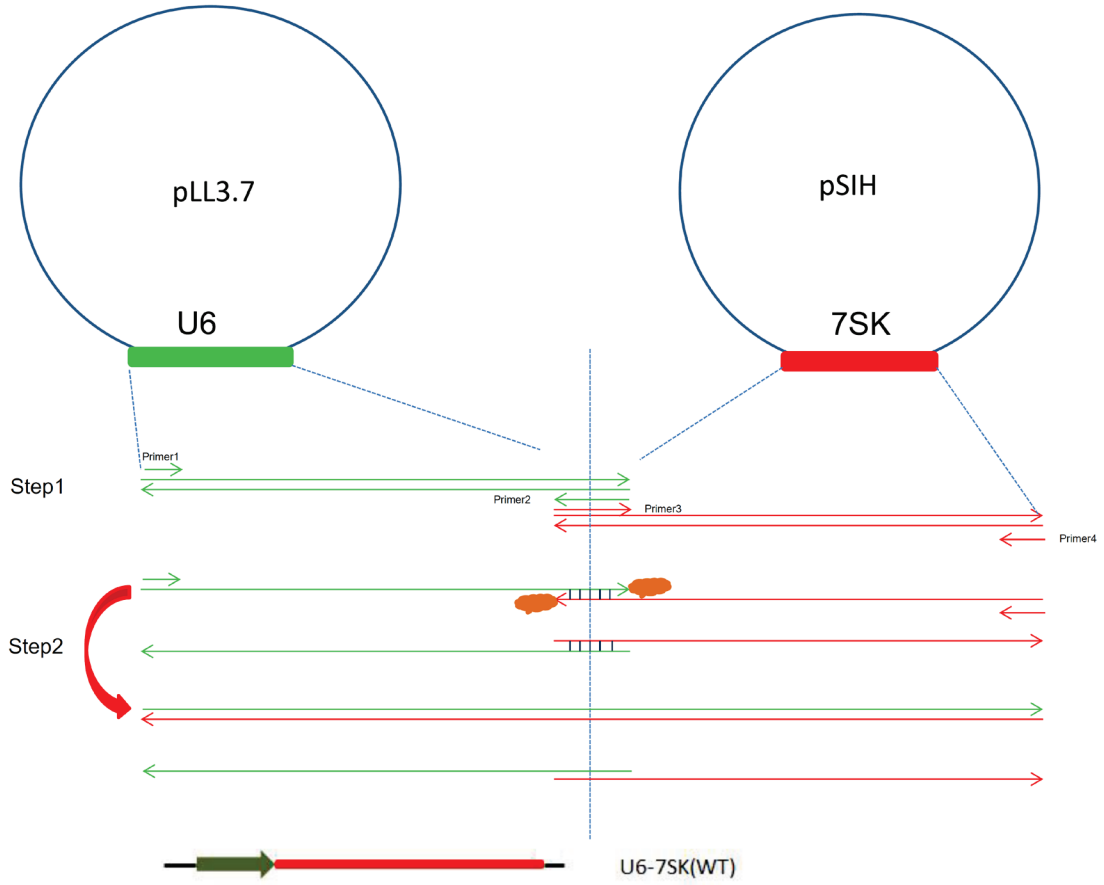

Figure 7: Schematic illustration of overlap PCR for generation of 7SK constructs

I designed Primer 1 and Primer 2 to amplify the U6 promoter region.
In parallel, I designed Primer 3 and Primer 4 to amplify the 7SK cDNA. Primer 3 was used as e the fusion primer with 25–30 bp homology to the sense strand of the 3' end of U6 and 20–25 bp of the sense strand of the 5' end of the 7SK.

Protocol

Step 1: Amplifation of the two separate fragments
For this purpose, two parallel PCR reactions were set up to amplify U6 promoter and 7SK. I used the Expand Long Template PCR protocol as follows, as an example for each reaction:

Reagent	**1x**
H2O	X µL
10 x Taq polymerase Buffer	2.5 µL

10 mM dNTP's	0.5 µL
10 µM Primer1 (or 3)	0.5 µL
10 µM Primer2 (or 4)	0.5 µL
(50 ng/µL) Plasmid	0.5 µL
Taq polymerase	Y µL
Total	25 µL

The PCR was run for 30 cycles on an Eppendorf thermocycler. Then the samples were loaded and seen as a band on a gel. The resulting cDNA was Gel purified, after cutting out the band that was obtained with the templates in the Step 2 PCR reaction.

1. 95 °C 5 min
2. 95 °C 30 sec
3. 60 °C 30 sec
4. 72 °C 30 sec
5. Go to Step 2 29x
6. 72 °C 5 min
7. 4 °C forever
8. END

Clean up the fragments. Use a Qiagen Gel Purification Kit to purify the products. Elute in 30 µl H_2O and check the concentration on the nanodrop.

Step2: Fuse the two fragments

Using the two products from Step1 as the templates for a single PCR reaction, fuse the two products into one. This reaction will either use Primer 1 and Primer 4 if the products are to be cloned.

Reagent	**1x**
H2O	X µL
10 x Taq polymerase Buffer	2.5 µL
10 mM dNTP's	0.5 µL
10 µM Primer1	0.5 µL
10 µM Primer4	0.5 µL
(50 ng/µL) U6	0.5 µL
(50 ng/µL) 7SK	0.5 µL
Taq polymerase	Y µL

Total	25 µL

Run the PCR for 30 cycles on Eppendorf thermocycler.

1. 95 °C 5 min
2. 95 °C 30 s
3. 60 °C 30 s
4. 72 °C 30 s
5. Go to Step 2 29x
6. 72 °C 5 min
7. 4 °C forever
8. END

The fused fragment was cleaned by running the entire 50 µL of the fusion reaction on a new 1.5% agarose gel + EtBr (made with 1xTAE) in a gel box with fresh 1xTAE. After the gel run was completed, (100V, 1hr), bands were cut out and the DNA extracted with a Qiagen Gel Extraction Kit. The DNA was eluted in 30 µL H_2O, then the concentration checked by the nanodrop device.

The resulting cDNA fragments were cloned into a vector by using 2 µL of cleaned fusion product in a pJET cloning reaction. 2 µL of the resulting cloning reaction were transformed into 50 µL TOP10 *E.coli*.

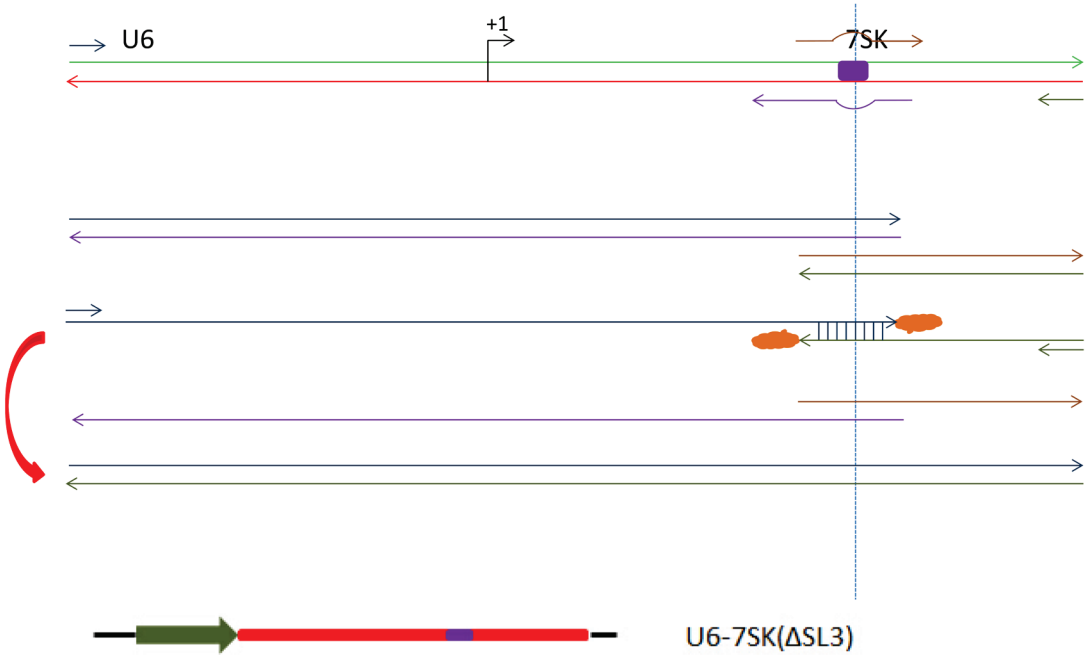

Figure 8: schematic illustration of the U6-7SK Δ SL3P overlap PCR reaction used to generate a 7SK Δ SL3P for expression under the U6 promoter

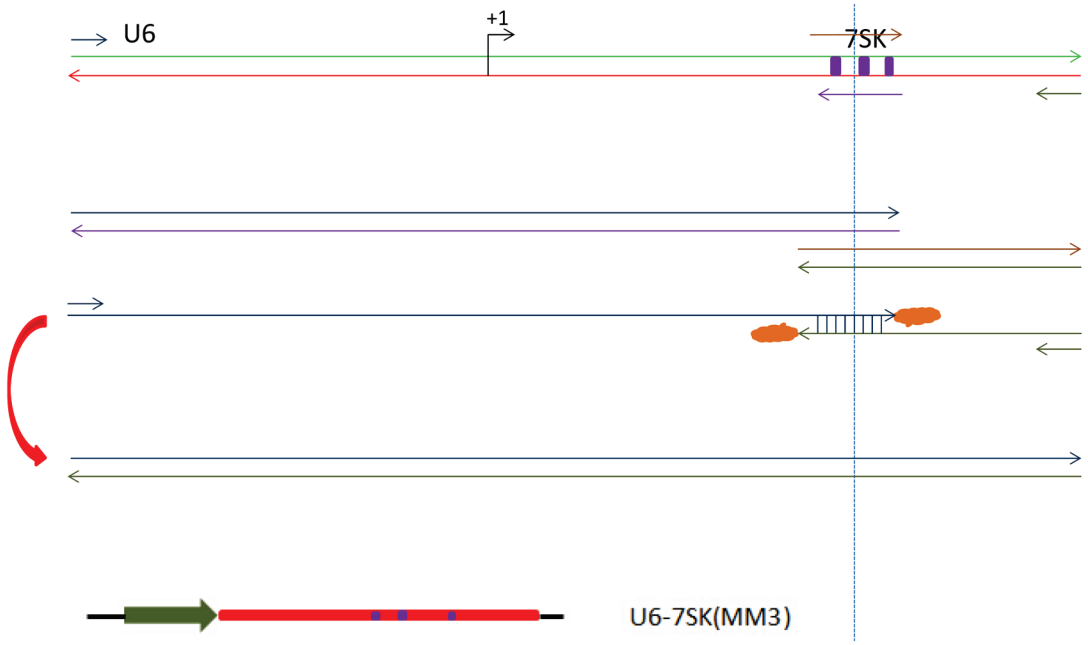

Figure 9: Schematic illustration of the generation of U6-7SKMM3 constructs by overlap PCR

pJET cloning

1. Set up the blunting reaction on ice:

Components	**Volume**
2X Reaction Buffer	10 µL
purified PCR product/other sticky-end DNA fragment	1 µL (0.15 pmol ends)
Water, nuclease-free	to 17 µL
DNA Blunting Enzyme	1 µL
Total volume	18 µL

The mixture was vortexed briefly and centrifuged for 3-5 s

2. Subsequently, the mixture was incubated at 70 °C for 5 min, and then chilled on

ice.

3. The ligation reaction was then set up on ice, followed by addition of the following to the blunting reaction mixture:

Component	Volume
pJET1.2/blunt Cloning Vector (50 ng/μL)	1 μL(0.05 pmol ends)
T4 DNA Ligase	1 μL
Total volume	20 μL

The resulting mixture was then vortexed briefly and centrifuged for 3-5 s to collect drops.

4. The ligation mixture was then incubated at room temperature (22 °C) for 5 min.

5. The ligation mixture was used directly for transformation. When transformation was postponed, the ligation mixture was kept at -20 °C, then thawed on ice and mixed carefully before transformation.

pSIH cloning

Sticky-end Ligation

The following protocol was developed and used for this procedure:

1. Prepare the following reaction mixture:

Component	volume
Linear vector DNA	20-100 ng
Insert DNA	1:1 to 5:1 molar ratio over
10x T4 DNA Ligase buffer	2 μL
Thermo Scientific T4 DNA Ligase	1 U
Water, nuclease-free	to 20 μL

Total	20 µL

2. Incubate 10 min at 22 °C.
3. Use up to 5 µL of the mixture for transformation of 50 µL of chemically competent cells.

NEBuilder HiFi DNA Assembly Cloning

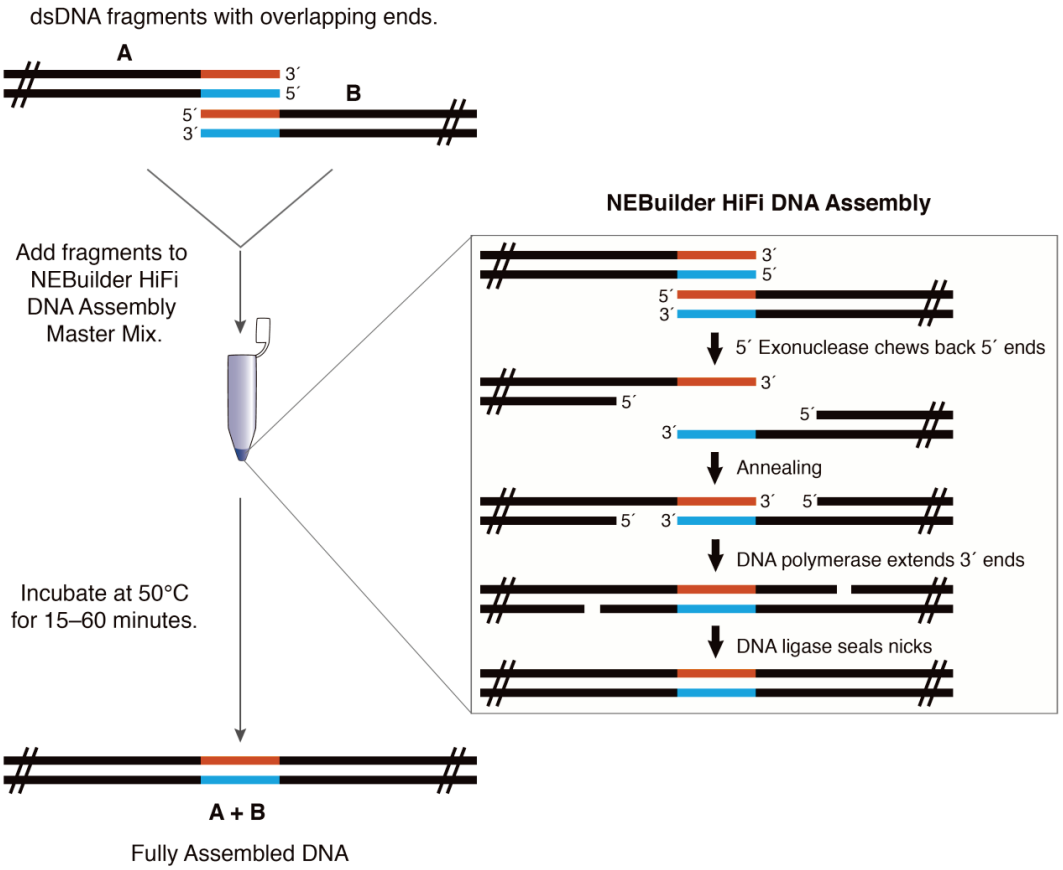

Figure 10: Schematic illustration of HiFi DNA Assembly (Source: NEBuilder®HiFi DNA Assembly Master Mix instruction manual)

The following HiFi DNA Assembly Protocol was developed and used for my experiments:

1. Set up the following reaction on ice:

Component	**Volume(2–3 Fragment)**
Recommended DNA Molar Ratio	vector:insert = 1:2

Total Amount of Fragments	X µL(0.03–0.2 pmols)
NEBuilder HiFi DNA Assembly Master Mix	10 µL
Deionized H_2O	10-X µL
Total Volume	20 µL

2. Incubate samples in a thermocycler at 50 °C for 15 min (when 2 or 3 fragments are being assembled) or 60 min (when 4–6 fragments are being assembled) (**Figure 10**). Following incubation, store samples on ice or at –20 °C for subsequent transformation.
3. Transform Top-10 Competent *E. coli* cells with 10 µL of the assembled product, following the transformation protocol.

***E.coli* storage**

500 µL of the overnight bacterial culture was added to 500 µL of 100% glycerol in a 2 mL screw top tube or cryovial and gently mixed.

Endotoxin free plasmids purification

Protocols used for this part of my thesis followed the user manual of Endotoxin-free plasmid DNA purification from MACHEREY-NAGEL GmbH & Co. KG

Lentivirus preparation and storage

Lentivirus preparation and storage followed the protocol that is established and optimized in the Michael Sendtner lab.

3.3.2. Design qPCR primers for 7SK mutants detection

The 7SK mutants and 7SK shRNA detection shows as follows (**Figure 11,12**)

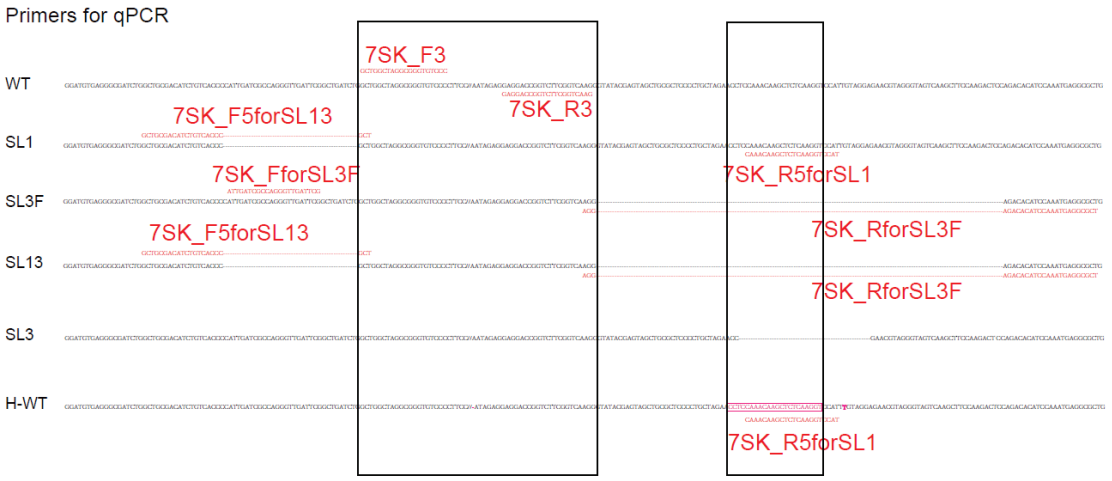

Figure 11: Primers used for detecting different 7SK mutations

3.3.3. 7SK shRNA detection by qPCR

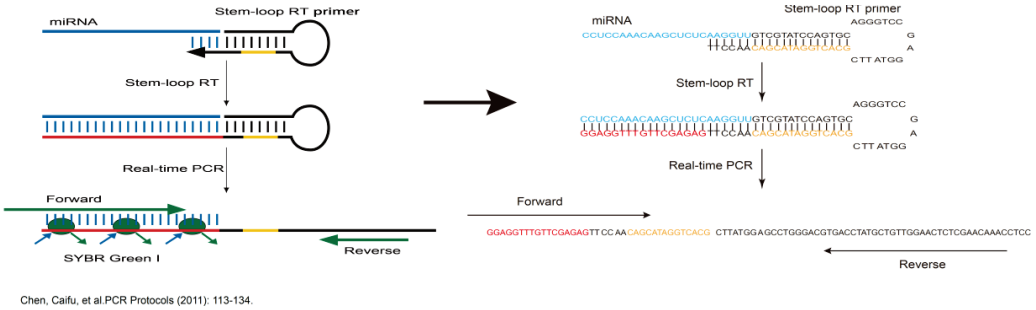

Figure 12: Schematic illustration of 7SK shRNA detection

3.3.4. Titer determination in Hela cells

1. For each 96 well, collect 20.000 cells in a total volume of 200 µL DMEM +10%FCS +1% P/S in 1st well, collect 10.000 cells in a total volume of 100 µL DMEM +10%FCS +1% P/S in 2-12 well.

Infect first well with 1µL of the supernatant, mix. Transfer 100 µL from well to well (mix by pipetting 5-10 times), creating a serial dilution in steps of 2 fold dilutions, ending up in tube #12 at a dilution of 2-12.

2. Incubate at 37 °C, 5% CO_2.

3. Check the dilutions for GFP expression/immunoreactivity (olympus) after 72 h, the last dilution where 80-100% cells are GFP gives information about the number of

infectious particles in your viral preparation as a measure of its quality (**Figure 13**).

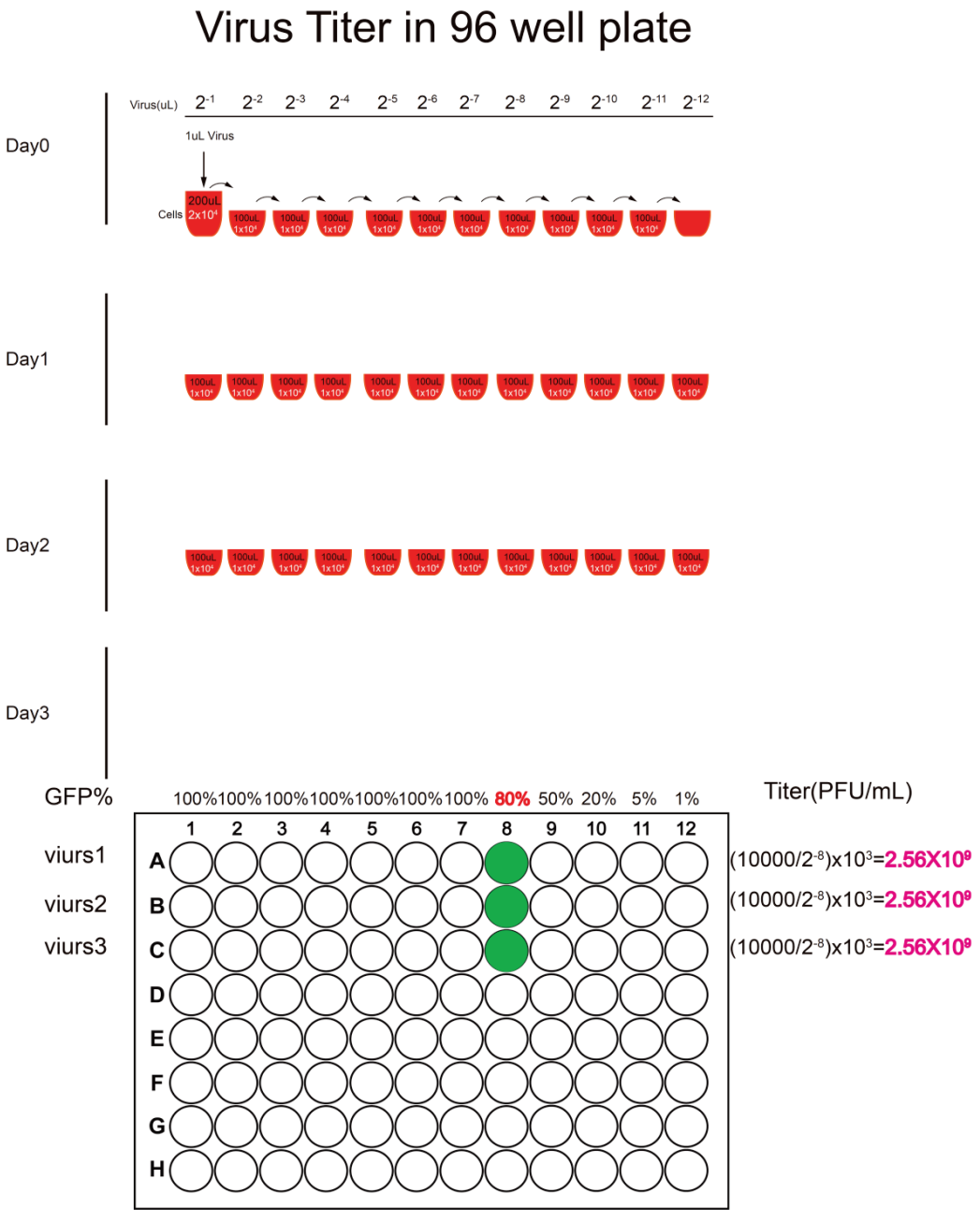

Figure 13: Flow chart of virus titration

The following protocol was used for identifying the optimal dilution of lentivirus for my experiments:

For 48 well plate, 20.000 HeLa cells were plated per well in 200 µL medium and mix with X= ((Titer/1000)/20.000)*10 µL virus.

3.3.5. Lentivirus transduction

After measuring the lentivirus titer, prepare one 24 well plate, and put 50,000 HeLa cells per well in 100 µL DMEM medium, then add virus, then keep 30 min, then add another 200 µL DMEM medium. Keep four days. Then harvest the cells for RNA extraction by using NucleoSpin RNA kit from Macherey-Nagel.

3.4. Investigation of 7SK binding to hnRNP R *in vitro*

RNA immunoprecipitation (RIP) followed by qPCR using recombinant His's-tagged hnRNP R (kindly provided by R. Sivadasan) and in vitro transcribed 7SK investigated the direct interaction between hnRNP R and 7SK.

3.4.1. Design primers for RNA *in vitro* transcription

Templates for *in vitro* transcription (**Figure 14**):

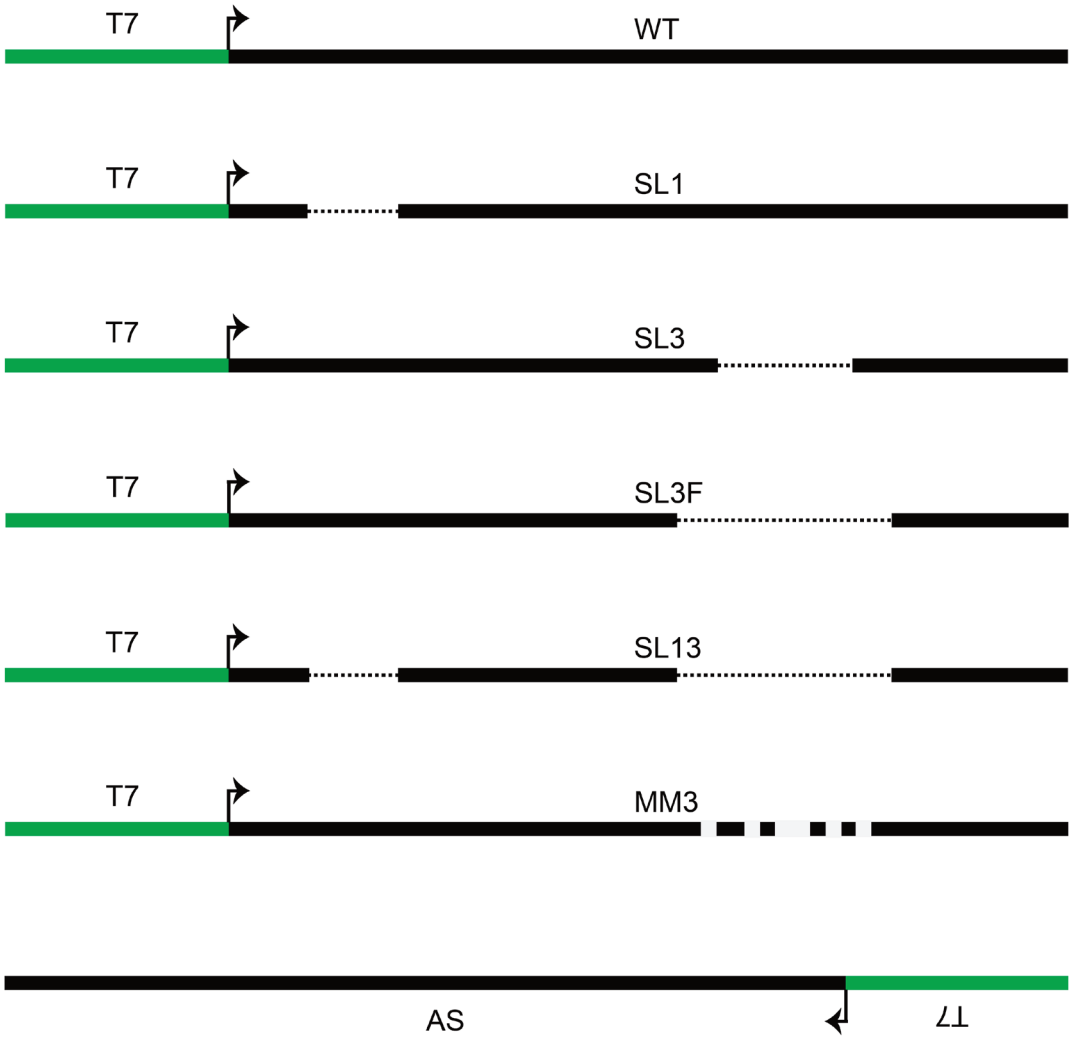

Figure 14: Schematic illustration of 7SK *in vitro* transcription

3.4.2. RNA *in vitro* transcription and purification

The following protocol was used for this part of my thesis:

1. Using PCR product as template DNA and purify the PCR product with NucleoSpin® Gel and PCR Clean-up kit from MACHEREY-NAGEL GmbH & Co. KG. Dissolve DNA in Molecular Grade Water
2. Prepare the following reaction mixture:

Component	Volume
5XTranscription buffer	10 µL
ATP/GTP/CTP/UTP Mix, 10 mM each	10 µL (2 mM final concentration)
Linear template DNA	1 µg
Thermo Scientific RiboLock RNase Inhibitor	1.25 µL (50 U)
T7 RNA Polymerase	30 U
Inorganic Pyrophosphatase (IPPase)	1 µL
Molecular Grade Water	to 50 µL

3. Incubate at 37 °C overnight.

4. Add 2 µL (2 U) of TuboDNase to remove template DNA mix and incubate at 37°C for 30 min.

5. Inactivate TuboDNase by phenol/chloroform extraction or by NucleoSpin® RNA kit from MACHEREY-NAGEL.

3.4.3. RIP-qPCR

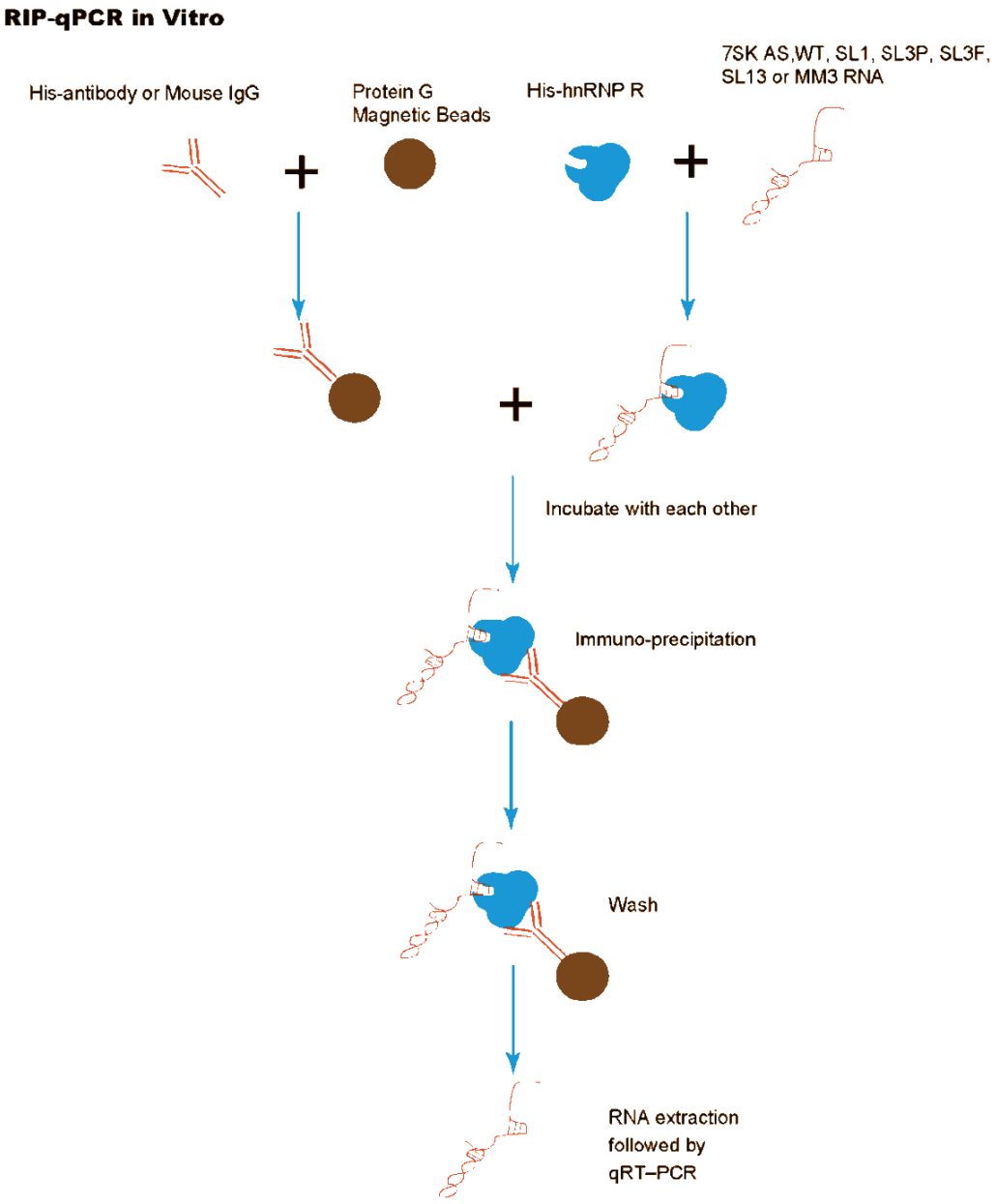

Figure 15: Schematic illustration of RIP-qPCR *in vitro*

The protocol of RIP-qPCR *in vitro* follows **Figure 15**.

7SKWT, SL1, SL3, SL3F, and SL13 are treated with TURBO DNase without purification.

1. Prepare 18 mL SA-RNP lysis buffer +1/1000 RNA +1/1000 RNAase inhibitor (for RNA dilution and washing).

2. Prepare 7SK RNA as following:

RNA	7SKWT	7SKSL1	7SKSL3P	7SKSL3F	7SKSL13
concentration(ng/μL)	0.226 ng/μL	0.205 ng/μL	0.206 ng/μL	0.162 ng/μL	0.140 ng/μL
volume(μL)	400	400	400	400	400
ribonuclear acid(V/V)	1/1000	1/1000	1/1000	1/1000	1/1000
RNAase inhibitor(V/V)	1/1000	1/1000	1/1000	1/1000	1/1000

And His-hnRNP R: 17.82 ng/μL—2500 μL in SA-RNP lysis buffer +1/1000 RA+1/1000 RNAase inhibitor

3. Prepare two tubes each add 70 μL G beads and put on the mag stand, Soak off the supernatant and add the following:

70μL G beads---1382.5 μL in SA-RNP lysis buffer +1/1000 RA+1/1000 RNAase inhibitor +17.5 μL (400ng/μL) Mouse IgG

70μL G beads---1393 μL in SA-RNP lysis buffer +1/1000 RA+1/1000 RNAase inhibitor +7 μL (1 ug/μL) anti-His

30 min .RT. rotate

4. 70 μL G beads group divide into 6 tubes, each is 200 μL

70 μL G beads group divide into 6 tubes, each is 200 μL

5. All the tubes put on the mag stand. Soak off the supernatant

Add 50 μL (17.82 ng/μL) His-hnRNP R+ 50 μL RNA [WT, SL1, SL3P, SL3F, SL13] in each tube. Cold room 30 min rotate

6. Centrifuge and put on the mag stand, soak off the supernatant

7. Wash all the beads 2 times with 1mL SA-RNP lysis buffer on the mag stand. Soak off the supernatant

8. Add 200 µL SA-RNP lysis buffer+1/1000 RA+1/1000 RNAase inhibitor +2 µL proteinase K [20 mg/mL]

9. Put on the thermomixer, 45 °C, 800 rpm, +-10 s, 2 h.

Centrifugation and put on the mag Rack, transfer the supernatant into new tubes

10. Add 200 µL Acid-Phenol: Chloroform, pH 4.5 (with IAA, 125:24:1), mix until an emulsion forms.

Input use 100 µL of RNA in SA-RNP lysis buffer

11. Spin 5 min 13.000 rpm, RT

12. Transfer the aqueous layer into a new tube.

13. Add 20 µL 3M sodium acetate,PH 5.5 ,mix ,1 µL Glyco-Blue (Ambion), then add 0.5 mL 100% Ethanol, mix.

14. Keep them in -20 °C overnight.

15. Spin 15 min 15,000 rpm at 4 °C

16. Remove supernatant and wash pellet with 0.5 mL 80% ice-cold ethanol.

17. Spin 15 min 15.000 rpm at 4 °C

18. Input pellet suspend in 10 0µL H2O

Samples pellet suspend in 20 µL H2O

Use 10 µL for reverse transcription

Step 3

19. Add

Random Hexamer	1 µL
H2O (samples)	10 µL
Total	11 µL

Transfer the supernatant in the PCR tube

20. 65 °C, 5 min, then put on ice

21. Add the following

5x reaction buffer	4 µL
RNAase inhibitor	1 µL
dNTP	2 µL
Transcriptase	2 µL

25 °C, 5 min, then 37 °C, 60 min, then 70 °C, 5 min, then 4 °C, 1 min.

22. 1:5 diluion

23. Take 2 µL for qPCR

24. Data analysis

3.4.4. Western blot

Protocol

Make separating gel as following formula in a suitable beaker. Ammonium persulfate and TEMED should be added before pouring gel.

1. Making 10% Resolving Gel (mL)

10% Resolving Gel

Final	**Component**
5 mL	Polyacrylamide. (37.5:1)
3.75 mL	1.5 M Tris-HCl(pH:8.8)
150 µL	10% SDS
150 µL	10% APS
6 µL	TEMED
5.95 mL	H2O
15 mL	Total

2. Pour the Resolving Gel

After adding ammonium persulfate and TEMED immediately mix the gel solution gently and carefully introduce the solution into the gel casting chamber. Stop the pouring when the gel solution reaches to about 6 cm height and layer about 0.5 mL isopropanol on top of the separating gel solution to keep gel surface flat. Allow the gel to polymerize within 10-30 min at room temperature.

3. Making 4% Stacking Gel (mL)

4% Stacking Gel

Final	**Component**
1.7 mL	Polyacrylamide. (37.5:1)
1.25 mL	1.0 M Tris-HCl(pH:6.8)
100 µL	10% SDS
100 µL	10% APS
10 µL	TEMED
6.8 mL	H2O
10 mL	Total

4. Pouring the stacking gel

When the gel has polymerized a distinct interface will appear between the separating gel and the isopropanol. Drain isopropanol and wash the surface with distilled water. After adding ammonium persulfate and TEMED immediately mix the gel solution gently and carefully introduce solution onto separating geL until solution reach top of the front plate. Carefully insert comb into gel until the bottom of teeth reaches the top of the front plate. Allow the gel to polymerize within 10-30 minutes.

5. Loading samples

After stacking gel has polymerized, and place the gel into the electrophoresis chamber. Add electrophoresis buffer to the inner and outer reservoir, remove comb carefully. Introduce sample solution, including molecular weight standard, into well (20-25ug total cell lysate/homogenate, unless otherwise specified).

6. Running Gel

Cover the lid and attach electrode plugs to the proper electrode. Turn on the power supply to 80V and run about 10 min. Change voltage to 160V when samples enter the stacking gel and form a single narrow line. Stop electrophoresis when dye front migrates to the bottom of the gel in about 40 min. Remove electrode plugs from electrodes and gel plates from the assembly.

7. Gel Transfer

A. Reagents and Materials

Transfer buffer 10X stock solution: 0.25M Tris, 2M Glycine. Add methanol to 20% after dilution to 1X buffer and just before use.
Blocking buffer: 5.0% non-fat dry milk in 1 X TBS, pH=7.4.
PVDF membrane

B. Equipment: Electro blotting apparatus: peQLab PerfectBlue™ 'Semi-Dry' Electro Blotter Power supply: Biometra Standard Power Pack P25.

C. Protocol

This protocol describes the steps following SDS-PAGE
.
7.1 PVDF membrane process: Cut PVDF membrane to the same size as the SDS-PAGE gel. Soak membrane sequentially in 20% methanol in 1X transfer buffer for at least 10 min.

7.2 Electro transfer
Arrange gel-membrane sandwich as described in the manufacturer's instruction. Set the power supply to 20V, 1000mA and transfer for 90 minutes at room temperature.

7.3 Blocking
a) Disconnect transfer apparatus, remove transfer cassette and transfer PVDF membrane to blocking buffer. Rock the blocking membrane on a shaker for at least 5 min at RT.
b) Follow Immunoblotting protocol as described.

7.4 Immunoblotting

A. Reagents and Materials

1X TBST

Primary antibody: In the list of antibodies for Western Blot

Secondary antibody: Goat anti-Rabbit IgG and Goat anti-Mouse IgG

Pierce™ ECL Western Blotting Substrate (Thermo Scientific™) X-ray film

B. Equipment

Rotary shaker

C. Protocol

This protocol is to be followed after Gel Transfer.

7.4.1. Primary antibodies preparation

a) The final primary antibody concentration should follow the product details for exact dilution to use.

7.4.2. Pretreat membrane: Wash the membrane in 1XTBST for 10min.

7.4.3. Primary antibodies incubation

a) Dilute the primary antibody in antibody dilution buffer to suitable antibody concentration, then shake overnight in the cold room.

7.4.4. Wash membrane: Pour off the primary antibody solution and wash membrane 3 times for 10 min each time with 1XTBST buffer.

7.4.5. Secondary antibodies incubation

a) Dilute secondary antibody in 1XTBST buffer (1:3,000 from 1mg/mL stock) and incubate with shaking for 1 h.

7.4.6. Wash membrane: Pour off primary antibody solution and wash membrane 3 times and for 15 minutes each time in 1XTBST buffer.

7.4.7. Development

a) Mix the two solutions of HRP substrate reagent in 1:1 ratio immediately prior to adding to the membrane. Incubate with the membrane for 1-3 min. Drain and remove

excess reagent and place the membrane in plastic wrap to ensure a dry surface for film exposure.

7.4.8. Exposure in darkroom

a) Exposure the membranes to X-ray film in the cassette for 1 min.

3.5. Investigation of 7SK binding to hnRNP R *in vivo*

The interaction between hnRNP R and 7SK in vivo was investigated by expressing different 7SK mutants in NSC34 cells followed by hnRNP R RIP qPCR from the cell lysate.

3.5.1. Transfection

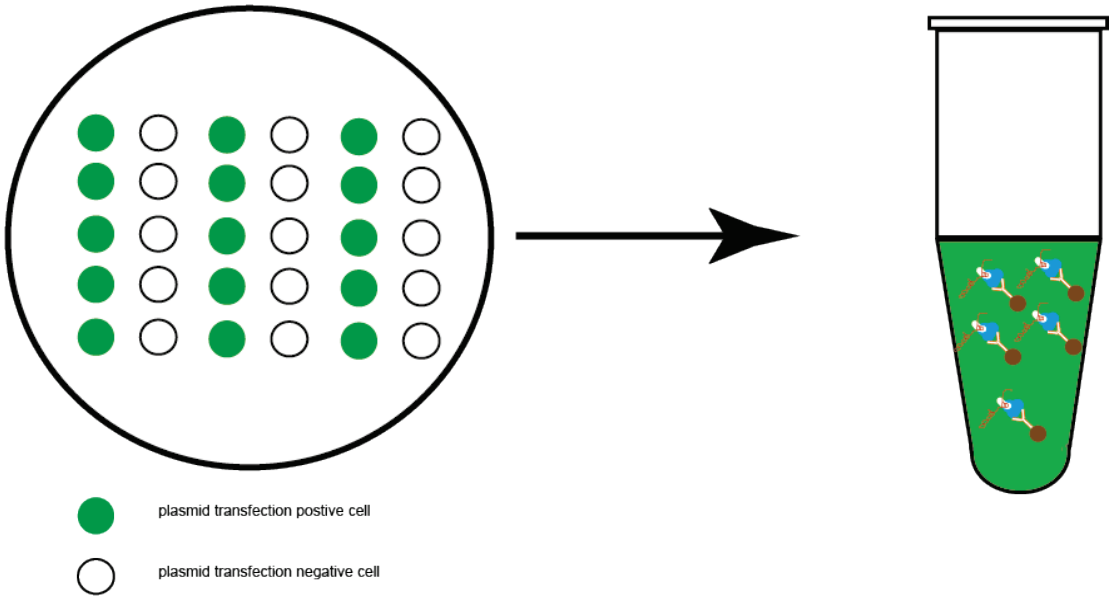

Figure 16: The schematic diagram of transfected and non-transfected NCS34 cells

Protocol:

plate	medium	cells	Plasmids	Opti-MEM	Tubofect
6 well plate	2 mL	1400.000	4 ug	400 µL	11.2 µL

1. Mix opti-MEM 400 µL, plasmids 4 ug, Tubofect 11.2 µL, then keep 20 min at room temperature.

2. Drop the mixture in the middle of each well of the 6 well plates, then add 1400.000

NSC34 cells in 2 mL DMEM. Shake the plate up and down.

3. Keep 48 h in 5% CO_2 incubator

4. Sock off the medium, wash the cells once by normal room temperature PBS, then harvest the cells by add 500 µL TrypLE.

5. Spin down the cells briefly, sock off the supernatant, then keep the cells on ice for next experiments or freeze in -80 °C.

3.5.2. RIP-qPCR

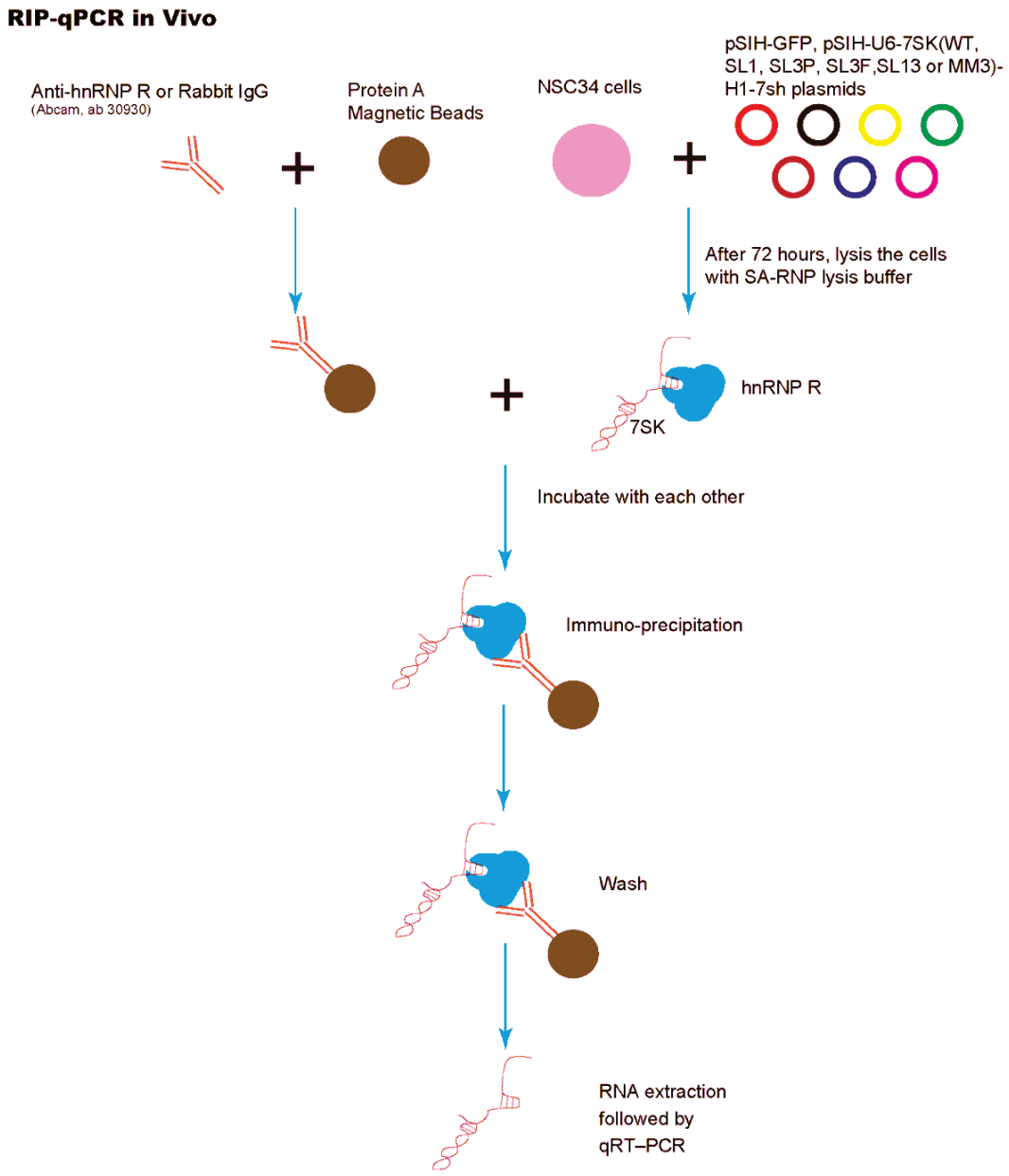

Figure 17: The schematic illustration of RIP-qPCR *in vivo*

The protocol of RIP-qPCR *in vitro* follows **Figure 17**.

Protocol:

1: Each tube adds 500 μL SA-RNP lysis buffer and pipette up and down to lysate the cells, then keep 15 min on ice.

2: 20.000 g. 15 min.4 °C

3: Transfer supernatant in a new tube, then transfer 2X200 μL into new two tubes, transfer 50μL into another new tube for RNA extraction as input, all the tubes keep on ice

9. At the same time, prepare the following:

1ug Rabbit-IgG	1ug Anti-hnRNP R (Abcam)
10μL Dyna beads A beads	10μL Dyna beads A beads
40μL 5XSA-RNP lysis buffer	40μL 5XSA-RNP lysis buffer
X μL H2O	X μL H2O
Total 200μL	Total 200μL

10. Rotate 30-40 min at room temperature.

11. Put on the magnetic stand, then suck off the supernatant.

12. Each tube adds 200μL NSC34 lysate.

13. 4°C, rotate 2 h.

14. Put on the magnetic stand, then suck off the supernatant.

15. Wash the beads 2 times by add 500μL SA-RNP wash buffer.Half for Western, half for RNA extraction.

16. RNA extraction by following the protocol of TRizol.

17. Elute the RNA in 50μL H_2O, and then take 5μL for reverse transcription.

3.6. Pull down of 7SK by using an antisense oligonucleotide

The advantage of using Biotin oligo to bind with 7SK is oligo can keep the secondary structure of 7SK, but different oligo has different affinity to bind with 7SK, so first we have to test different oligoes. Biotinylated 7SK snRNA has been used widely recently,Liu et al [22] using this method found that a unique cohort of jumonji C-domain-containing protein 6 (JMJD6) and bromodomain-containing protein 4 (Brd4) cobound distal enhancers, termed anti-pause enhancers (A-PEs), regulate promoter-proximal pause release of a large subset of transcription units via long-range interactions. Brd4-dependent JMJD6 recruitment on A-PEs mediates erasure of H4R3me2(s), which is directly read by 7SK snRNA, and decapping demethylation of

7SK snRNA, ensuring the dismissal of the 7SK snRNA/HEXIM inhibitory complex. The interactions of both JMJD6 and Brd4 with the P-TEFb complex permit its activation and pause release of regulated coding genes. However, Biotinylated 7SK snRNA has some disadvantages, such as 7SK cannot fold properly because of Biotin integrated on 7SK randomly. Therefore, this will cause a lot of nonspecific binding on 7SK snRNA.

Biotinylated anti-7SK oligo can target the 95-114 of 7SK, Luo prove that 7SK snRNA is involved in C-myc deregulation during transformation induction [80]. Yang et al used biotinylated antisense 2′ -O-methyl RNA oligonucleotide that is complementary to a region in 7SK from nucleotide 221-242 and found that 7SK small nuclear RNA inhibits the CDK9/cyclin T1 kinase to control transcription [35, 81].

3.6.1. Testing different antisense oligonucleotide for 7SK binding

I designed 10 biotinylated oligoes which can target different region of 7SK (**Figure 18**).

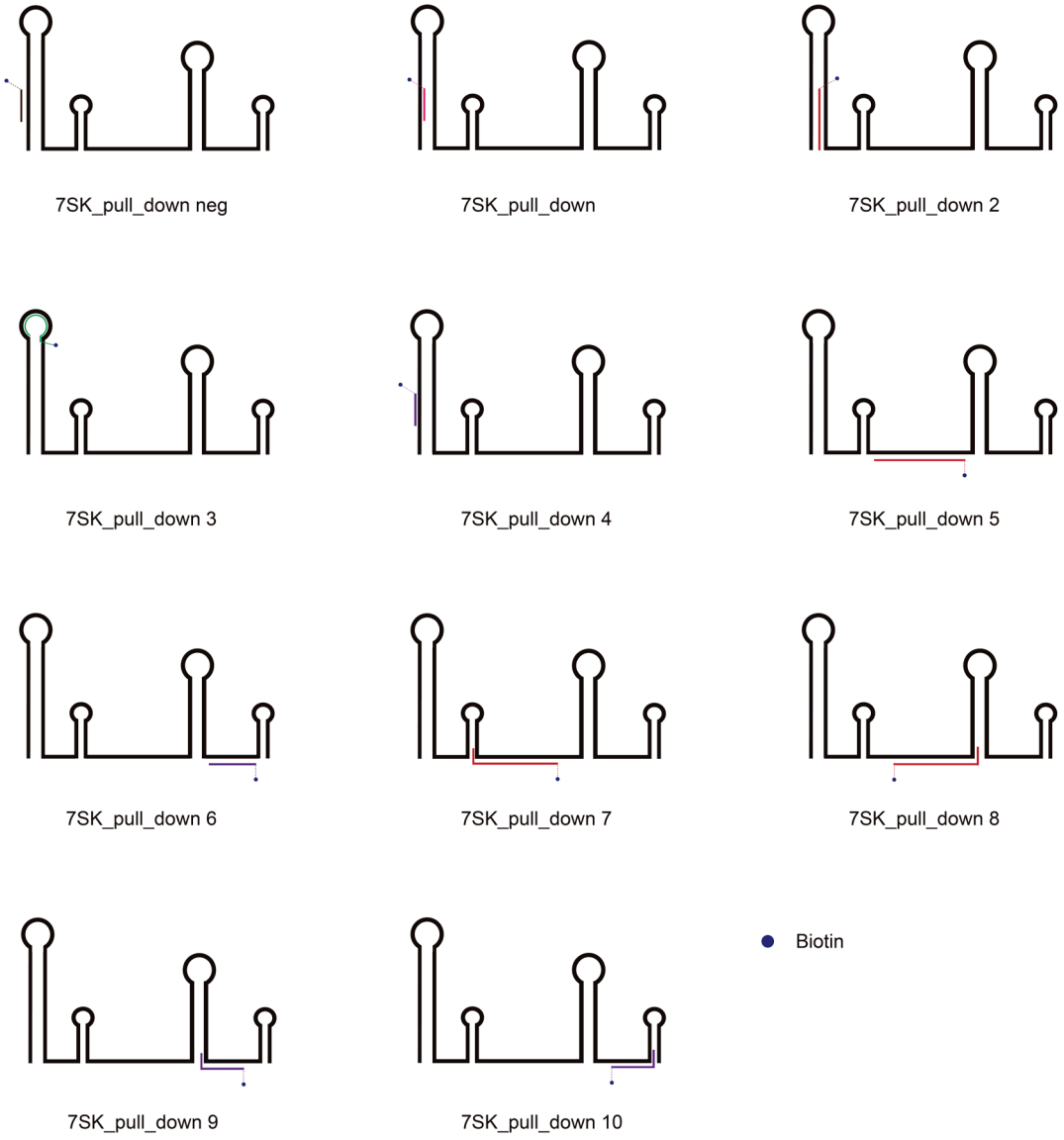

Figure 18: The schematic illustration of target region on 7SK by Biotinylated antisense oligo

Protocol

Step1

RNA in vitro transcription and purification

1. Use KAPA Hifi Hotstart Readymix (KAPA Biosystems), use pSIH plasmid as template and primer T7-7SKUP, T7-7SKDN get T7-7SKWT, use primer T7-7SKUPAS, T7-7SKDNAS get T7-7SKWTAS PCR product.

2. Purify the PCR product by NucleoSpin Gel and PCR Clean-up kit

3. RNA in vitro transcription follows the protocol of T7 RNA polymerase (20 U/μL) (thermo)

4. Add 2μL tuboDNAase in the 50μL reaction, keep 1 h in 37 °C, and purify the RNA by Nucleospin RNA kit (Macherey-Nagel)

5. Dissolve the RNA in RNAase free H_2O, Check the concentration by nanodrop.keep the RNA in -20 °C (one month) or -80 °C (one year)

Step2

Check the RNA binding on streptavidin magnetic beads

1. Take 7SKWT 2000 ng in 20 μL H_2O, keep 65 °C for 5 min, and then keep on ice for 3 min

2. Add the following:

2. 2 μL (10 pmol/μL) different Biotin oligoes

10 μL 5X SA-RNP lysis buffer

17.8 μL H_2O

50 μL total

Into each tube, keep 10 min on 37 °C, then keep on ice.

3. Each tube add 10 μL streptavidin magnetic beads and 200 μL SA-RNP lysis buffer

4. Rotate 30 min in 4 °C,

5. Put the tube on the magnetic stand, transfer the supernatant in a new tube, take 26μL supernatant into a new tube and keep on ice.

6. Wash 2x with 200 μL SA-RNP lysis buffer, take 20 μL supernatant into a new tube and keep on ice.

7. Elute the beads in the 50 μL RNA elution buffer.

8.For supernatant, wash 1 and wash 2 each tube add 26 μL 2XRNA loading buffer, then all the tubes put in 70 °C for 10 min, then keep on ice

9. Immediately run 2.5% RNAase free TBE agarose gel.400V, 6min.

3.6.2. Optimization of 7SK and antisense oligoes for *in vitro* binding

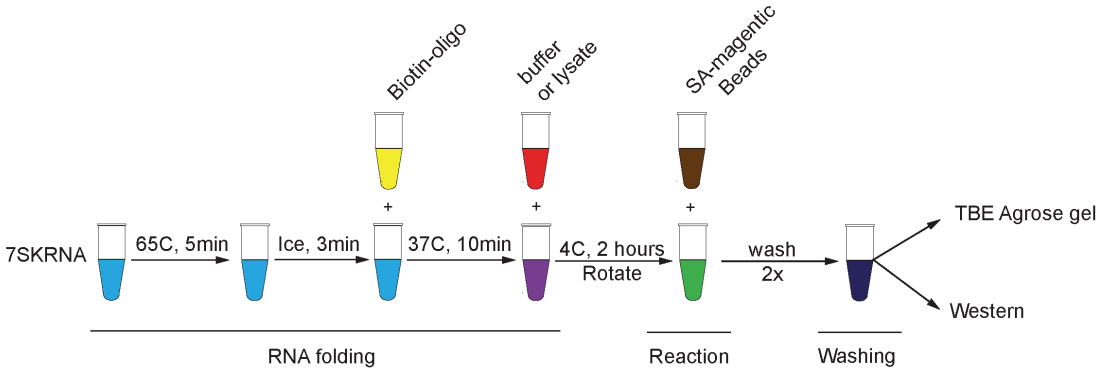

Figure 19: The flow chart of 7SK and Biotinylated antisense oligo binding to streptavidin beads

Protocol

Step1

RNA in vitro transcription and purification

1. Use KAPA Hifi Hotstart Readymix (KAPA Biosystems), use pSIH plasmid as template and primer T7-7SKUP, T7-7SKDN get T7-7SKWT, use primer T7-7SKUPAS, T7-7SKDNAS get T7-7SKWTAS PCR product.
2. Purify the PCR product by NucleoSpin Gel and PCR Clean-up kit
3. RNA in vitro transcription follows the protocol of T7 RNA polymerase (20 U/μL) (thermo)
4. Add 2 μL tuboDNAase in the 50 μL reaction, keep 1 h at 37 °C, and purify the RNA by Nucleospin RNA kit (Macherey-Nagel)
5. Dissolve the RNA in RNAase free H_2O, Check the concentration by nanodrop.keep the RNA in -20 °C (one month) or -80 °C (one year)

Step2

Check the RNA binding on streptavidin magnetic beads

1. Take

7SKWT RNA 0 ng, 2000 ng, 5000 ng, 10000 ng

In 20 μL H_2O, keep 65° C for 5 min, then keep on ice for 3 min

2. Add the following:

0 μL, 2.2 μL, 5.3 μL, 11 μL (10 pmol/μL) Biotin-TEG-Short-PD5

10 μL 5X SA-RNP lysis buffer

17.8 µL H2O
50 µL total
Into each tube, keep 10 min on 37 °C, then keep on ice.
3. Each tube add 10 µL streptavidin magnetic beads and 200 µL SA-RNP lysis buffer
4. Rotate 30 min in 4 °C,
5. Put the tube on the magnetic stand, transfer the supernatant in a new tube, take 26 µL supernatant into a new tube and keep on ice.
6. Wash 2x with 200µL SA-RNP lysis buffer, take 20 µL supernatant into a new tube and keep on ice.
7. Elute the beads in the 50 µL RNA elution buffer.
8. For supernatant, wash 1 and wash 2 each tube add 26 µL 2XRNA loading buffer, then all the tubes put in 70 °C for 10 min, then keep on ice
9. Immediately run 2.5% RNAase free TBE agarose gel.400 V, 6 min.

3.6.3. Optimization of NCS34 lysate for pulling down 7SK interactors

The protocol follows "3.4.2"

3.7. 7SKWT, SL3P but not SL1, SL3F, SL13 binds to pTEFb *in vivo*

For testing 7SK and 7SK different mutation forms binds CDK9, cyclinT1 *in vivo.*First, I did 7SK and antisense oligoes bind to streptavidin magnetic beads *in vitro, then* the next step do the western.

3.7.1. Binding 7SK mutations by using antisense oligos

Protocol

Step1

RNA in vitro transcription and purification
1. Use KAPA Hifi Hotstart Readymix (KAPA Biosystems), use pSIH plasmid as template and primer T7-7SK UP, T7-7SK DN get T7-7SK WT, T7-7SK SL1, T7-7SK SL3, T7-7SK SL3F, T7-7SK SL13, T7-7SK MM3 PCR product, use primer T7-7SK UP AS, T7-7SK DN AS get T7-7SK WT AS PCR product.
2. Purify the PCR product by NucleoSpin Gel and PCR Clean-up kit

3. RNA in vitro transcription follows the protocol of T7 RNA polymerase (20 U/μL) (thermo)

4. Add 1 μL tuboDNAase in the 50 μL reaction, keep 30 min in 37 °C, and purify the RNA by Nucleospin RNA kit (Macherey-Nagel)

5. Dissolve the RNA in RNAase free H_2O; Check the concentration by nanodrop.keep the RNA in -20 °C or -80 °C.

Step2

Check the RNA binding on streptavidin magnetic beads

1. Take

RNA	7SKWTAS	7SKWT	7SKSL1	7SKSL3P	7SKSL3F	7SKSL13	7SKMM3
ng	2000 ng	2000 ng	1812 ng	1820 ng	1432 ng	1240 ng	2000 ng

In 20 μL H_2O, keep 65 °C for 5 min, then keep on ice for 3 min

2. Add the following:

2.2 μL (10 pmol/μL) Biotin-TEG-Short-PD5 (for 7SK AS need 2.2 μL (10 pmol/μL) Biotin-TEG-Sense 5)

10 μL 5X SA-RNP lysis buffer

17.8 μL H2O

50 μL total

Into each tube, keep 10 min on 37 °C, then keep on ice.

3. Each tube adds 10 μL streptavidin magnetic beads and 200 μL SA-RNP lysis buffer.

4. Rotate 30 min in 4°C,

5. Put the tube on the magnetic stand, transfer 26 μL supernatant in a new tube, 2XRNA loading buffer, and keep on ice.

6. Wash 2x with 200 μL SA-RNP lysis buffer

7. Elute the beads in the 50 μL RNA elution buffer.

8. Put the supernatant and beads in 70 °C for 10 min, and then keep on ice

9. Immediately run 2.5% RNAase free TBE agarose gel. 400 V, 6 min.

3.7.2. Western blot

Protocol

The protocol same as section“3.2.4”

1. After the RNA binding with the oligoes, add 200 µL NSC34 lysate in each tube.
2. Rotate 2 h in 4 °C,
3. Each tube add 10 µL streptavidin magnetic beads
4. Rotate 30 min in 4 °C.
5. Put the tube on the magnetic stand.
6. Wash 2x with 200 µL SA-RNP wash buffer.
7. Elute the beads in the 60 µL 1xlaemmli buffer.
8. Divide into 3 tubes each, take one tube for western.

3.8. Pull down 7SK/hnRNPs complex by Biotin-labeled RNA oligo

3.8.1. Biotin oligo screen for 7SK binding *In vivo*

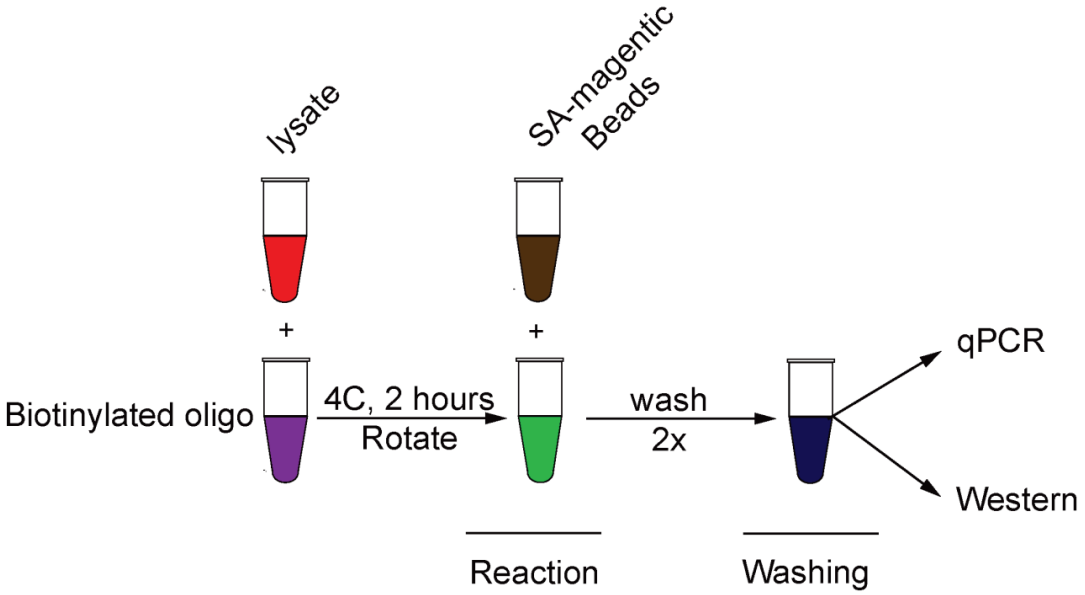

Figure 20: The flow chart of pulling down endogenous 7SK by Biotinylated antisense oligo

Protocol

Step1: NSC34 lysate preparation

1. Take 3 NSC34 pellets (one 10 cm dish is one pellet) from -80°C.
2. Keep on ice for 5 min, then to each add 1 mL SA-RNP lysis buffer, dissociate the cells and transfer into the new tube for 15 min on ice.
3. 20.000 g, 15 min, 4 °C.
5. Transfer the supernatant into a new tube and keep on ice.

Step2: Biotinylated oligo preparation

Dilute Biotin oligo, 2, 3, 4, 5, 6, 7, 8, 9, and 10 into 10 pmol/µL and keep on ice.

7. Preparing 11 tubes, each tube adds 200 µL NSC34 lysate.
8. The first tube adds 5 µL H_2O, the next tubes add 5 µL each oligo.
9. Rotate 2 h in 4 °C,
10. Each tube add 10 µL streptavidin magnetic beads
11. Rotate 30 min in 4°C.
12. Put the tube on the magnetic stand.
13. Wash 2x with 200 µL SA-RNP lysis buffer.
14. Elute the beads in 20 µL H2O.
15. Extract RNA by TRIZOL.

3.8.2. Optimization oligo, beads, lysate for 7SK binding *In vivo*

After confirming Biotin oligo RNA 4 has the highest efficiency, design a negative control oligo which does not bind 7SK.

Protocol

Step1: NSC34 lysate preparation

1. Take 3 NSC34 pellets (one 10 cm dish is one pellet) from -80°C.
2. Keep on ice for 5 min, then to each add 1 mL SA-RNP lysis buffer, dissociate the cells and transfer into the new tube for 15 min on ice.
3. 20.000 g, 15 min, 4 °C.
4. Transfer the supernatant into a new tube and keep on ice.

Step2: Biotinylated oligo preparation

Dilute Biotin oligo scr 4, Biotin oligo PD4 into 10 pmol/µL and keep on ice.

5. Prepae 5 tubes, To the 1, 2, 3 tubes add 1600 µL NSC34 lysate, to the 4, 5 tubes add 200 µL NSC34 lysate.
6. Tube 1 add nothing, tube 2 and tube 4 add 5 µL Biotin oligo scr4, and tube 3 and tube 5 add 5 µL Biotin oligo PD4.
7. Rotate 2 h in 4 °C,
8. Each tube add 10 µL streptavidin magnetic beads

9. Rotate 30 min in 4 °C.
10. Put the tube on the magnetic stand.
11. Wash 2x with 200 µL SA-RNP lysis buffer.
12. Elute the beads in 20 µL H2O,
13. Do western or extract RNA by TRIZOL.

3.9. Digitonin mediated fractionation in NSC34 cells

Fractionation on cell line is a very useful technique to investigate the cytosolic particles and nuclear particles; it can study how proteins or RNAs are transported or shuttled between nuclear and cytoplasm. Furthermore, it can also study the RNP complex alteration in the cytosolic and nuclear fraction.

A different detergent has been used for fractionation, such as Triton X-100 [82], the method which they used in the paper has some problems: one is the Triton X-100 can break the organelle membrane and nuclear membrane, so it is difficult to get a pure cytosolic fraction. Another problem is the cells are harvested and released from the dish or the flask, the cellulars compartment in the cytosolic fraction and the nuclear fraction will change a lot. Such as some proteins and RNAs should stay in the nucleus, then they will transfer to cytosolic fraction, and vice versa.

NP40 [83] wasused in this paper, maybe low concentration of NP40 is a good choice for breaking the cell membrane, but this method still has some defects: the organic compartment with cytosolic fraction will mix up. So when studying the organelles or the cytosolic compartment functions, there will be some contamination between each other.

Anyway, Triton X-100 or NP40 both have some defects, so we use digitonin instead for separating pure cytosolic fractions without organelles and nuclear fraction contamination (**Figure 21**).

Another advantage of this method is that we treat the cell with digitonin directly on the dish, so the cell has the smallest destroy and can keep its integrity.

Overall, digitonin is the best choice so far for us.

Digitonin is one of the mildest detergents, which makes the cell membrane solublization. However, without destruction the organelles and nuclear membrane, in

this case only the cytosolic fraction can be separated.

Detergent	MW (Da) monomer	MW (Da) micelle	CMC (mM) 25°C	Aggregation No.	Cloud Point (°C)	Avg. Micellar Weight	Strength	Dialyzable	Applications
SDS	289	18,000	7-10	62	>100	18,000	Harsh	Yes	Cell lysis, Electrophoresis, WB, hybridization
Triton X-100	625	90,000	0.2-0.9	100-155	65	80,000	Mild	No	Enzyme immunoassays, IP, Membrane solubilization
CHAPS	615	6,150	6	10	>100	6,150	Mild	Yes	IEF, IP
NP-40	680	90,000	0.059		45-50		Mild	No	IEF
n-dodecyl-β-D-maltoside	511		0.15	98		50,000			Protein Crystallization
Tween-20	1228		0.06		76		Mild	No	WB, ELISA, Enzyme immunoassays
Digitonin	1229	70,000	<0.5	60		70,000	Mild	No	Membrane solubilization

Figure 21: Properties and main applications of common detergents. Information from the University of Florida, BCH6206. WB, western blotting; IP, immunoprecipitation; IEF, isoelectric focusing; (https://www.labome.com/method/Detergents-Triton-X-100-Tween-20-and-More.html)

3.9.1. Digitonin concentration optimization for fractionation

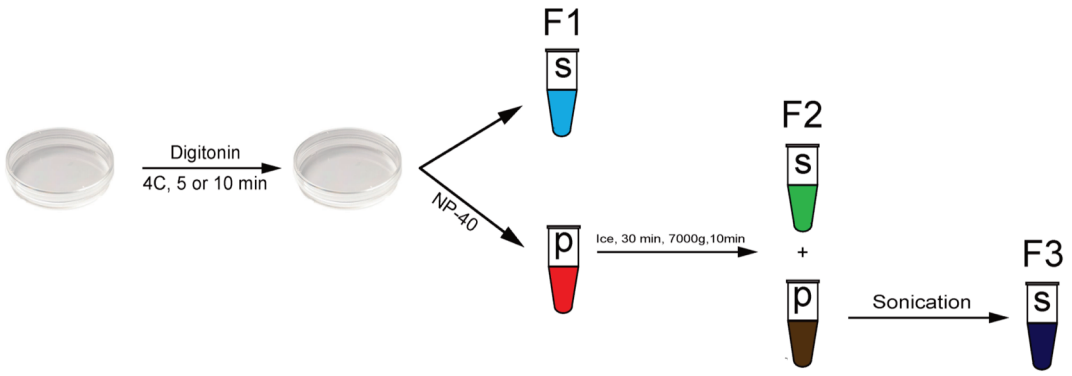

F1: cytosolic
F2: organelles, nuclear soluble
F3: nuclear insoluble

Buffer F1	
HEPES pH7.0	10 mM
KCl	100 mM
MgCl2	5 mM
Digitonin	x µg/ml

Buffer F2/3	
HEPES pH7.0	10 mM
KCl	100 mM
MgCl2	5 mM
NP-40	0.5%

Figure 22: Schematic illustration of cell fractionation by Digitonin for NSC34 cells

Regent

1. Digitonin stock solution:5 mg/mL in super clean water.
(Put the solution in 99°C for 2 min before aliquot, then aliquot into 100 µL each, freeze in –20°C avoid of light).

2. Polysome lysis buffer A: 10 mM HEPES-KOH; 100 mM KCl, 5 mM $MgCl_2$. pH7.0.
3. Polysome lysis buffer B: 10 mM HEPES-KOH; 100 mM KCl, 5 mM $MgCl_2$, 0.5% NP40.

Protocol

1. Prepare 800.000 NSC34/well in 12 well plates in 2 mL DMEM medium.
2. Keep 1 day.
3. Wash once with ice-cold DPBS(thermal).
4. Each well adds 600 µL ice-cold 0-250 ug/mL digitonin (before using the stock, heat in 99 °C for 1-2 min, then dilute in Polysome lysis buffer A buffer).
5. Keep in 4 °C 10 min without shaking.
6. Transfer supernatant into the tube lived with“cytoplasm fraction”
7. Then wash the cells very carefully with ice-cold DBPS once.
8. Then add 600 µL Polysome lysis buffer B in the good pipette up and down to lysis the cells, then transfer into tube labeled with“organles+nuclear soluble fraction”.
9. Keep the“organles+nuclear soluble fraction” tube on ice for 15 min, meanwhile to spindown the“cytoplasm fraction” by 2000 g,10 min, transfer the supernatant into new tube labeled with “F1”.
10. After 15 min on ice, “organles+nuclear soluble fraction” 20000 g, 15 min. then transfer the supernatant into a new tube labeled with“F2”.
11. Wash the tube once with ice-cold DPBS then add 300 µL Polysome lysis buffer B, sonication to dissociate the chromatin.labled with“F3”.
12. Load the same volume of F1, F2, and F3 for western to check Gapdh, calnexin, histone H3.

3.9.2. Testing 25 ug/mL Digitonin in 10 cm dish

Regent

1. Digitonin stock solution:5 mg/mL in super clean water.
(Put the solution in 99°C for 2 min before aliquot, then aliquot into 100 µL each, freeze in –20°C avoid of light).

2. Polysome lysis buffer A: 10 mM HEPES-KOH; 100 mM KCl, 5 mM $MgCl_2$. pH7.0.
3. Polysome lysis buffer B: 10 mM HEPES-KOH; 100 mM KCl, 5 mM $MgCl_2$, 0.5% NP40.

Protocol

1. Prepare 4.4X10^6 NSC34 cells in 10 dishes in 8 mL DMEM medium.
2. Keep 1 day.
3. Wash once with ice-cold DPBS(thermo).
4. Each well adds 4 mL ice-cold 25 ug/mL digitonin (before using the stock, heat in 99°C for 1-2 min, then dilute in Polysome lysis buffer A buffer).

4. Keep in 4 °C for 10 min without shaking.
5. Transfer supernatant into the tube lived with“cytoplasm fraction”.
6. Then wash the cells very carefully with ice-cold DBPS once.
7. Then add 4 mL Polysome lysis buffer B in the good people up and down to lysis the cells, then transfer into tube labeled with“organles+nuclear soluble fraction”.
8. Keep the“organles+nuclear soluble fraction” tube on ice for 15 min, meanwhile to spindown the“cytoplasm fraction” by 2000 g,10 min, transfer the supernatant into new tube labeled with “F1”.
9. After 15 min on ice, “organles+nuclear soluble fraction” 20000 g, 15 min. then transfer the supernatant into a new tube labeled with“F2”.
10. Wash the tube once with ice-cold DPBS then add 300 µL Polysome lysis buffer B, sonication to dissociate the chromatin.labled with“F3”.
11. Load the same volume of F1, F2, and F3 for western to check Gapdh, calnexin, histone H3.

3.9.3. Testing different time treatment by Digitonin on 10 cm dish

The protocol same as “3.9.2”, but the treatment time using 5 min or 10 min

3.10. Digitonin mediated fractionation in mouse primary motoneurons

Regent

1. Digitonin stock solution: 5 mg/mL in super clean water.
(Put the solution in 99 °C for 2 min before aliquot, then aliquot into 100 µL each, freeze in –20 °C avoid of light).

2. Polysome lysis buffer A: 10 mM HEPES-KOH; 100 mM KCl, 5 mM $MgCl_2$. pH7.0.
3. Polysome lysis buffer B: 10 mM HEPES-KOH; 100 mM KCl, 5 mM $MgCl_2$, 0.5% NP40.
Protocol

1. Prepare 400.000 motoneurons/well in 24 well plates in 1 mL neuron basal medium, Keep 7 d.
2. Wash once with ice-cold DPBS(thermo).
3. Each well adds 300 µL ice-cold 200 ug/mL digitonin (before using the stock, heat in 99 °C for 1-2 min, then dilute in Polysome lysis buffer A buffer).
4. Keep in 4 °C for 10 min without shaking.
5. Transfer supernatant into the tube, labeled with“cytoplasm fraction”.
6. Then wash the cells very carefully with ice-cold DBPS once.
7. Then add 300 µL Polysome lysis buffer B in the good pipette up and down to lysis the cells, then transfer into tube labeled with“organles+nuclear soluble fraction”.
8. Keep the“organles+nuclear soluble fraction” tube on ice for 15 min, meanwhile to spindown the“cytoplasm fraction” by 2000 g,10 min, transfer the supernatant into new tube labeled with “F1”
9. After 15 min on ice, “organles+nuclear soluble fraction” 20000 g, 15 min. then transfer the supernatant into a new tube labeled with“F2”
10. Wash the tube once with ice-cold DPBS then add 300 µL Polysome lysis buffer B, sonication to dissociate the chromatin.labled with“F3”
11. Load the same volume of F1, F2, and F3 for western to check Gapdh, calnexin, histone H3.

3.11. Proteomics

Biotinylated oligoes are used for pulling down endogenous RNA and its binding

proteins is a very useful and popμLar method [42, 84-86]. Elodie et al used Hela nuclear soluble extract as bait and incubate with 7SK antisense oligo, and check the 7SK binding proteins, some known 7SK binding proteins are found, such as Larp7, hnRNP A1, hnRNP A2/B1, hnRNP R, hnRNP Q. also some novel proteins, like RHA [42]. Sylvain et al used Hela nuclear insoluble extract as bait and incubate with 7SK antisense oligo, and check the 7SK binding proteins, little elongation complex are found is associate with 7SK. Overall, antisense oligo has been broadly used for many years and different cell line, but for pulling endogenous 7SK and its binding proteins in NSC34 cells or mouse primary motoneurons has not been investigated yet.

Protocol

Harvest NSC34 cells ● timing 30 min **the entire step should be RNAase free**

1| NSC34 cell first was growed in 10 cm dish (prepare 10 or more) in DMEM with 10% FCS, 1% P/S, 1% glutamax. Harvest the cells when the cells are 80-90% confluent.

2| Sock off the medium, wash once with warm DPBS (sigma, without $MgCl_2$, $CaCl_2$) then sock off the DPBS, add 3 mL warm TrypLE, keep 3 min in the incubator.

3| Add 5 mL warm medium then transfer in 15 mL falcon, 0.2x1000 RCF for 4 min, sock off the supernatant, wash once with ice-cold DPBS, and freeze in -80 °C.

Pull down ● timing 3 h

4| Take 8 falcon of cells and add 1 mL polysome lysis buffer-B in each tube, dissociate it by pipetting up and down, vortex a little bit and then transfer into the 1.5 mL tube, labeled with 1 2 3 4 5 6 7 8. Keep on ice for 15 min.

5| At the same time prepare 10 pmol/μL Biotin_Scramble RNA 4 and Biotin_PD RNA 4.

6| Centrifuge the lysate at 16000 g, 15 min, 4°C, then transfer (1+2), (3+4), (5+6), (7+8) tube supernatant into new 2 mL tube labeled with A B C D and keep on ice.

7| Prepare 8X1.5 mL tubes and label with

Scr4 1 2 3 4

PD4 1 2 3 4

Each Scr4 and PD4 tube add 600 µL NSC34 lysate from tube A B C D.

Scr4 1 2 3 4 tube each tube add 15 µL (10 pmol/µL) Biotin Scramble RNA 4

PD4 1 2 3 4 tube each tube add 15 µL (10 pmol/µL) Biotin_PD RNA 4.

8| Rotate 2 h at 4°C cold room.

9| each tube add 30 µL piece streptavidin magnetic beads.

10| then rotate 30 min 4°C at the cold room.

11| put the tubes on the magnetic stand, sock off the supernatant.

Wash the beads 2 times with 1mL polysome lysis buffer-B and 2 times with polysome lysis buffer-A by turning around the tube 8 times on the stand.

12| Each tube add 600 µL polysome lysis buffer-A and dissociate the beads, transfer 100 µL beads into new 1.5 mL tube, put the tubes on the stand sock off the supernatant, add 10 µL 1XLDS loading buffer in the 100 µL tube, the 500 µL tube put in the liquid N_2 and freeze in -80 °C for at least 6 months.

Silver staining ● timing 4 h

13| Sliver staining follows the protocol from Pro. Dr. Michael Sendtner lab.

3.12. Silver staining

1. Incubate the gel in Fixer (40% ethanol, 10% acetic acid, 50% H2O) for 1 hr.

2. Wash the gel in H_2O for at least 30 min. NB! Overnight washing with several changes of water will remove all acetic acid, reduce background staining and increase sensitivity.

3. Sensitize the gel in 0.02% sodium thiosulfate (0.04 g $Na_2S_2O_3$, 200 mL H_2O) for only 1 min. NB! Longer time will decrease peptide recovery from the gel.

4. Wash gel in H_2O for 3 x 20 s.

5. Incubate gel for 20 min in 4 °C cold 0.1% silver nitrate solution (0.2 g $AgNO_3$, 200 mL H_2O, 0.02% formaldehyde (add 40 µL 35% formaldehyde just before use). NB!

Staining is enhanced with cold $AgNO_3$.

6. Wash the gel in H_2O for 3 x 20 s.

7. Place the gel in a new staining tray. NB! Residual $AgNO_3$ on the gel surface and staining tray will increase background staining.

8. Wash the gel in H_2O for 1 min.

9. Develop the gel in 3% sodium carbonate (7.5 g Na_2CO_3 in 250 mL H_2O), 0.05% formaldehyde (add 125 µL 35% formaldehyde just before use). NB! Change developer solution immediately when it turns yellow. Terminate when the staining is sufficient.

10. Wash the gel in H_2O for 20 s.

11. Terminate staining in 5% acetic acid for 5 min.

12. Leave the gel at 4 °C in 1% acetic for storage. Prior to MS analysis the gel is washed in water for 3 x 10 min to ensure complete removal of acetic acid.

3.13. Simply Blue staining

1. After electrophoresis, rinse the mini-gel 3 times for 5 min with 100 mL deionized water to remove SDS and buffer salts, which interfere with binding of the dye to the protein. Discard each rinse.

2. Add a suffic'ent volume of SimplyBlue™ SafeStain (~20 mL) to cover the mini-gel, then incubate for 1 hour at room temperature with gentle shaking. Bands begin to develop within minutes. After incubation, discard the stain.

Note: The gel can be stained for up to 3 h, but after 3 h, sensitivity decreases. If you need to leave the gel overnight in the stain, add 2 mL of 20% NaCl (w/v) in water for every 20 mL of stain. This procedure will not affect sensitivity.

3. Wash the mini-gel with 100 mL of water for 1–3 h.

Note: The gel can be left in the water for several days without loss of sensitivity.

There is a small amount of dye in the water that is in equilibrium with the dye bound to the protein, so proteins remain blue.

4. To obtain the clearest background for photography, perform a second 1-hour wash with 100 mL of water

3.14. Total RNA analysis

RNA Isolation with Trizol Reagent

1 mL Trizol (using a small amount of tissue) for 50-100 mg tissue or 10^7 cells. Sample volume should not exceed 10% of the volume of Trizol.

RNA Extraction

1. Take 100 µL lysates, which used for IP after 2 h reaction, add 1 mL TRIZOL and mix well.
2. Allow 5 min incubation at room temperature.
3. Add 200 µL Chloroform/1 mL Trizol.
4. Vortex.
5. Let sit for 10 min at room temperature.
6. Centrifuge at 12000 g for 15 min at 4 µL
7. The sample will separate in 3 layers- Phase separation.
a. Top layer clear aqueous phase = RNA.
b. Middle layer white cloudy phase = DNA.
c. Bottom layer red phenol phase = protein.
8. Extract 80% of the RNA layer leaving 20% behind in the tube.
9. Transfer the 80% RNA layer to a new, labeled tube, each adds 1-2 µL glycoBlue.

RNA Precipitation

1. Add 0.5 mL isopropanol/1 mL Trizol
2. Invert tubes 5X or vortex for 10 s.
3. Let sit for 10 min at room temperature.
4. Centrifuge at 12,000 g for 10 min at 4 °C.

5. Remove supernatant by pipette (Be careful not to disturb the pellet)

RNA Wash

1. Wash with 1 mL cold 80% EtOH (20% RNase, DNase so on free molecular water).
2. Vortex pellet.
3. Centrifuge at 9,100 rpm for 5 min at 4 °C.
4. Remove supernatant using the pipette (Be careful not to disturb the pellet).
5. Allow drying at room temperature for 5 min.

Solubilization

1. Turn on heat block (low setting) to 55 °C and put water in wells
2. Dissolve RNA pellet in 30 µL H2O and mix well (15 sec).
3. Incubate 2 min at 55 °C in heat block.

Take reading

Nanodrop2000
Purity = A260/A280, Purity should be between 1.8-2.0

Run 2% TBE agarose gel

1. Prepare 2%TBE agarose gel in RNase free 1XTBE buffer.
2. Add 2 ug total RNA in 2xRNA loading dye, the total is 30 µL.
8. Incubate at 70 °C for 3-5 min. (in heat block).
9. Chill on ice (immediately) 2-3 min.
10. Run 2%TBE agarose gel at 400 V.
11. Take the picture from the gel analyzer.

3.15. Co-Immunoprecipitation

3.15.1. Co-Immunoprecipitaion in total NSC34 cells

NSC-34 cells were grown in 10 cm dishes until 80-90% confluency. Cells were

washed once with ice-cold DPBS and collected by scraping. Cells were lysed in 1 ml lysis buffer B [10 mM HEPES (pH 7.0), 100 mM KCl, 5 mM MgCl2, 0.5% NP-40] on ice for 15 min. Lysates were centrifuged at 20,000×g for 15 min at 4 °C. 10 µl Dynabeads Protein G or A (depending on the antibody species) (Invitrogen) and 1 µg antibody or IgG control were added to 200 µL lysis buffer and rotated for 30-40 min at RT. Then 200 µL lysate were added to the antibody-bound beads and rotated for 2 h at 4°C. Beads were washed twice with lysis buffer B and proteins were eluted in 1× Laemmli buffer [50 mM Tris-HCl (pH 6.8), 1% sodium dodecyl sulfate, 6% glycerol, 1% β-mercaptoethanol, 0.004% bromophenolblue]. Proteins were size-separated by SDS-PAGE and analyzed by immunoblotting. For RNase treatment, 3 µL RNase A (Thermo Fisher Scientific) were added to 200 µL lysate and incubated at 37 °C for 10 min before proceeding with co-immunoprecipitation.

3.15.2. Co-Immunoprecipitaion in fractionated NSC34 cells

For co-Immunoprecipitaion in fractionated NSC34 cells, 800 uL different fractions from NSC34 cells was used for Co-IP. For RNase treatment, 10 µL RNase A (Thermo Fisher Scientific) were added to 800 µL different fractions and incubated at 37 °C for 10 min before proceeding with co-immunoprecipitation.

3.16. Co-sedimentation assay

Protocol:

1. make 50 mL 10x polysome buffer without NP-40:

	1x	10x
HEPES pH7.0	10 mM	100 mM
KCl	100 mM	1 M
$MgCl_2$	5 mM	50 mM

2. make 4 sucrose solutions of 20 mL:

	sucrose	10x buffer	water
5%	1 g	2 mL	to 20 mL
10%	2 g	2 mL	to 20 mL
15%	3 g	2 mL	to 20 mL
20%	4 g	2 mL	to 20 mL

3. make gradients:

- Add 2.5 mL 20% sucrose solution to tube and freeze at -80 °C.
- Add 2.5 mL 15% sucrose solution to tube and freeze at -80 °C.
- Add 2.5 mL 10% sucrose solution to tube and freeze at -80 °C.
- Add 2.5 mL 5% sucrose solution to tube and freeze at -80 °C.

4. Take gradient out of -80 °C and leave at 4 °C in the fridge overnight.
5. lyse cells in polysome buffer (with NP-40) and add 500 µL lysate with a concentration of 4 ug/µL onto the gradient
6. Carefully balance the tubes and spin at 29,000 rpm for 5 h in SW 41 Ti rotor.
7. After centrifugation collect 0.5 mL fractions with pipette and analyze 20 µL of each fraction on Western.

4. Results

4.1. Cloning

In order to investigate the role of different structural elements of 7SK for its cellular function, I generated a series of rescue constructs using the lentiviral expression vector pSIH, which also included elements for suppression of endogenous 7SK. These constructs transcribe an shRNA for knockdown of endogenous 7SK and simultaneously express wild-type or mutant forms of 7SK. The mutants were designed to harbor a deletion of SL1, a partial deletion of SL3 (SL3P), a full deletion of SL3 (SL3F), a deletion of both SL1 and SL3 (SL13) or point mutations in the region targeted by the shRNA (MM3). For visualization of transduction efficiency, EGFP is expressed from the CMV promoter (**Figure 23**). Following the generation of lentiviral particles, their titer was determined by transduction of HeLa cells with serial dilutions of the viruses.

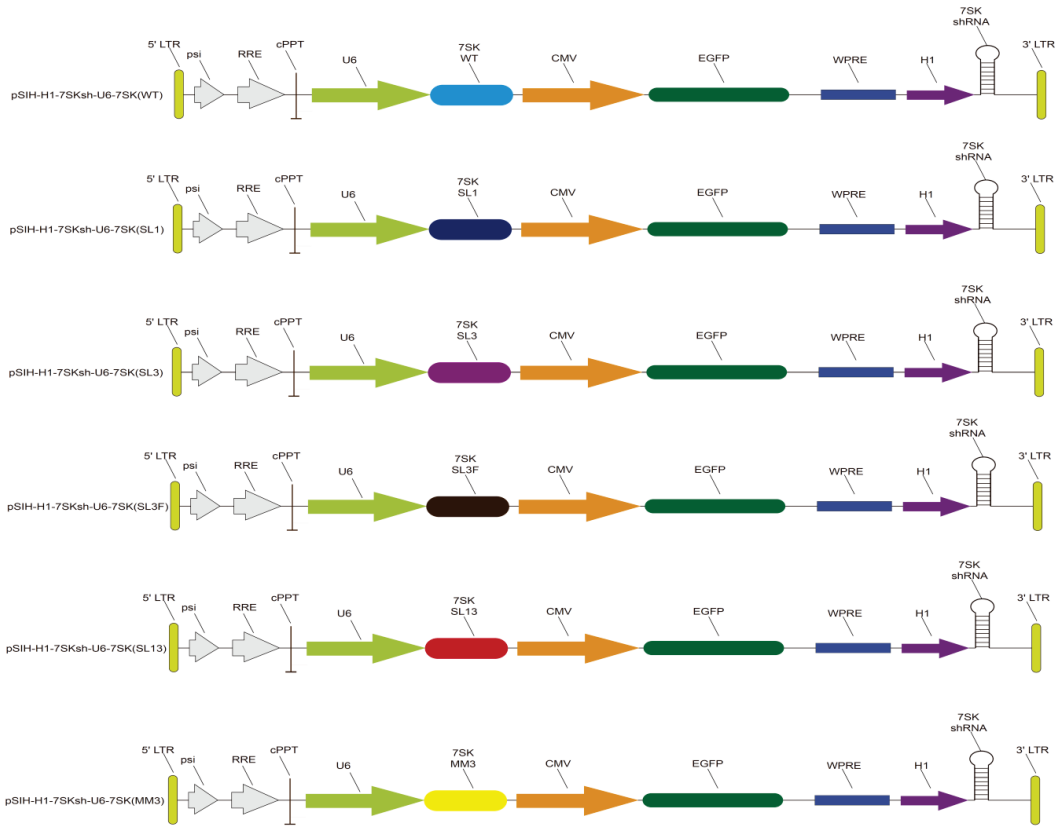

Figure 23: Schematic representation of 7SK viral rescue constructs. The plasmids express an shRNA against 7SK driven by the H1 promoter as well as 7SK wild-type or mutant forms driven by the U6 promoter. For visualization of transduction efficiency, EGFP is expressed from a CMV promoter.

4.2. Lentivirus-mediated 7SK rescue in HeLa cells

4.2.1. 7SK shRNA detection

In order to validate the functionality of the viral constructs and recombinant lentiviruses, I transduced HeLa cells with viruses expressing the 7SK shRNA alone or co-expressing 7SK SL1, SL3F and SL13. RNA was extracted from these cells and reverse-transcribed with a primer specific for the shRNA sequence. The cDNA was used for qPCR reactions and the products were resolved by agarose gel electrophoresis. As a result, all three rescue constructs (SL1, SL3F, and SL13) efficiently express the shRNA similar to the construct expressing the shRNA alone (**Figure 24**).

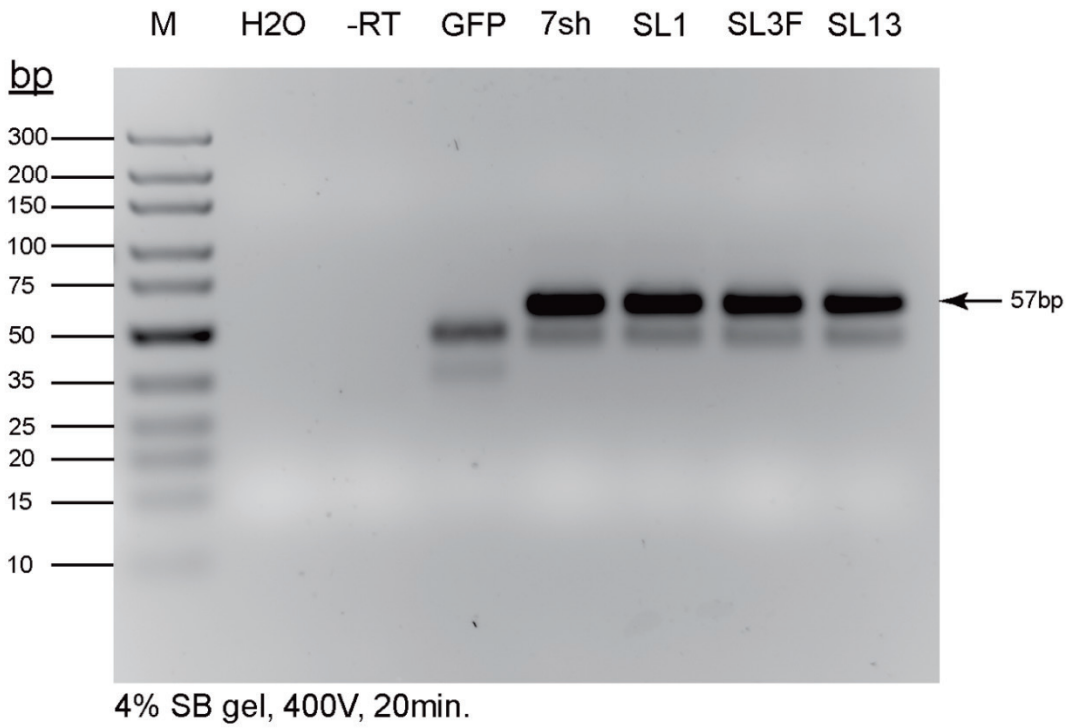

Figure 24: Gel electrophoresis in 4.0% SB agarose gel of 7SK shRNA (57 bp) to show the efficacy of 7SK shRNA expression. The 7SK shRNA (57 bp) product from qPCR of total RNA synthesized by the first strand cDNA from HeLa cells transduced with GFP, 7sh, 7SKWT+7sh, 7SKSL1+7sh, 7SKSL3F+7sh, 7SKSL13+7sh virus. Lane M, MLR DNA marker (Thermo)

4.2.2. 7SK mutation quantification by qPCR

As a next step, I quantified the total 7SK levels as well as the levels of the individual 7SK mutants in HeLa cells transduced with the lentiviruses. I found that the lentivirus expressing the 7SK shRNA alone efficiently reduced 7SK levels to 10-20% (**Figures 25 and 26**). When 7SK wild-type or mutant forms were co-expressed, total 7SK levels composed of endogenous and exogenous 7SK were similar to controls. This result shows that the lentiviral constructs can be used to efficiently knock down endogenous 7SK and replace it with different mutant forms.

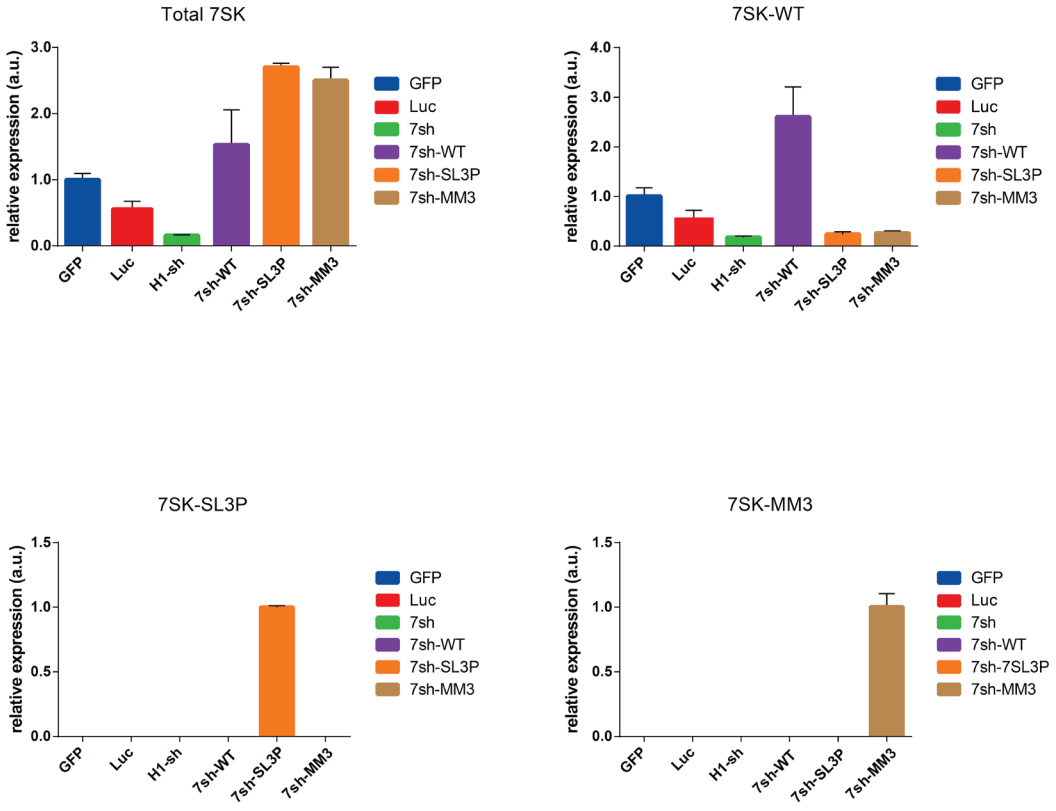

Figure 25: Bar graph showing 7SK levels following transduction with lentiviruses. Data show relative expression of total 7SK, 7SKWT, 7SK-SL3P and 7SK-MM3 following normalization to *Gapdh*.

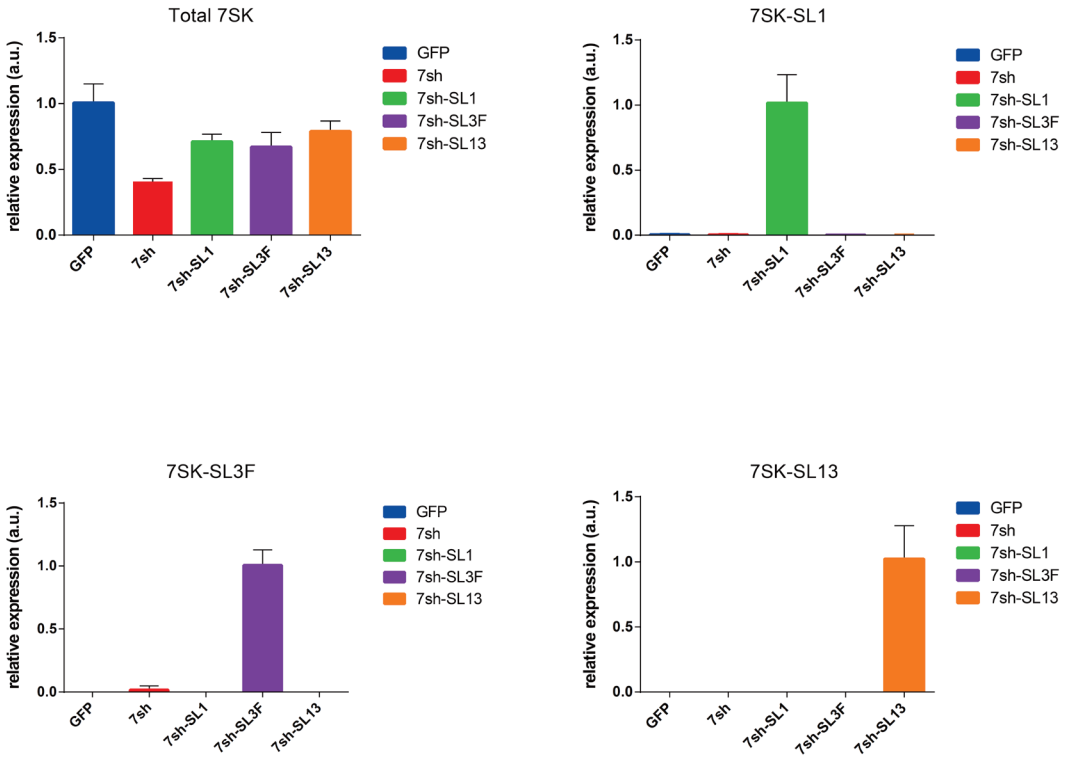

Figure 26: Bar graph showing 7SK levels following transduction with lentiviruses. Data show relative expression of total 7SK, 7SK-SL1, 7SK-3F, 7SK-SL13 following normalization to *Gapdh*.

4.3. 7SK binds hnRNP R *in vitro*

4.3.1. RNA *in vitro* transcription and purification

Analysis of the hnRNP R RNA interactome by iCLIP revealed that 7SK is the top interacting RNA and that hnRNP R crosslinking sites on 7SK are located in SL1 and SL3 regions. In order to verify that hnRNP R binds to these regions, I performed pulldown experiments in which I used recombinant His-tagged hnRNP R as bait for purification of different 7SK deletion mutants. As a first step, I generated a series of 7SK snRNA constructs in wild-type and mutant forms by *in vitro* transcription (**Figure 27**). 7SK wild-type (WT) and antisense (AS) control, 7SK harboring deletions of SL1, SL3 (partial (P) or full (F)) and both SL1 and 3 (SL13), and 7SK containing a mismatch in the region targeted by the shRNA (MM3). These 7SK mutants were the same as those previously cloned into the pSIH rescue constructs.

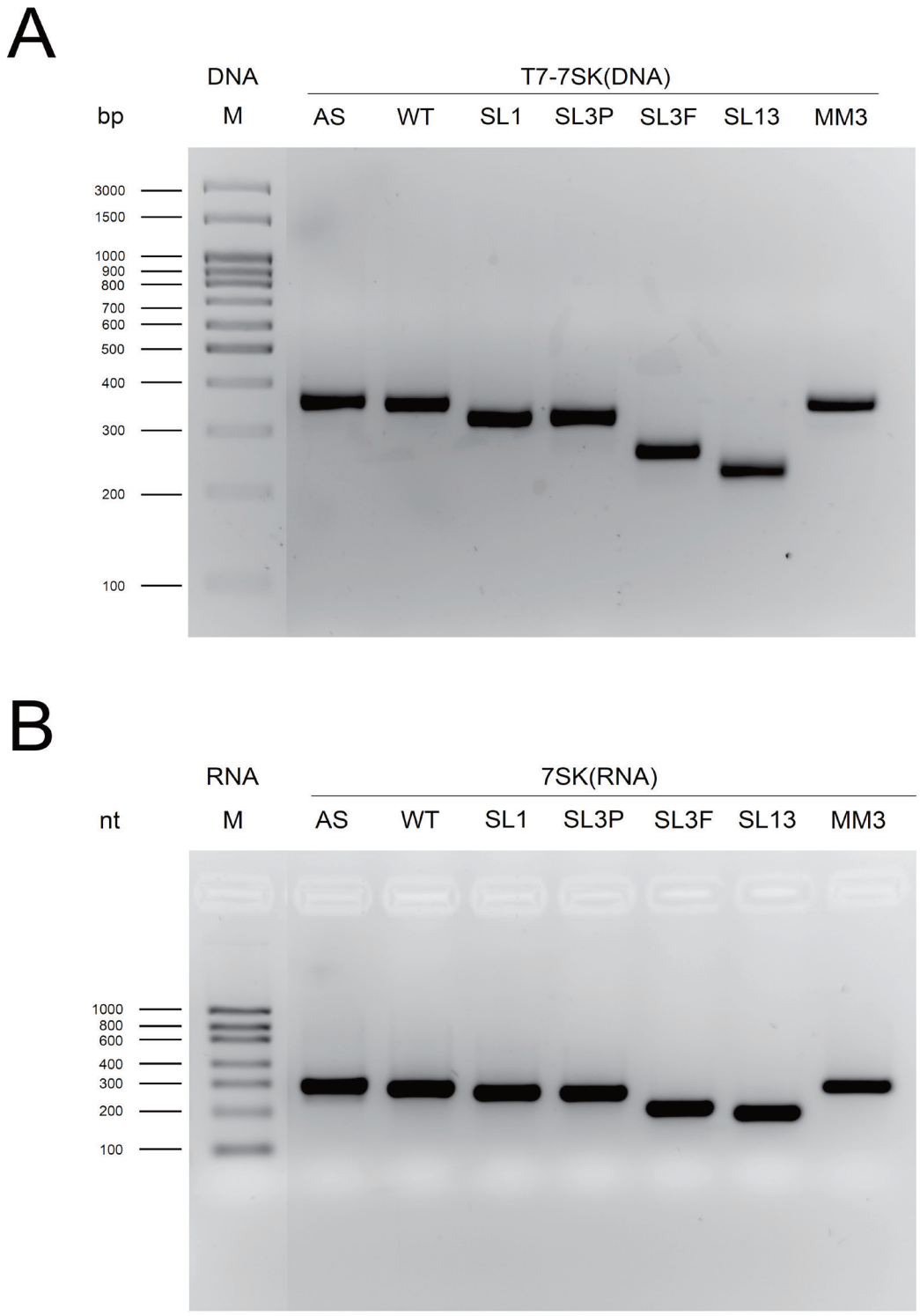

Figure 27: Gel electrophoresis in 2.5% TBE agarose gel of T7-7SK AS, WT, SL1, SL3P, SL3F, SL13, MM3 DNA, and 7SK RNA to verify altered nucleotide length of deletion constructs.

A: PCR product after purification by NucleoSpin® Gel and PCR Clean-up from

MACHEREY-NAGEL. 500 ng/each sample, Lane M, 100 bp-3000 bp DNA Rainbow Ladder from GENEON GMBH

B: 7SK RNA after purification by NucleoSpin RNA kit from MACHEREY-NAGEL. 1000 ng/each, sample, Lane M, RiboRuler Low Range RNA Ladder from Thermo Fisher.

4.3.2. His-hnRNP R protein binds on Protein G beads

As a next step, I tested the binding of His-hnRNP R on protein G beads conjugated with anti-His antibodies. As a result, I found that His-hnRNP R efficiently bound to protein G beads coated with anti-His antibody but not to beads conjugated with mouse IgG control antibodies (**Figure 28**).

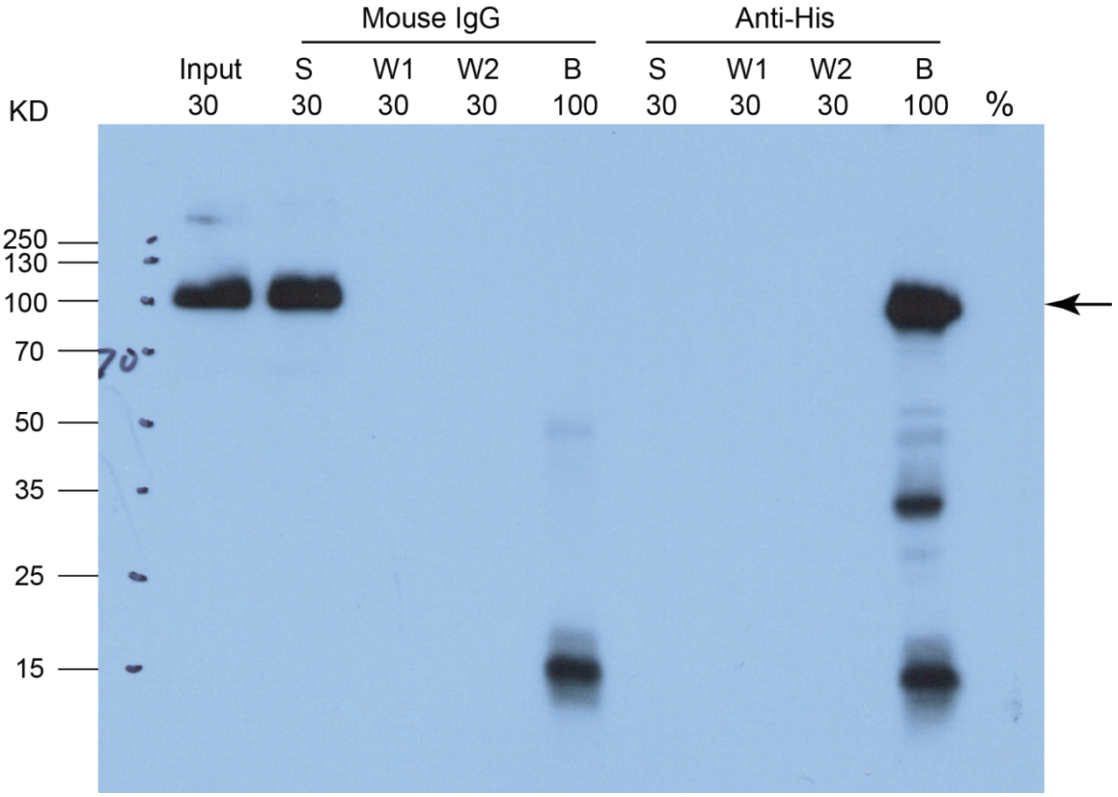

Figure 28: Western blotting shows recombinant His-hnRNP R protein binding to Anti-His antibody but not Mouse-IgG coupled Protein G Dynabeads™. Beads:10 µL, Mouse –IgG:1 ug, Anti-His antibody:1ug, recombinant His-hnRNP R protein:891 ng. Reaction volume is 200 µL. Lane M, PageRuler Prestained Protein Ladder, 10 to 180 kDa from Thermo Fisher Scientific.

In order to further control for possible interactions with the anti-His antibody or the His

peptide itself, I set up an additional control reaction in which His-hnRNP R was immunopurified with anti-His-conjugated protein G beads in the presence of an excess amount of His peptide. As a result, 5 µg of His peptide fully prevented His-hnRNP R from binding to the anti-His beads (**Figure 29**)

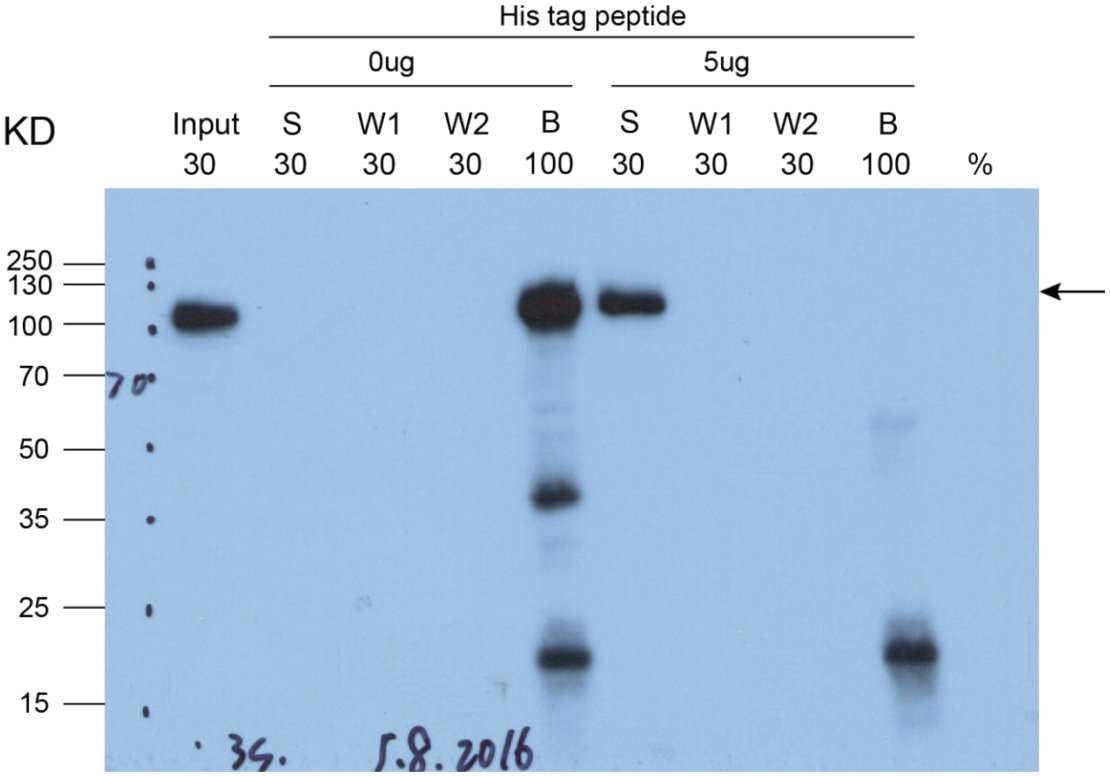

Figure 29: Western blotting shows recombinant His-hnRNP R protein binding with or without His-tag peptide treated Anti-His antibody coupled Protein G Dynabeads™. Beads:10 µL, Anti-His antibody:1 ug, His-tag peptide: 0 ug or 5 ug. recombinant His-hnRNP R protein:891 ng.
Reaction volume is 200 µL. Lane M, PageRuler Prestained Protein Ladder, 10 to 180 kDa from Thermo Fisher Scientific.

4.3.3. RIP-qPCR

After having optimized binding of His-hnRNP R to beads I set up pull down reactions by incubating beads bound to His-hnRNP R or respective controls with 7SK WT or AS. I found that 7SK WT was efficiently co-purified by His-hnRNP R bound to beads through anti-His, but not in control reactions containing mouse IgG or anti-His antibody with an excess of His peptide (**Figure 30**). In contrast to 7SK WT, binding of its antisense version to His-hnRNP R was significantly reduced. This result indicates that 7SK directly interacts with hnRNP R.

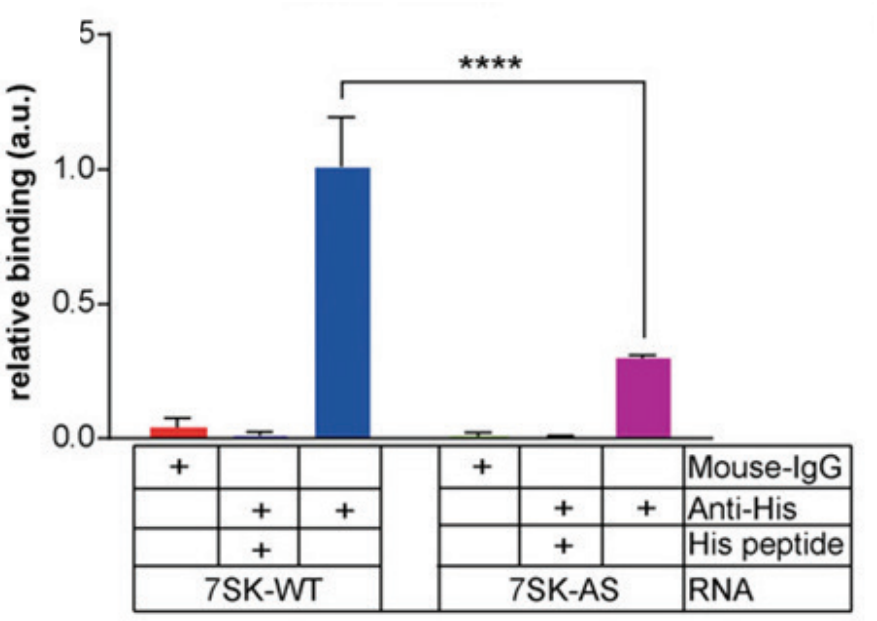

Figure 30: RNA immunoprecipitation of hnRNP R *in vitro* binding reactions containing recombinant His-tagged hnRNP R and either 7SK snRNA (7SK-WT) or its antisense version (7SK-AS) as the negative control. To control for the specificity of the immunoprecipitation, mouse IgG antibody was used or an excess of His peptide was included in the hnRNP R immunoprecipitation.

I also evaluated the propensity of the 7SK deletion mutants to interact with His-hnRNP R. I found that deletion of either SL1 or 3 alone or in combination significantly reduced the ability of 7SK to interact with hnRNP R (**Figure 31**). Therefore, this finding is in agreement with the notion that the hnRNP R crosslinking sites in SL1 and SL3 identified by iCLIP represent the hnRNP R binding sites on 7SK.

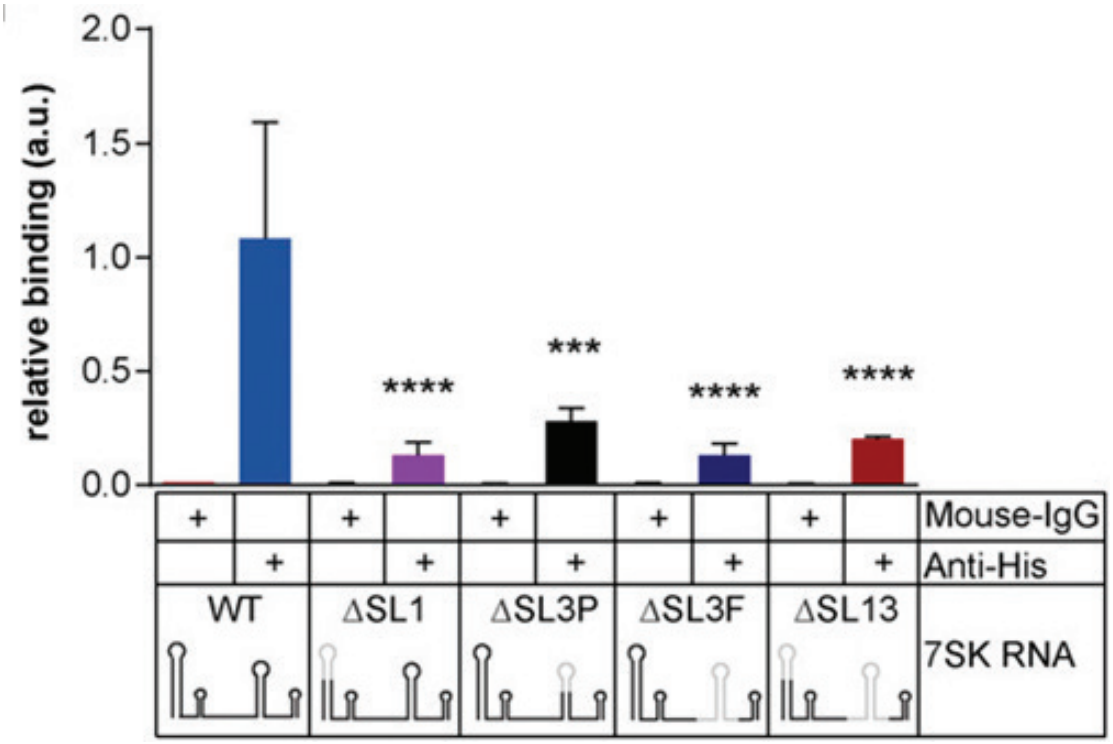

Figure 31: RNA immunoprecipitation of hnRNP R *in vitro* to investigate binding of 7SK deletion mutants to hnRNP R

Binding reactions containing recombinant His-tagged hnRNP R and 7SK snRNAs harboring the indicated mutations. A schematic representation of the 7SK snRNAs is shown with deleted regions depicted in gray. Data in D–F are mean ± SD; **P ≤ 0.01, ***P ≤ 0.001, ****P ≤ 0.0001; two-way ANOVA with Tukey's multiple comparisons test.

4.4. 7SK binds hnRNP R *in vivo*

After having shown that hnRNP R binds to 7SK *in vitro*, next I investigated their interaction *in vivo*.

For this purpose I immunoprecipitated endogenous hnRNP R from NSC34 cells transfected with the pSIH plasmids for knocking down endogenous 7SK and simultaneously overexpressing the 7SK mutants described above. Since transfection efficiency in NSC34 cells is ~50% half of the cells are transfected and express mutant 7SK whereas the other half are non-transfected expressing endogenous 7SK. Therefore, the interaction of hnRNP R with endogenous 7SK from non-transfected cells serves as an internal control for the efficiency of the RNA immunoprecipitation procedure.

Following immunoprecipitation, hnRNP R was detectable in the eluate when anti-hnRNP R antibody was used for purification but not when rabbit IgG was used (control) (**Figure 32**). RNA extraction from the eluates to detect bound RNAs revealed that hnRNP R efficiently co-immunoprecipitated endogenous 7SK (**Figure 33**). In contrast, 7SK mutants were co-immunoprecipitated significantly less compared to endogenous 7SK. Whilst deletion of SL1 (SL1 and SL13 mutants) and full deletion of SL3 (SL3F) completely abolished binding to hnRNP R, partial deletion of SL3 (SL3P) and mismatch mutations (MM3) still partially retained their binding ability to hnRNP R. This result, therefore, agrees with the in vitro binding assay in that both SL1 and SL3 of 7SK are critical for its interaction with hnRNP R under these conditions. The ability of the SL3P mutant to interact with hnRNP R *in vivo* but not *in vitro* might indicate that additional proteins modify the strength of interaction of hnRNP R with SL3 in cells.

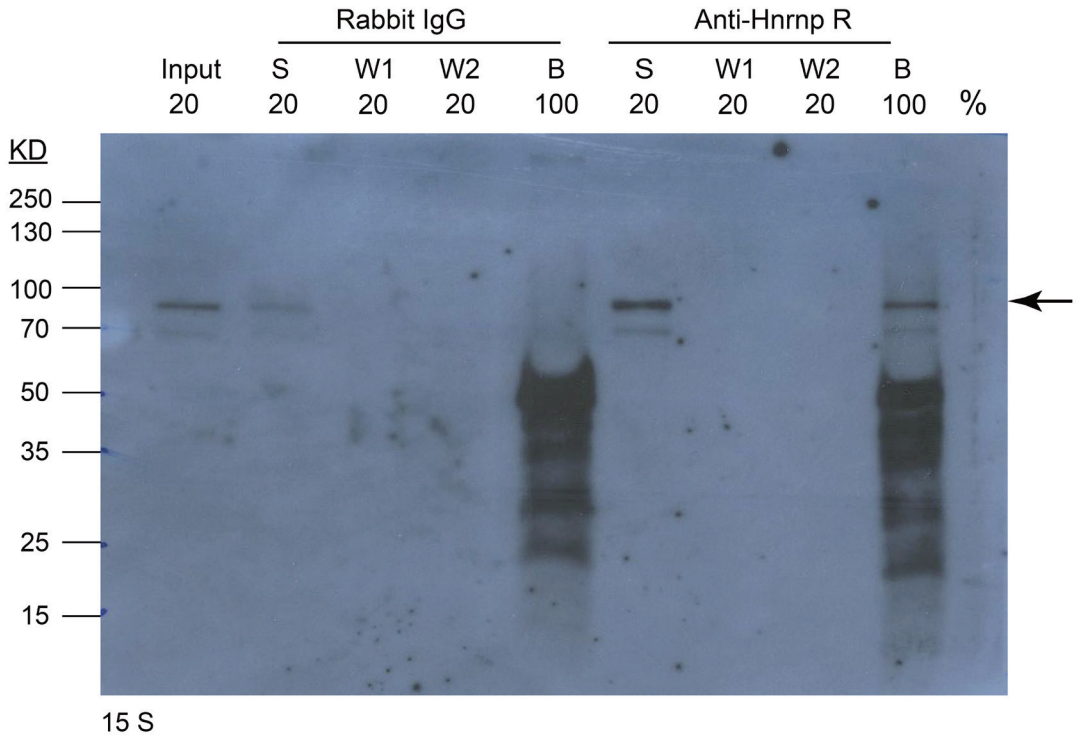

Figure 32: Western blotting shows hnRNP R antibody from Abcam which recognizes C-terminus of Human hnRNP R for pulling down endogenous hnRNP R from NSC34 lysate. Beads:10 µL, Rabbit–IgG:1 ug, Anti- hnRNP R antibody:1 ug, NSC34 lysate:1/5 10 cm dish. Reaction volume is 200 µL. Lane M, PageRuler Prestained Protein Ladder, 10 to 180 kDa from Thermo Fisher Scientific.

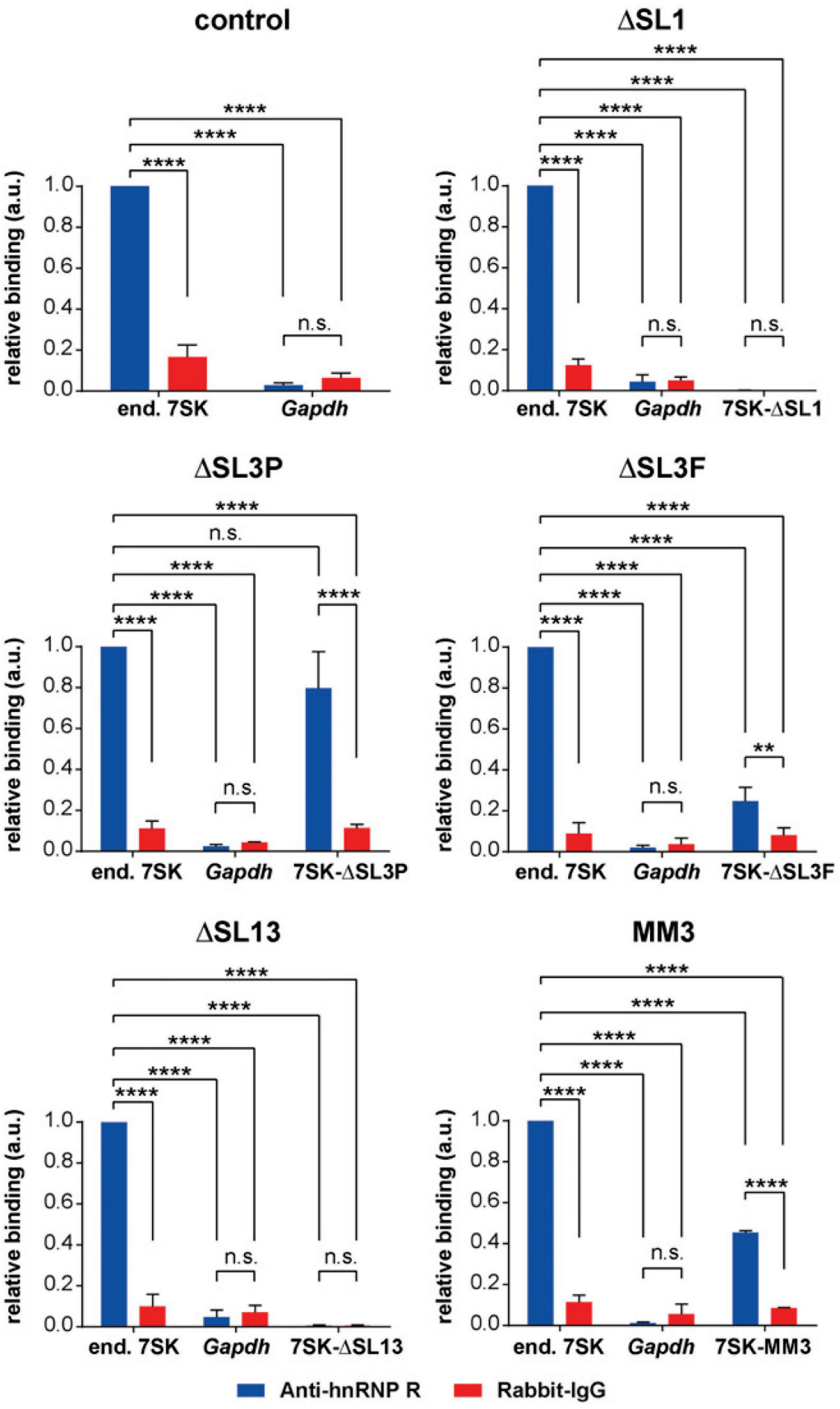

Figure 33: Interaction of hnRNP R with 7SK *in vivo*

qPCR analysis of 7SK mutants co-precipitated by anti-hnRNP R or IgG control from NSC-34 cells transfected with 7SK expression plasmids.

RNA immunoprecipitations of hnRNP R from lysates of NSC34 cells transfected with expression constructs for knocking down endogenous 7SK and overexpressing wild type or mutant 7SK. As control, the empty plasmid was used. To control for the specificity of the immunoprecipitations, rabbit IgG antibody was used, and precipitated RNA was tested for the presence of Gapdh by qPCR. Data are mean ± SD; **P ≤ 0.01, ****P ≤ 0.0001; n.s., not significant; two-way ANOVA with Tukey's multiple-comparisons test. The end, endogenous.

4.5. RNA-mediated pull down of 7SK interacting proteins

4.5.1. Testing different antisense oligos for pull down 7SK

As an additional approach to investigate interactions of proteins with 7SK, I performed RNA pulldown experiments in which 7SK snRNA generated by *in vitro* transcription is coupled to streptavidin beads through a biotinylated antisense oligonucleotide and incubated with cell lysates. As a first step, I designed several biotinylated antisense oligonucleotides and assessed their ability to couple 7SK wild-type RNA to streptavidin beads. I found that oligonucleotides #3, #5 and #6 efficiently pulled down 7SK snRNA. Since oligonucleotide, #3 binds to SL1, which is a binding site for several proteins including HEXIM1, I decided to use oligonucleotide #5 for further experiments (**Figure 34**). This oligonucleotide binds to the region between SL2 and SL3 and, therefore, is expected to not perturb the binding of proteins to SL1 or 3.

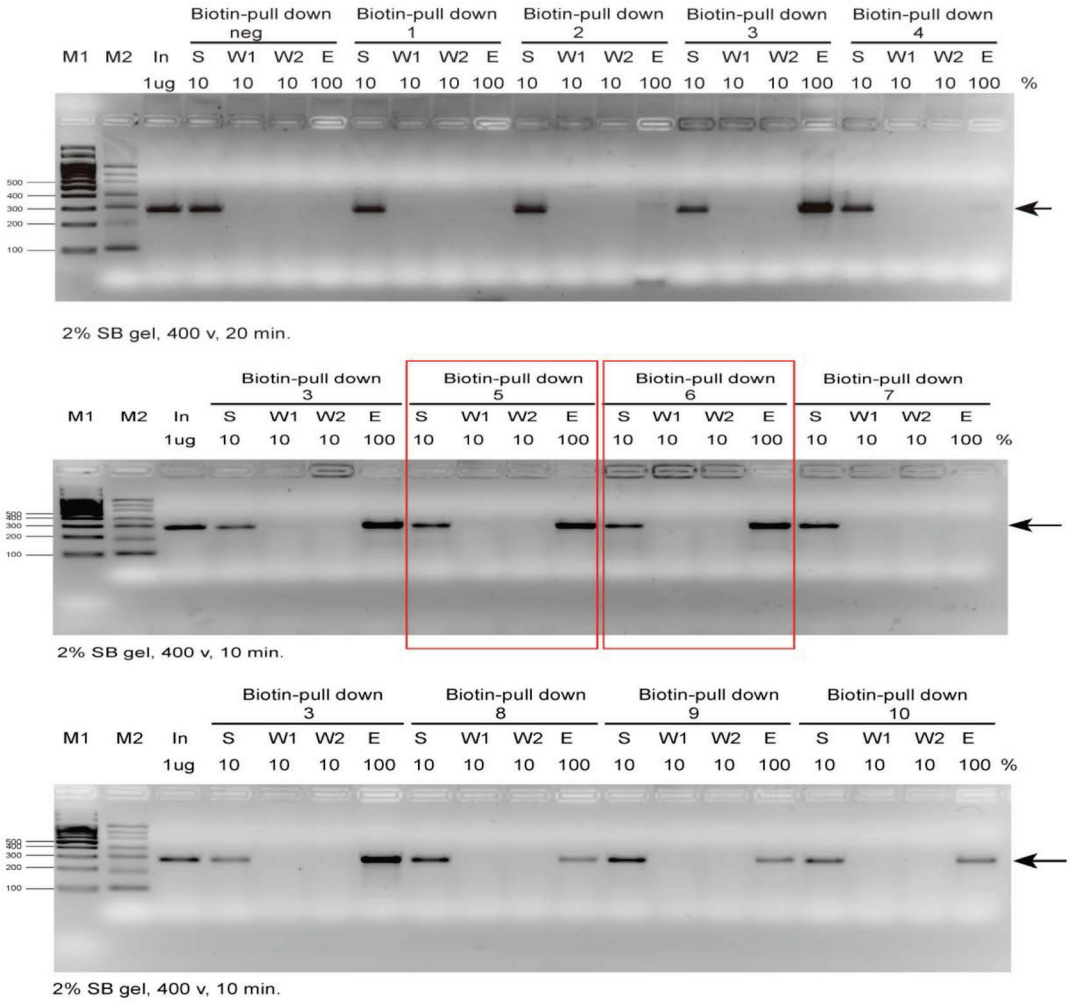

Figure 34: Testing of biotinylated oligonucleotides for 7SK pulldown

Gel electrophoresis showing the efficiency of 7SK pulldown with different biotinylated oligonucleotides, which target different regions of 7SKWT RNA for *in vitro* binding. In, input; S, supernatant; W, wash; E, eluate.

Lane M, RiboRuler Low Range RNA Ladder from Thermo Fisher Scientific. Lane M, 100 bp-3000 bp DNA Rainbow Ladder from GENEON GMBH.

4.5.2. RNA optimization binding on streptavidin magnetic beads

As a next step, I optimized the amounts of 7SK wild-type RNA and antisense oligonucleotide for binding to streptavidin beads (**Figure 35**) and pulling down endogenous Larp7 from NSC34 cell lysate. As a result, 2 µg 7SK snRNA, 22 pmol antisense oligonucleotide and 10 µL streptavidin were found as optimal.

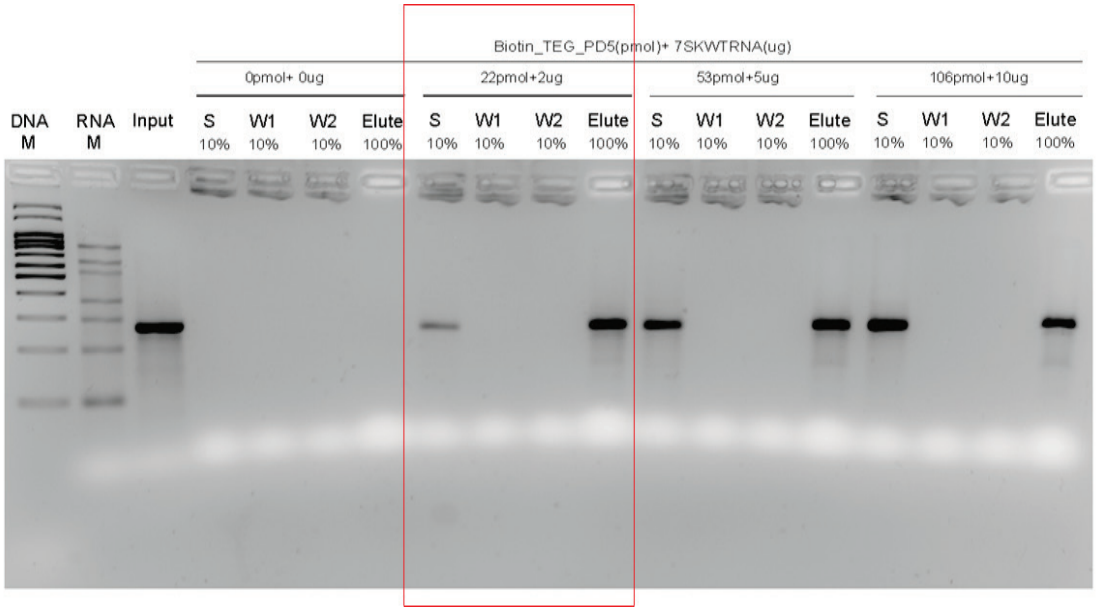

Figure 35: Optimization of oligonucleotide and RNA amounts for 7SK pulldown
Gel electrophoresis in 2.5% TBE agarose gel tests the different amount of Biotin-PD5 coupled 7SKWT RNA after *in vitro* binding to 10 µL Streptavidin Magnetic Beads. Lane RNA M, RiboRuler Low Range RNA Ladder from Thermo Fisher Scientific. Lane DNA M, 100 bp-3000 bp DNA Rainbow Ladder from GENEON GMBH

After optimization of the amounts of 7SK wild-type RNA and antisense oligonucleotide for binding to streptavidin beads, I investigated the amount of NSC34 cell lysate that is sufficient to pull down endogenous Larp7 from cell extracts, using 7SK pulldown. As a result, 2 µg 7SK snRNA, 22 pmol antisense oligonucleotide, 10 µL streptavidin and 200 µL NSC34 cell lysate (1/5 10 cm dish cells) were found to be optimal (**Figure 36)**.

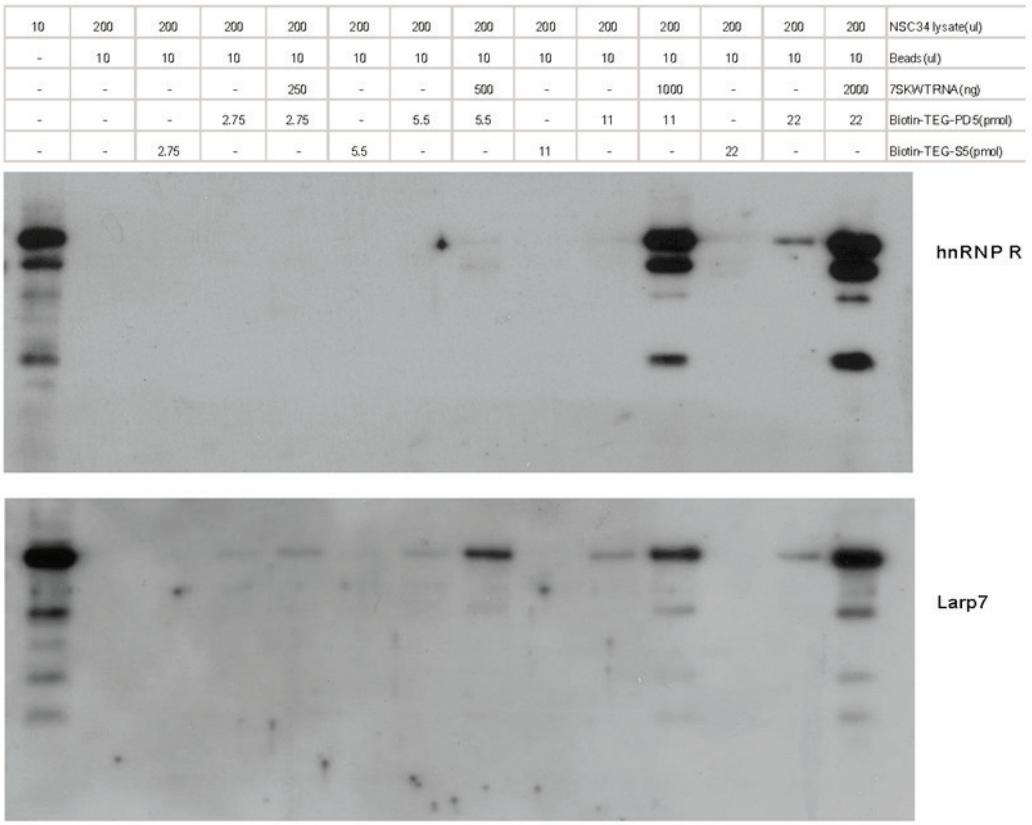

Figure 36: Optimization of conditions for pulldown of 7SK-associated proteins from NSC-34 lysate

Western blotting shows that increasing amount of Biotin_PD5+7SKWT RNA can pull down more endogenous hnRNP R and Larp7 from NSC34 lysates by using 7SK antisense oligonucleotide coupled streptavidin magnetic beads, Beads:10 µL, NSC34 lysate:1/5 10 cm dish. Reaction volume is 200 µL.

4.5.3. 7SKWT, SL3P, 3F, but not SL1 or SL13 bind CDK9 and cyclinT1 *in vivo*

After optimizing the amounts of 7SK RNA and antisense oligonucleotide for binding to streptavidin beads, I tested the binding of different 7SK mutants to streptavidin beads (**Figure 37**). For this purpose, the same molar amount of the 7SK mutants was used. The *in vitro* binding result shows that all the 7SK mutants can bind to streptavidin beads very effectively via the antisense oligonucleotide.

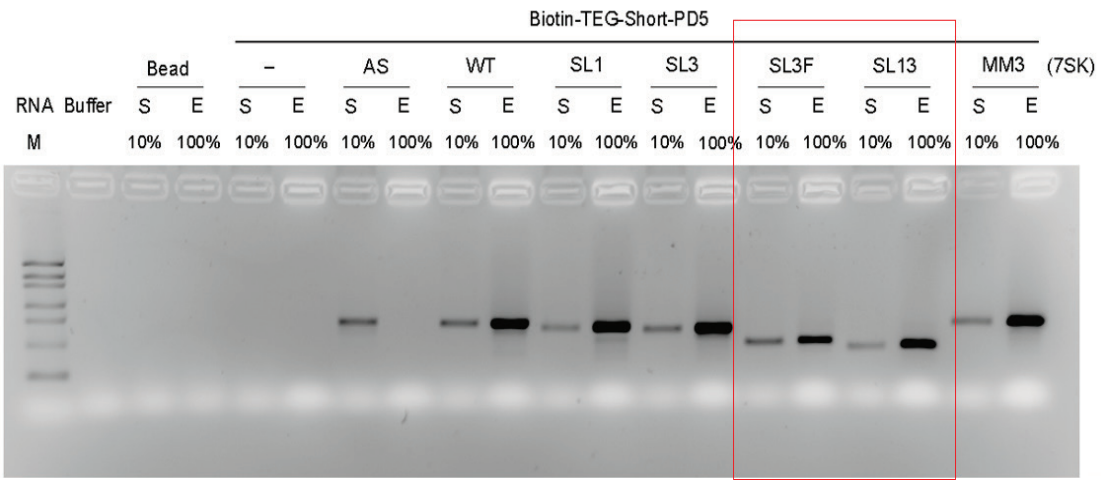

Figure 37: Immobilization of in vitro-transcribed 7SK snRNAs on streptavidin beads using a biotinylated antisense oligonucleotide. Agarose gel electrophoresis of the eluted RNA (E, 100% loading) and the RNA remaining in the supernatant (S, 10% loading). Lane M, RiboRuler Low Range RNA Ladder from Thermo Fisher Scientific.

Next, I investigated to what extent the 7SK RNA mutants can interact with Larp7, CyclinT1, and Cdk9. For this purpose 7SK wild-type or mutant RNAs were incubated with NSC34 lysate followed by antisense oligonucleotide-mediated pulldown using Streptavidin beads. As a result, I found that Larp7 interacts with wild-type 7SK and all 7SK deletion mutants in agreement with the notion that Larp7 interacts with SL4 of 7SK and none of the mutants harbors deletions in SL4. No Larp7 interaction was detected on the 7SK antisense RNA as a control. In contrast to Larp7, binding of CyclinT1 and Cdk9 to 7SK was disrupted by the deletion of SL1 but not of SL3. This result supports a previous study in which SL1 was found to be the binding site for Hexim1 which recruits the pTEFb complex to 7SK [39]. Importantly, the binding ability of 7SK to CyclinT1 and Cdk9 was retained by the full deletion of SL3 (SL3F). Given my previous finding that hnRNP R binding to 7SK is lost upon full deletion of SL3 this result further shows that 7SK/pTEFb and 7SK/hnRNP R complexes are separate from each other (**Figure 38**).

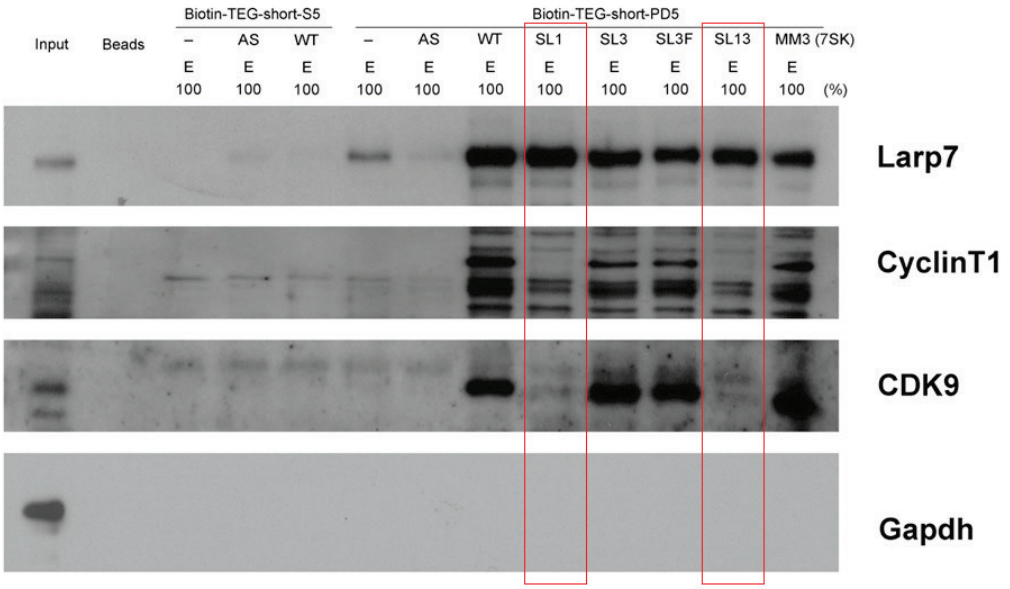

Figure 38: Western blot analysis of proteins bound to 7SK snRNAs. As control, 7SK wild-type (WT) and antisense (AS) were purified using either an antisense oligonucleotide that binds to wild type or a sense oligonucleotide that binds to antisense.

4.6. Digitonin-mediated fractionation on NSC34 cells

hnRNP R is not only present in the nucleus but also in the cytoplasm of motoneurons [66], and 7SK also can be detected in the cytoplasm of motoneurons by in situ hybridization [87]. In order to investigate the subcellular distribution of 7SK-interacting proteins in the nucleus and cytosolic fraction. I applied a fractionation protocol that uses buffers containing digitonin or NP-40 to sequentially extract the cytosolic fraction (F1), the organellar and nuclear soluble fraction (F2) and the nuclear insoluble fraction (F3). First, I used the NSC34 cell line to optimize the fractionation protocol. I use Gapdh as the marker for the cytosolic fraction, Calnexin (CNX), an integral protein of the endoplasmic reticulum (ER), it later turned out that the nuclear soluble fraction and the organellar fraction were co-fractioned, and Histone H3 as the nuclear insoluble marker. I found that using 25-35 ug/mL digitonin and 10 min incubation could completely separate the cytosolic fraction from the organellar and nuclear soluble fraction and from the nuclear insoluble fraction (**Figure 39, 40, 41)**. The soluble nuclear and cytoplasmic organellar fraction were co-purified. I also

checked 7SK in different fractions by qPCR and found that 7SK is present mostly in the nuclear soluble fraction but also detectable in the cytosolic and nuclear insoluble fraction (**Figure 43**), this result is also consistent with previously published data [21, 68, 88-90]

4.6.1. Optimization of digitonin concentration

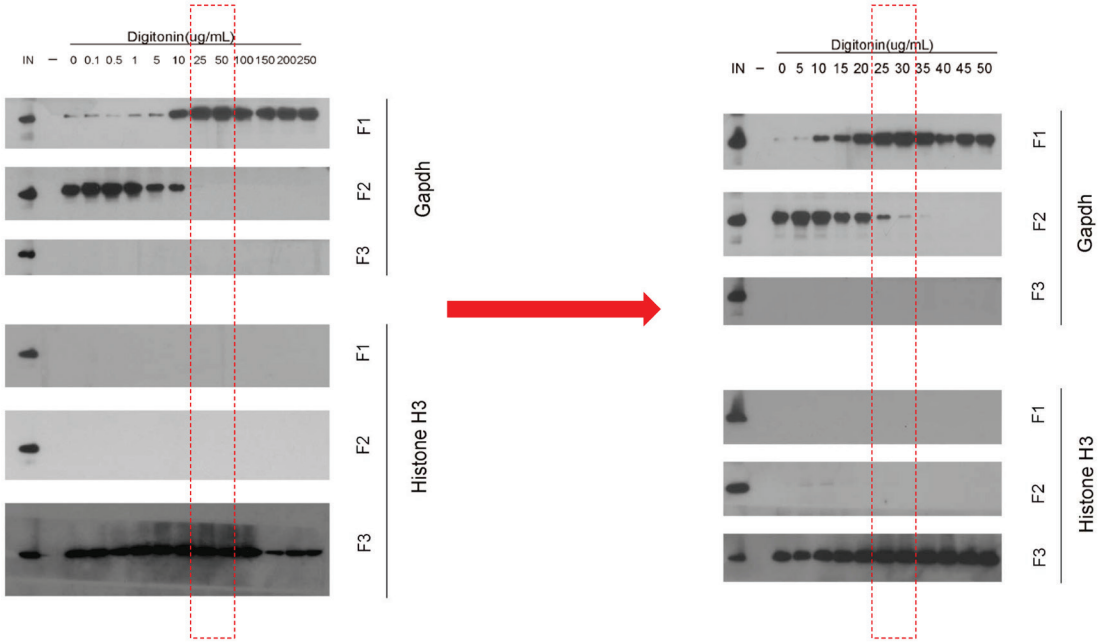

Figure 39: Western blot analysis for optimization of digitonin concentration for cellular fractionation

The cytosolic fraction marker Gapdh shows that the cytoplasm can be separated from other fractions at 25 ug/mL digitonin for 10mins treatment. F3: nuclear insoluble fraction marker HisotoneH3 is found in the F3 after treated at 25 ug/mL digitonin.

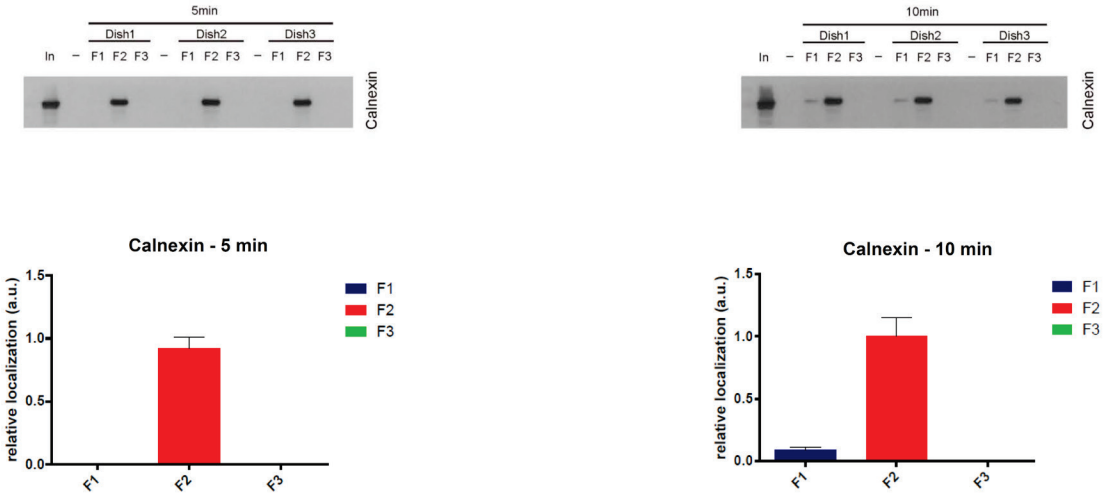

Figure 40: Western blot analysis of Calnexin in subcellular fractions following exposure to digitonin for 5 or 10 min

The Organelle plus nuclear soluble fraction was detected using the endoplasmic reticulum a marker Calnexin. Calnexin is retained in the organelles without being released to the cytosolic fraction at 25 ug/mL digitonin for 10 min treatment.

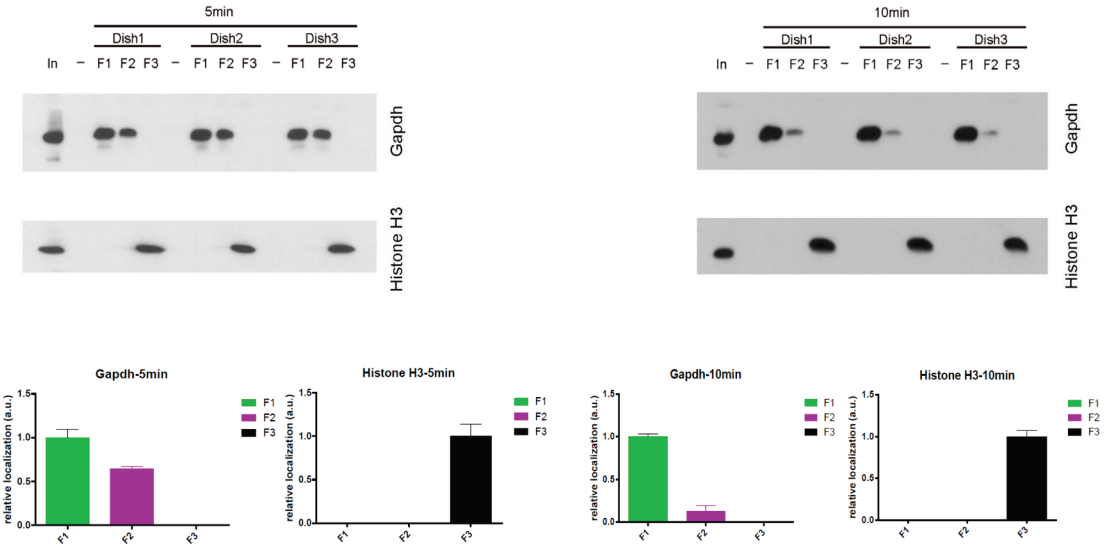

Figure 41: Western blot analysis of Gapdh and Histone H3 in subcellular fractions following exposure to digitonin for 5 or 10 min

After 5 min treatment with digitonin, Gapdh is found both in F1 and F2 fractions, and it becomes more enriched to the F1 fraction after 10 min, indicative of a better separation of the cytosolic soluble and the organelle fraction. The insoluble nuclear

fraction is completely separated from F1 and F2 at both time points, as indicated by staining of this fraction with a Histone H3 antibody.

4.6.2. Subcellular distribution of 7SK-interacting proteins

As a next step, I checked 7SK-interacting proteins in different fractions by Western blotting (**Figure 42)**. hnRNP R, A1 and A2B1 are located mostly in the nuclear insoluble fraction, most likely caused by their binding to nascent RNA associated with chromatin. Similar to the distribution of 7SK, Larp7 was mostly present in the nuclear soluble fraction but also detectable in the cytosolic and nuclear insoluble fraction suggesting that 7SK complexes can shuttle between nucleus and cytoplasm and also interact with chromatin. In agreement with this notion, I detected Hexim1 in the cytosolic fraction as well. As expected, Smn was abundant in the cytosolic fraction where it has been shown to exert its canonical function in snRNP biogenesis.

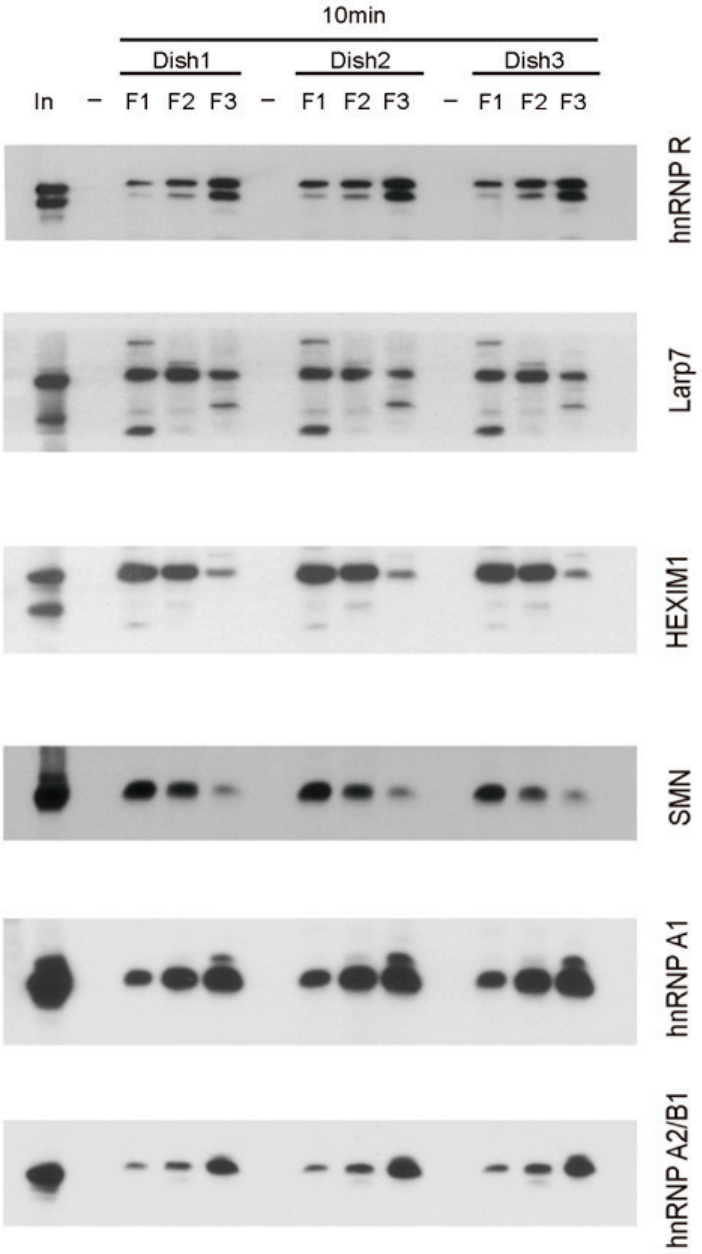

Figure 42: Western analysis of 7SK-interacting proteins in different fractions in NSC34 cells.

4.6.3. qPCR

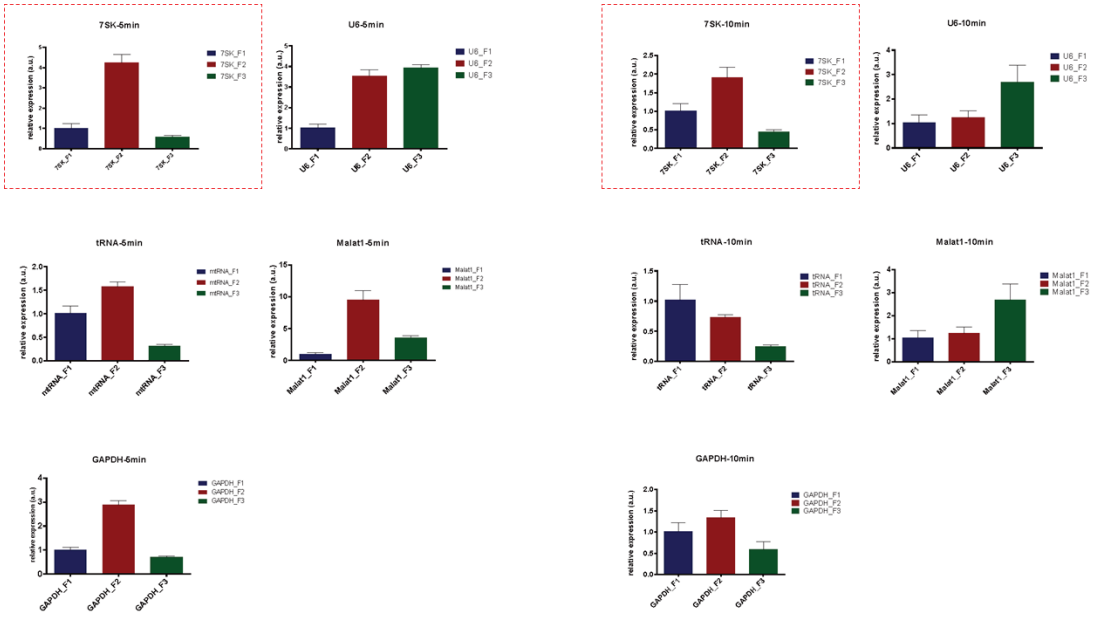

Figure 43: qPCR analysis of the subcellular distribution of RNAs.

4.7. Digitonin-mediated fractionation on motoneurons

As a next step, I used this fractionation procedure for primary mouse embryonic motoneurons. Such motoneuron cultures are used as *in vitro* models for ALS (Amyotrophic lateral sclerosis) and SMA (Spinal muscular atrophy), two common and severe forms of motoneuron disease for which the pathogenesis is still not clear. Fractionation of motoneurons gives us one good direction to find out alterations in subcellular distributions of RNA and protein in the cytosolic or nuclear fractions

Different cell types need different concentrations of digitonin. So first, I had to optimize the digitonin concentration also on motoneurons. I found that the Gapdh protein could completely release from the cytosol without breaking down the endoplasmic reticulum and nuclear membrane at 200 ug/mL digitonin (**Figure 44**).

4.7.1. Optimization of digitonin concentration on primary motoneurons

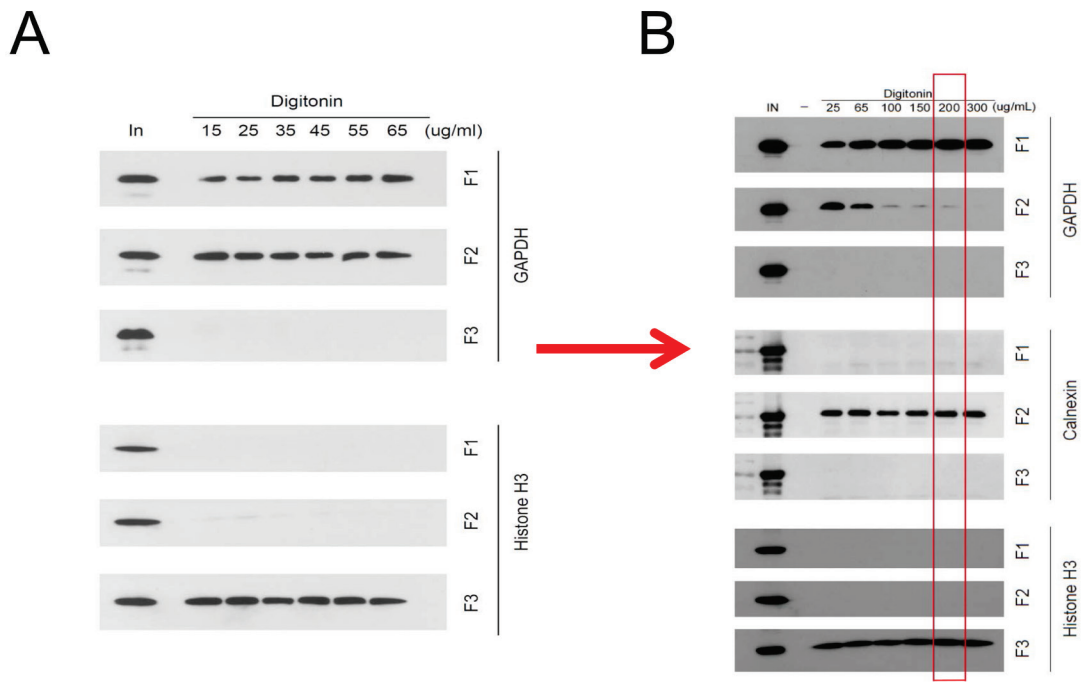

Figure 44: Optimization of digitonin concentration for the subcellular fractionation of motoneurons. The presence of Gapdh in the F1 fraction was used as readout. The cytosolic fraction marker Gapdh is most highly enriched in the cytoplasm at 200 ug/mL digitonin for 10 min treatment. F2: organelles plus nuclear marker Calnexin is still separated from the soluble cytoplasm at 200 ug/mL digitonin for 10 min treatment. F3: nuclear insoluble fraction marker Histone H3 is retained in the F3 fraction after treatment with 200 ug/mL digitonin for 10 min.

After optimization of the digitonin concentration for fractionating primary motoneurons, I validated the concentration on 24 well plates. The Western shows that 200 ug/mL digitonin is optimal (**Figure 45**).

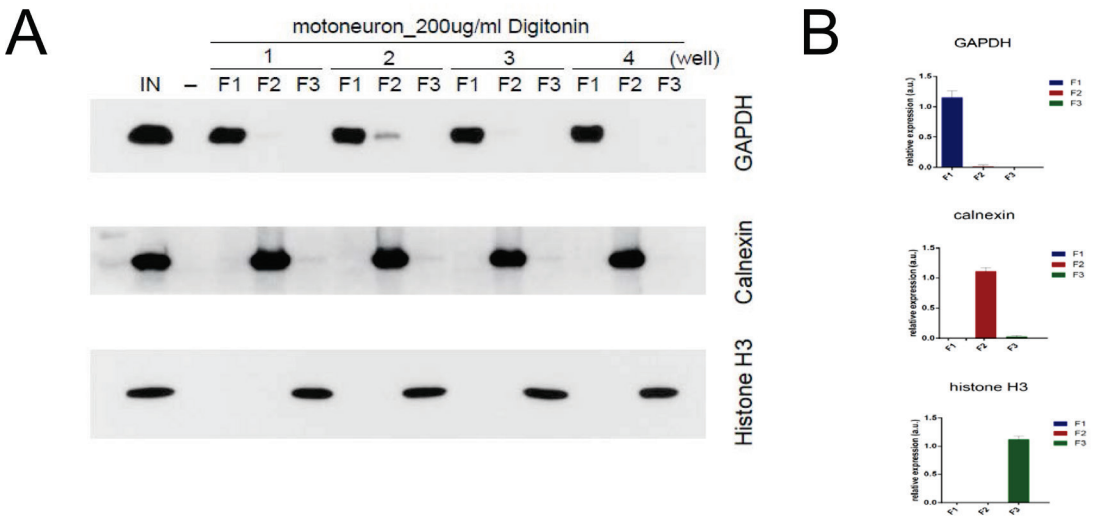

Figure 45: Western blot analysis F1, F2, F3 markers following subcellular fractionation of motoneurons

Western blotting shows that motoneuron fractionation by using 200 ug/mL) of digitonin in 24 well plates is suitable for optimal separation. In each well, 400.000 cells are kept for 7 d before performing the fractionation. Replicates were performed with 4 wells, and the enrichment of Gapdh in the F1 fraction was checked: The cytosolic fraction marker Gapdh is most highly enriched in the cytoplasm fraction F1 at 200 ug/mL digitonin after 10 min treatment. F2: organelles plus nuclear marker Calnexin is enriched and separated from the cytoplasm at 200 ug/mL digitonin for 10 min treatment. F3: nuclear insoluble fraction marker HisotoneH3 is retained in the F3 fraction after treatment at 200 ug/mL digitonin for 10 min. The right part of the figure shows a bar graph with the quantification of the Western blot bands.

4.7.2. Subcellular distribution of 7SK-interacting proteins in motoneurons

As a next step, I checked 7SK-interacting proteins in different fractions by Western blotting. Similar to NSC34 cells, hnRNP R was mostly located in the nuclear insoluble fraction. Larp7 was mostly located in the nuclear soluble fraction but was also detectable in the cytosolic and nuclear insoluble fractions. Smn was abundant in the cytosolic fraction (**Figure 46**).

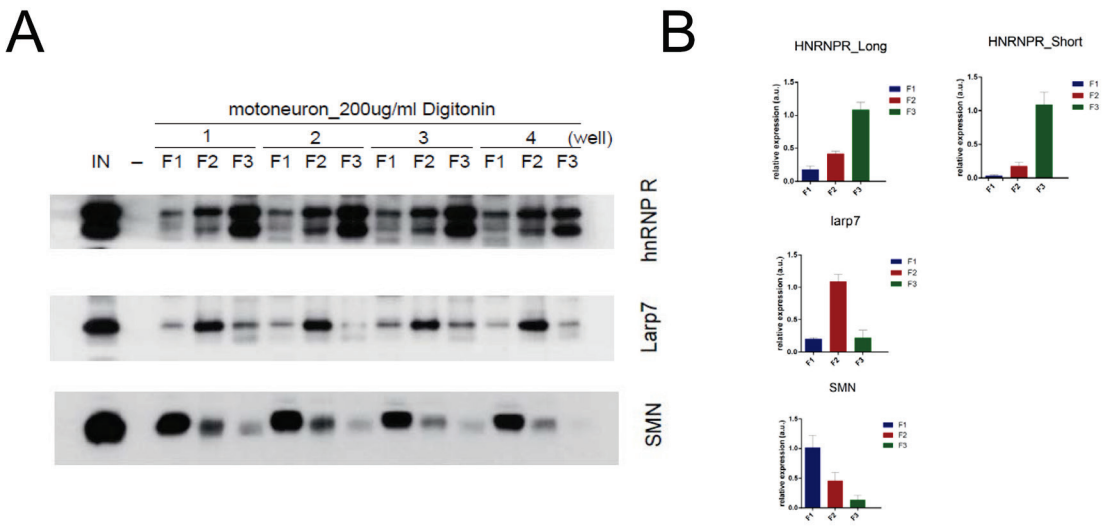

Figure 46: Subcellular distribution of 7SK-interacting proteins in motoneurons.

As a next step, I checked 7SK and other RNAs in different fractions by qPCR (**Figure 47**). This figure shows that 7SK is mostly located in the nuclear soluble fractions. This is to be expected because the main functions of 7SK is regulation of transcription [20]. U1 snRNA is mostly located in the nuclear soluble fraction because the U1 snRNP assembly and splicing mainly occur in the nucleus. This is also consistent with published data [91-93].

MALAT1, also known as nuclear enriched abundant transcript-2 (NEAT2), is a highly abundant and conserved nuclear lncRNA [94-96]. Our data also proved that MALAT1 is localized in the nucleus.

Gapdh protein is localized in the cytosolic fraction. In contrast to NSC34 cells, most of the Gapdh mRNA also localized in the cytosolic fraction in motoneurons. This appears plausible because motoneurons are fractionated at day 6, at this time point they are highly polarized. The proteins and the RNAs encoding cytosolic proteins are widely distributed in the cytosol and transported to the axons, and thus the separation from nuclear fractions is more efficient.

4.7.3. qPCR

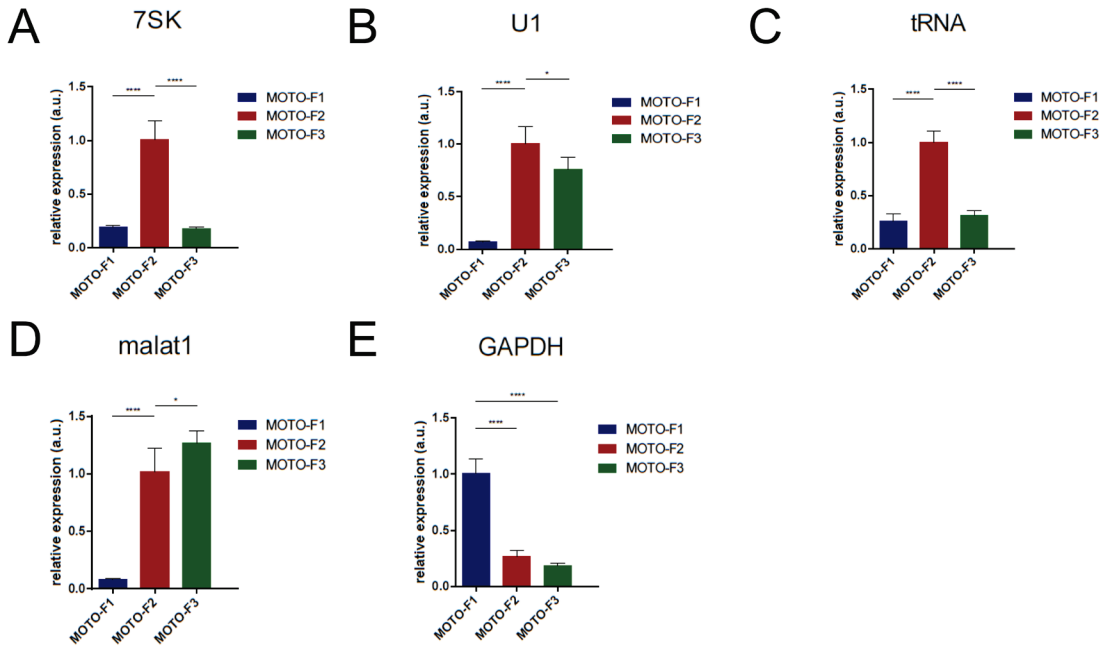

Figure 47: Bar graph showing the qPCR result of the RNAs from F1: cytosolic fraction. F2: organelles plus nuclear soluble fraction. F3: nuclear insoluble fraction. Most 7SK is in F2 fraction, most U1, malat1 are in F3 fraction, tRNA in motoneurons, in contrast to NSC34 is most highly enriched in the F2 fraction. Most of the Gapdh mRNA is found in F1 fraction.

4.8. Pulldown of endogenous 7SK/hnRNP complexes

As a next step in order to investigate other 7SK binding proteins besides hnRNP R and hnRNP A1, I did the pull-down assay with 7SK antisense oligonucleotide for pull down of endogenous 7SK/hnRNP complexes (**Figure 48, 49, 50**). As a first step, I tested different oligos that target different regions of 7SK for pulling down endogenous 7SK. One oligo that targets the stem loop 1 region was the best choice. The same oligo was also used by Van Herreweghe in 2007 [42] to pull down 7SK complex from Hela nuclear extracts. In a second step, I optimized the amount of oligo, streptavidin beads and NSC34 lysate. I found that 50 pmoL Biotinylated oligo, 10 µL streptavidin beads, 200 µL NSC34 lysate (1/5 dish) is the best choice.

4.8.1. Testing of antisense oligonucleotides for pull down 7SK

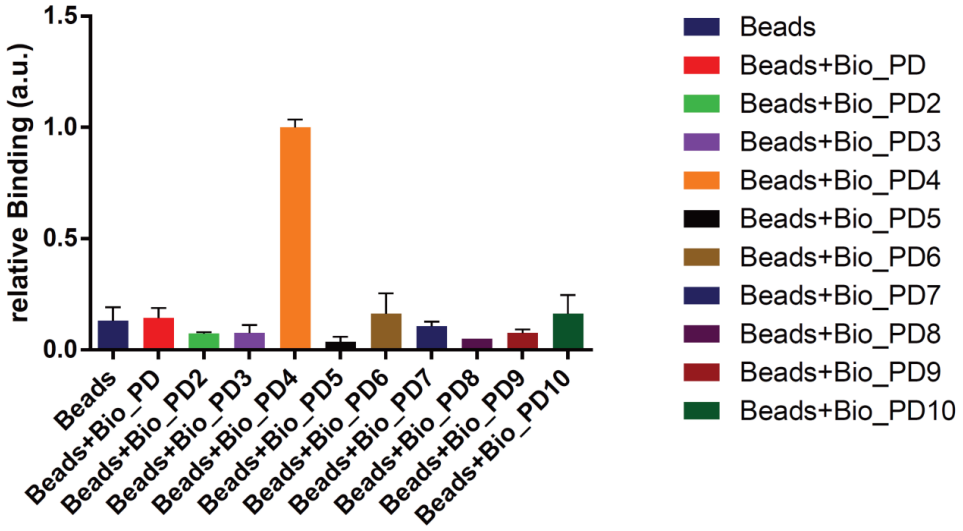

Figure 48: Testing of different oligonucleotides for pulldown of endogenous 7SK

Bar graph shows the qPCR result for different Biotin-coupled oligonucleotides for endogenous 7SK *in vivo* binding. These results show that that Biotin_PD4 oligo has the highest efficiency to pull down 7SK and 7SK bound RNA/protein complexes.

4.8.2. Optimization of pull down conditions with oligonucleotide 4

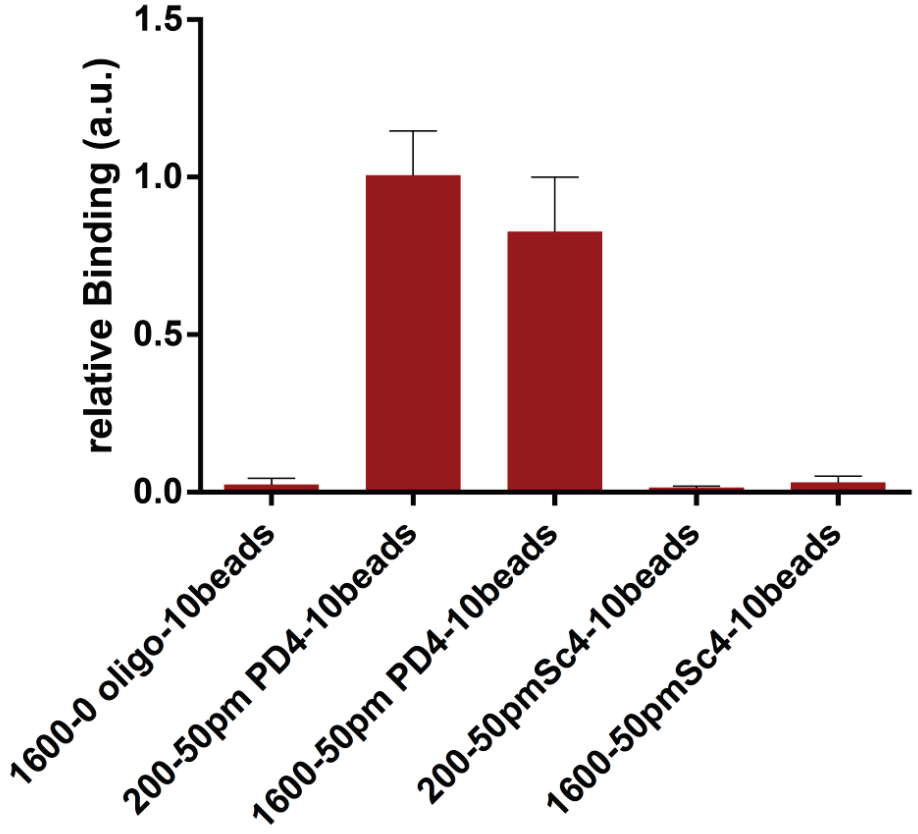

Figure 49: Bar graph showing the 7SK qPCR result for different amounts of NSC34 lysate after Biotin PD4 binding und immunoprecipitation of endogenous 7SK. 200 or 1600 µl lysate were used as input.

This result indicates that increasing the amount of NSC34 lysate from 200 to 1600 µL does not improve the binding efficiency.

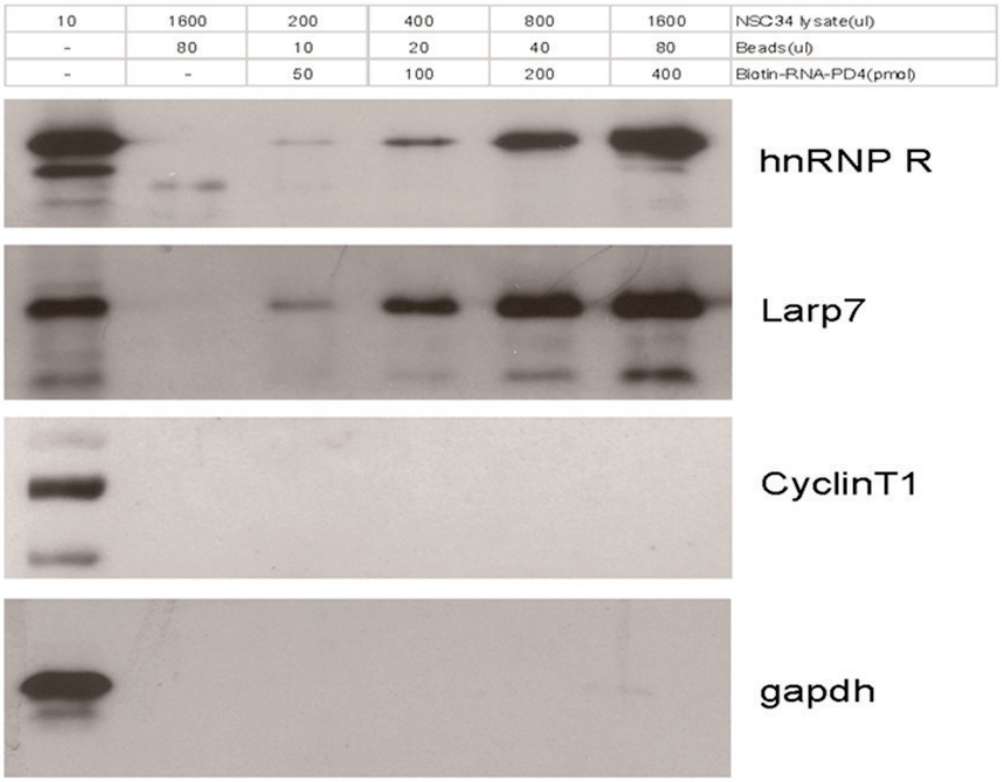

Figure 50: Western blot analysis of proteins that interact with immunoprecipitated 7SK.

These results indicate that increasing the amount of beads, oligo, and NSC34 lysate can improve the hnRNP R and Larp7 binding efficiency but not the interaction and/or pulldown of CyclinT1 and Gapdh.

After optimization of the concentrations for oligo, beads, NSC34 lysate, I performed qPCR to make sure that the oligonucleotide pulls down only 7SK and not other RNAs. **Figure 51** shows that this oligonucleotide-mediated pulldown only immunoprecipitated 7SK but not Malat1, B-actin mRNA, U1, 7SL, and Gapdh mRNA. Those are common and abundant RNAs. In summary. The oligo-mediated pulldown is very specific for 7SK.

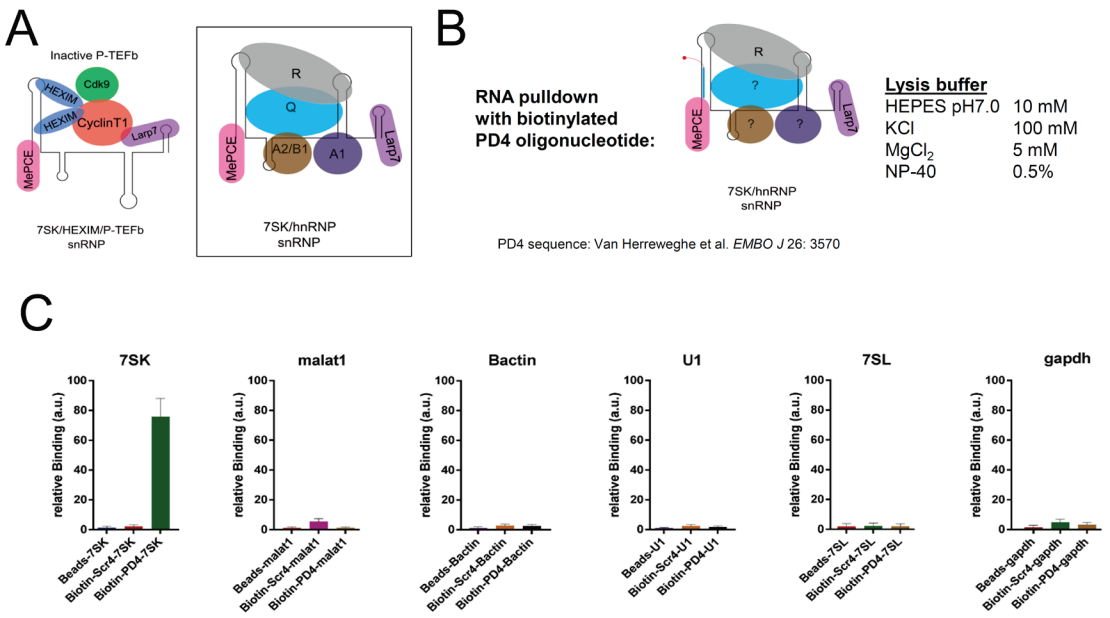

Figure 51: Validation of 7SK pulldown by the Biotin_RNA PD4 oligonucleotide. (A) Diagram of the 7SK/p-TEFb complex and 7SK/hnRNPs complexes. (B) Diagram of the Biotin_RNA PD4 oligo target region on 7SK and the buffer used for 7SK complex pulling down. (C) Validation that 7SK can only be pulled down by Biotin_RNA PD4 oligo, not by beads or randomly designed oligo.

4.9. Proteomic analysis of 7SK-interacting proteins in NSC34 cells

As a next step before sending the samples to the lab of our collaboration partner (Prof. Matthias Mann, MPI for Biochemistry, Munich-Martinsried) I performed a PAGE with subsequent silver staining of the gel and simply blue staining to make sure that the Biotin oligo can pull down proteins (**Figure 52**). These precipitated proteins were then identified and analyzed by Jakob Bader and Felix Meissner, MPI for Biochemistry, Munich. These colleagues also analyzed the data. These data revealed that the 7SK oligo could also pull down the Smn-SmB complex (**Figure 53**).

Smn is the abbreviation for survival motor neuron gene. There are two Smn genes in humans: Smn1 and Smn2. Lack of Smn protein due to mutations or deletions of the human Smn1 gene are causative for spinal muscular atrophy (SMA), a neurodegenerative motoneuron disease. In healthy individuals, the survival motor neuron 1 (*Smn1*) gene produces 100% full length (FL) Smn protein while the *Smn2*

gene produces ~10% FL Smn and ~90% of a non-functional product that lacks exon 7 (SmnΔ7) encoded domains due to aberrant alternative splicing. In SMA patients, the *Smn1* gene is lost due to mutations or deletions. *Smn2* remains and the small amount of FL Smn is sufficient for survival. The number of *Smn2* copies correlates with disease severity, with a lower copy number being linked to more severe types of SMA [97]. So far, only a few therapies are effective. Marco A. Passini and his colleagues used an adeno-associated virus (AAV) vector expressing human Smn (AAV8-hSmn) to inject into the CNS of mice modeling SMA, they found that the injected mice had wide spread expression of Smn throughout the spinal cord, and the expression of this transgene ranslated into robust improvement in skeletal muscle physiology, including increased myofiber size and improved neuromuscular junction architecture. Treatment with AAV8-hSmn increased the median life span of mice with SMA-like disease to 50 days compared with 15 days for untreated controls. Moreover, injecting mice with SMA-like disease with a human Smn–expressing self-complementary AAV vector — a vector that leads to earlier onset of gene expression compared with standard AAV vectors — led to improved efficacy of gene therapy, including a substantial extension in median survival to 157 days [98]. As a second line of therapy development, an oligonucleotide that caused suppression of the splice inhibitor for exon 7 inclusion from *Smn2*-derived transcripts was developed and tested from mice to humans. Spinraza was first invented in 2004 but reported in 2006 by Singh [99], Spinraza was approved by the FDA at the end of 2016. So far it is the most widely used drug that has been approved on humans with SMA [100].

Smn is part of a stable multiprotein complex that is found in all metazoan cells in the cytoplasm and in nuclear Gems. The Smn complex contains in addition to Smn, at least six other proteins, named Gemins2–7, and plays an essential role in the assembly of the spliceosomal small nuclear ribonucleoproteins (snRNPs). Through its binding to specific sequences contained within snRNAs, the Smn complex surveys the correct identity of the target RNAs and facilitates snRNP assembly with spliceosomal proteins. Based on its ability to interact with several other proteins and RNA components of cellular RNPs, it is likely that the Smn complex functions as an assembly some in the formation of diverse RNP particles, some of which may be of particular importance to motoneurons. Therefore, we decided to study the association of the Smn complex with 7SK/hnRNPs complex in more detail, in order to understand the role of this interaction for the cellular function of the Smn complex. This may help to develop further therapeutic strategies for this neurodegenerative disease [101].

4.9.1. Silver staining and Simply Blue staining

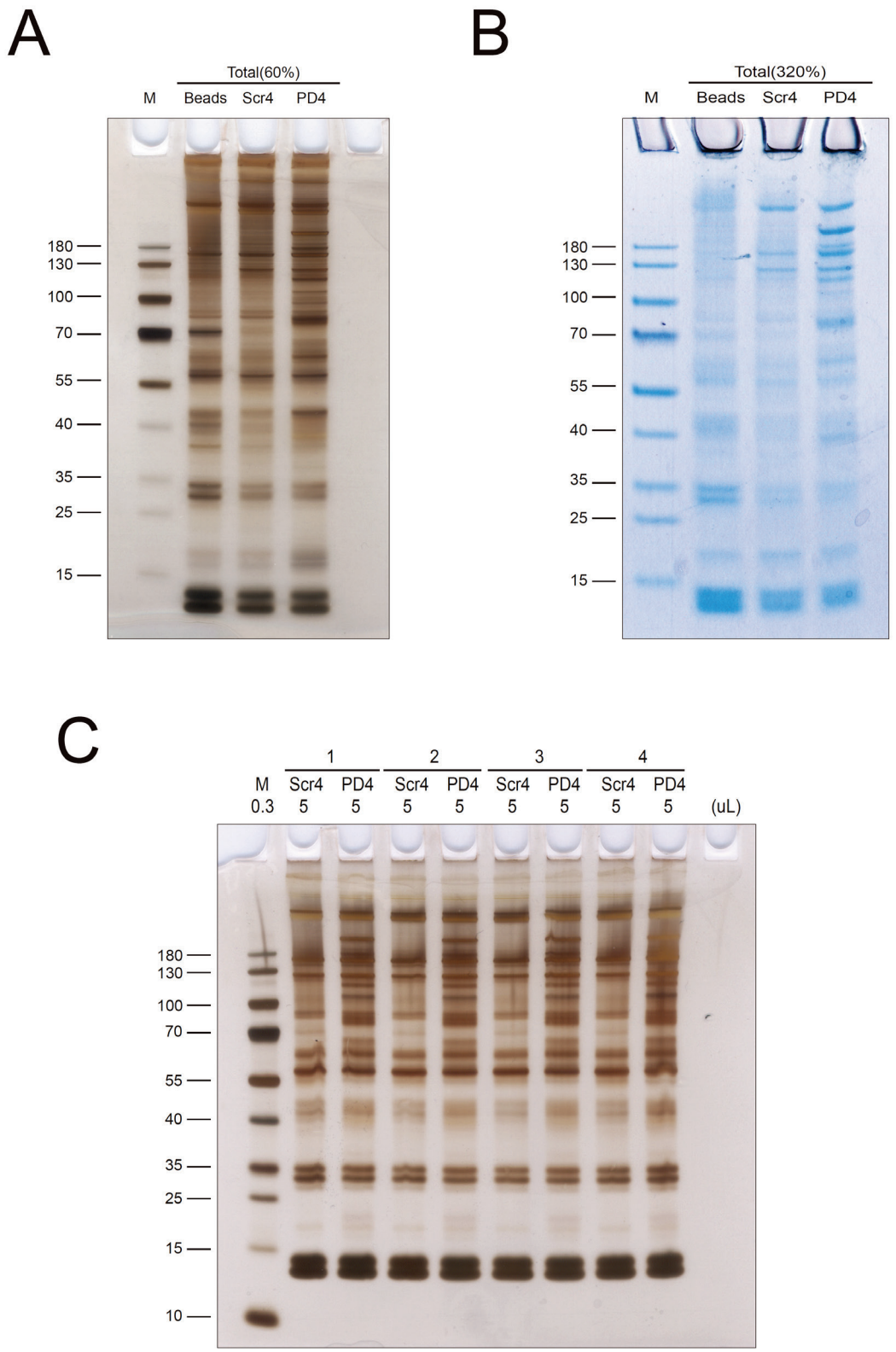

Figure 52: Silver staining and Simply Blue staining of 7SK oligonucleotide

precipitates from NSC34 cell extracts

Silver staining and Simply Blue staining show the protein bands that are pulled down by streptavidin magnetic beads or Biotin_Scramble RNA oligo that does not target 7SK or Biotin_PD4 RNA oligo that targets 7SK C17-G33 region. In the picture, specific protein bands are found which are pulled down by Biotin_PD4 RNA oligo.

4.9.2. Proteomics data analysis

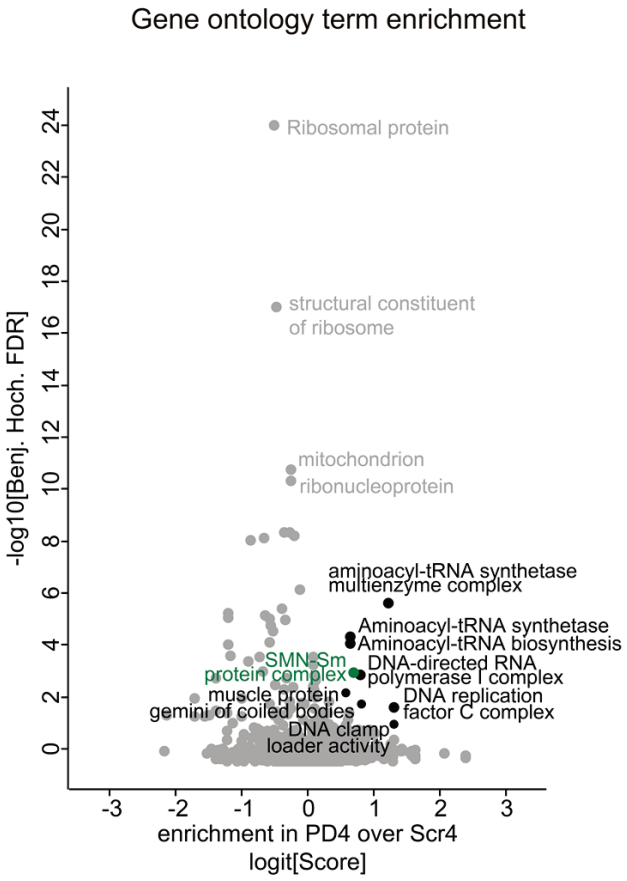

Figure 53: Go term analysis of proteins that are pulled down by Biotin_PD4 oligo from NSC34 total cell lysate.

4.9.3. Proteomics data validation

After obtaining the proteomics data, I selected hnRNP R, Larp7, HEXIM1, hnRNP A1, hnRNP A2B1, Gapdh to confirm that the oligonucleotide can pull down the proteins that had been identified by mass spectrometry. **Figure 54** shows that the antisense

oligo can pull down hnRNP R, Larp7, hnRNP A1 but not HEXIM1, hnRNP A2B1 that are established interaction partners for 7SK in the p-TEF regulatory complex. Similary, Gapdh as an unspecific housekeeping protein was also not pulled down.

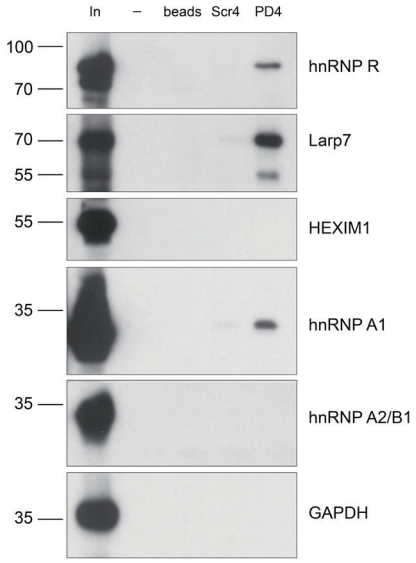

Figure 54: Proteomics data validation. Biotin RNA oligo can pull down hnRNP R, Larp7, hnRNP A1 that all are on the list of interaction proteins identified by mass spectrometric analysis.

4.10. hnRNP A1 and R belong to 7SK/hnRNP complex not 7SK/HEXIM1/pTEFb complex

In addition to the 7SK/HEXIM1/P-TEFb complex, a number of hnRNPs have been identified as interactors of 7SK more recently [31]. Among these are the hnRNPs A1, A2/B1, Q, and R.

As a next step, I therefore also checked hnRNP A1, another very important RNA binding protein involved in amyotrophic lateral sclerosis (ALS) [43, 44].

hnRNP A1 is highly expressed in neural cells [102]. It has two RRMs and a Gly-rich domain at the C-terminus. HnRNPA1 preferentially binds to UAGGGA/U sequences and cooperates with other hnRNPs to regulate splicing, including splicing of its own transcripts, and pathological splicing events [50, 57, 103-106]. In addition to its role in splicing, hnRNP A1 also has functions in modulating mRNA stability, export, transport, localization, and translation as well as miRNA processing [107-109]; Moreover,

hnRNP A1 is recruited to stress granules upon stress [110].

Mutations in hnRNP A1 underlie less than 1% of ALS cases [111]. Kim and colleagues identified hnRNP A1 missense mutations in a family affected by ALS and in two families with multisystem proteinopathy (MSP) affecting the brain, moto neurons, muscle, and bone [54]. Cytoplasmic accumulation and nuclear clearance of mutant hnRNP A1 have been observed in patient muscle tissue [54]. Interestingly, hnRNP A1 staining in postmortem tissue of sporadic ALS patients was reduced in the nuclei of motor neurons relative to that of control tissue and did not colocalize with TDP-43 inclusions [112]. ALS associated mutations in the Gly-rich LC domain of hnRNPA1, which mediates phase separation [113], have been shown to increase incorporation into stress granules, strengthen steric zipper motifs and accelerate fibrillization compared to wild-type hnRNP A1 [54, 113]. Additional mutations in hnRNP A1 were later identified by targeted sequencing of sporadic ALS patients and in an ALS family with flail arm syndrome [114]. hnRNP A1 knockout mice are embryonic lethal, while heterozygous animals display a cardiac phenotype and show many changes in alternative splicing of muscle development-related genes [115]. This evidence supports an important role for hnRNP A1 in alternative splicing, but further animal studies are required to investigate its role in ALS pathogenesis.

In order to investigate the interaction of hnRNP A1 with the 7SK complex, I performed co-immunoprecipitation of hnRNP A1 from NSC34 cell lysate in the presence or absence of RNase A. In order to make sure that the RNA is completely degraded by RNase A I extracted the total RNA from the supernatant after incubation of the NSC34 cell lysate with the antibody and pulling down complexes. As a result, the 18S and 28S rRNA were completely degraded after RNase A treatment (**Figure 55**). I then investigated hnRNP A1 protein interactors by Western blotting of the immunoprecipitate for selected candidates. I found that hnRNP A1 binds hnRNP R, Larp7 and Smn in an RNA-dependent manner (**Figure 56**).

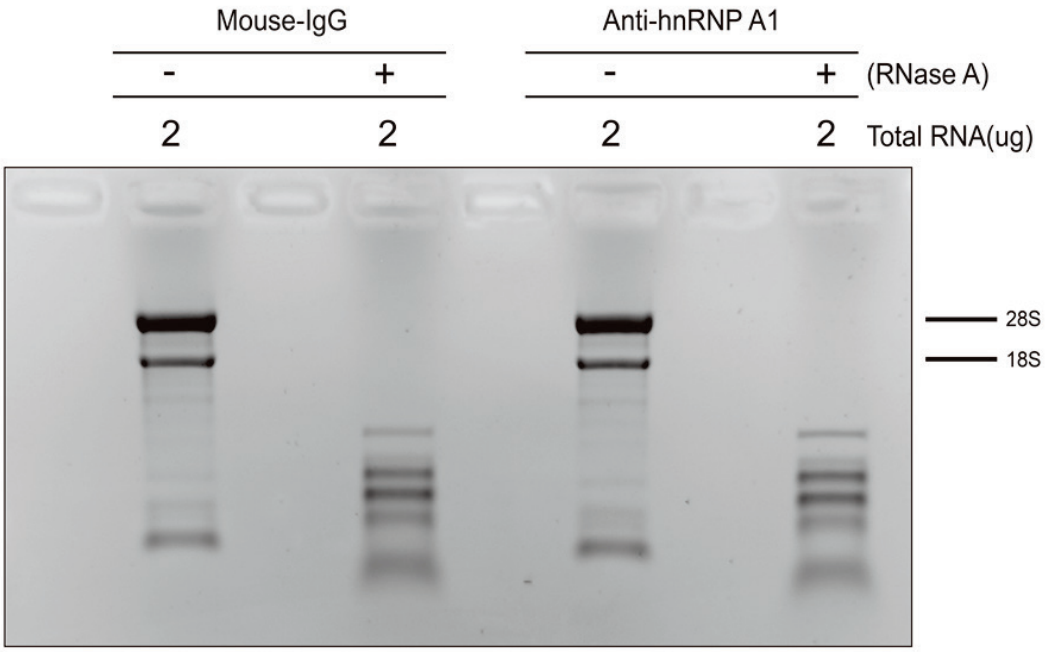

Figure 55: Gel electrophoresis in 1.5% TBE agarose gel of total RNAs that are extracted from the NSC34 lysate supernatant of Mouse-IgG control and hnRNP A1 samples. The upper band is 28S, the lower one is 18S. After RNase A treatment the RNA was completely degraded.

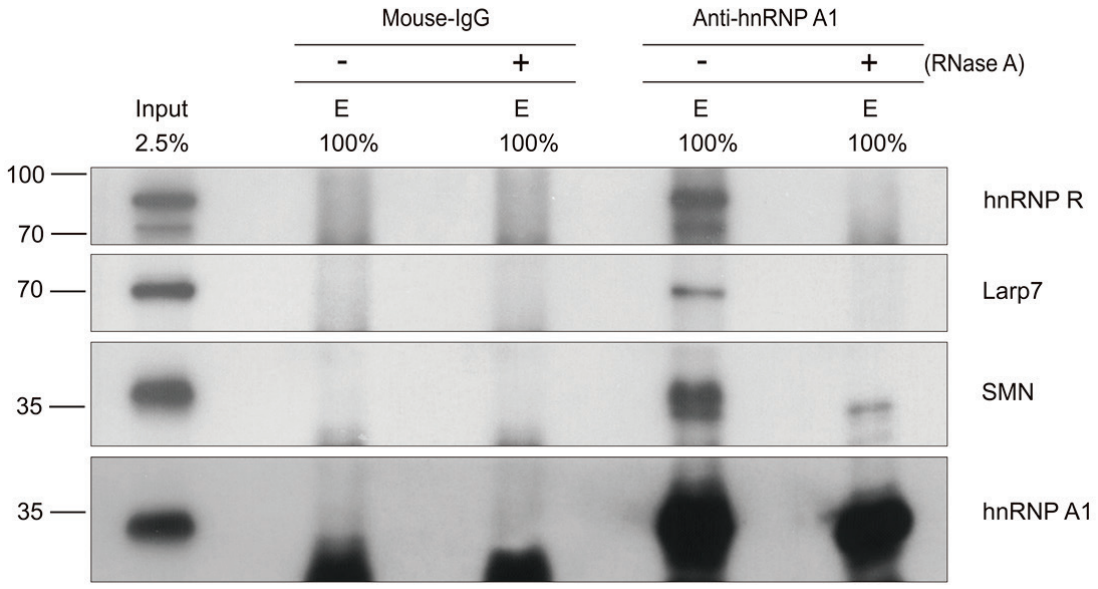

Figure 56: Western blot analysis of proteins that are co-immunoprecipitated by hnRNP A1 antibody. This result shows that hnRNP A1 can co-immunoprecipitate hnRNP R, Larp7, Smn without RNase A treatment. After RNase A treatment the

binding of hnRNP R, Larp7, Smn to hnRNP A1 is abolished, indicating that hnRNP A1 binds hnRNP R, Larp7, and that Smn binding is indirect.

4.11. Smn is part of a 7SK/hnRNPs complex, not 7SK/HEXIM1/pTEFb complex

After we found that the oligo could also pull down the Smn-SmB complex, we further investigated whether Smn can bind with 7SK/hnRNP complex. I performed Co-IP to check Smn binding by using a Larp7 antibody, because 90% of the 7SK snRNA is bound to Larp7 via its 3'-end [20]. Thus, if Smn-SmB complex binds 7SK, it should also interact with Larp7. In agreement, Smn co-immunoprecipitated with anti-Larp7 (**Figure 57**).

As a next step, I did Co-IP by using cyclinT1 antibody. I found that cyclinT1 antibody can pull down Larp7, HEXIM1, but not hnRNP R, hnRNP A1, Smn, Gapdh (**Figure 58**). I also did Co-IP by using hnRNP A1 antibody. This experiment revealed that hnRNP A1 antibody could pull down hnRNP R, Larp7, but not cyclinT1, HEXIM1, Gapdh (**Figure 59**). Furthermore, I also did Co-IP by using an Smn antibody (**Figure 60**). This experiment showed that the Smn antibody can pull down hnRNP R, Larp7, hnRNP A1, but not HEXIM1 and Gapdh. Based on the forward and reverse Co-IP I found that Smn is part of a 7SK/hnRNPs complex but not a 7SK/HEXIM1/pTEFb complex binding partner.

As a next step, I treated the NSC34 lysate with RNase A. Then I performed a Co-IP by using Smn antibody to check whether Smn binds to 7SK/hnRNP complex and whether this interaction depends on RNA. This experiment showed that after RNase A treatment Smn still binds to Larp7, but hnRNP R, hnRNP A1 binding are abolished (**Figure 61**). Taken together, Smn interacts with hnRNP R, hnRNP A1 in an RNA-dependent manner but binds with Larp7 in an RNA-independent manner.

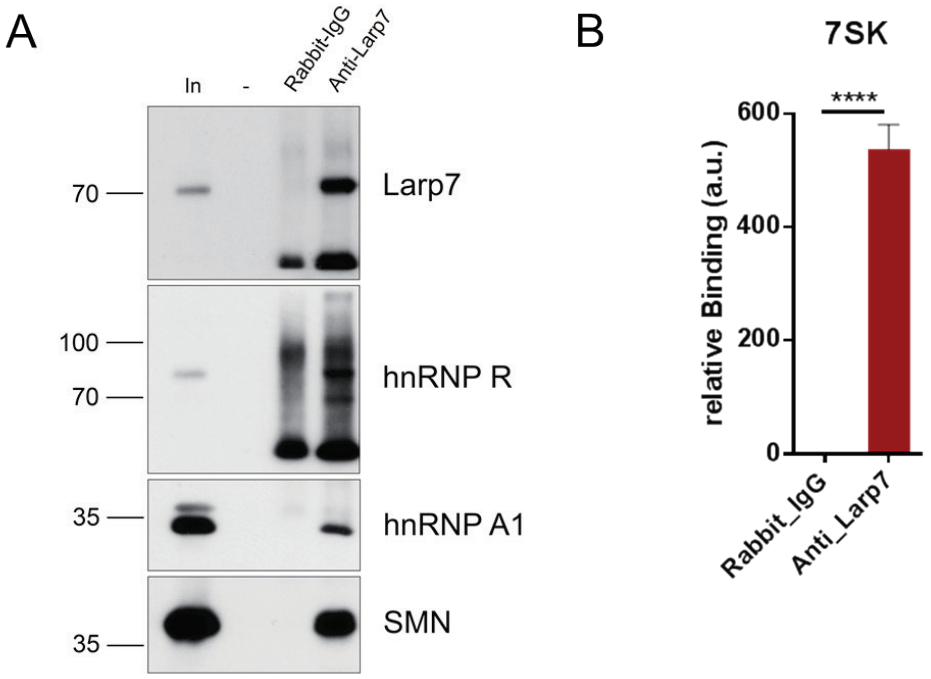

Figure 57: Western blotting of proteins that are pulled down by Larp7 antibody. The experiment revealed that Larp7 binds hnRNP R, hnRNP A1, and Smn. qPCR shows that Larp7 interacts heavily with 7SK.

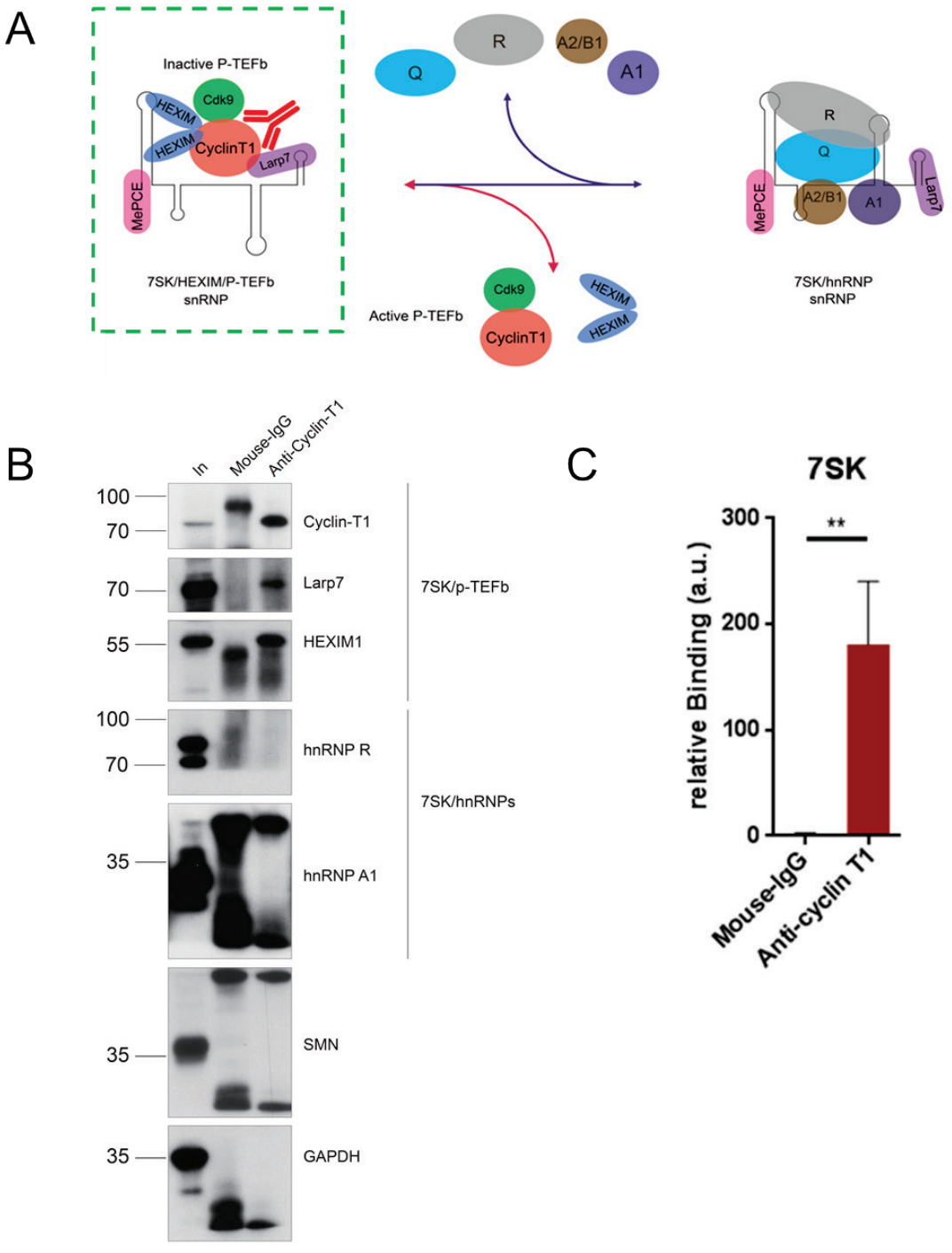

Figure 58: Western blot analysis of proteins that are pulled down by cyclinT1 antibody. (A) The carton illustrates the compartments of the classical 7SK/HEXIM/pTEFb complex in the box. On the right side, the interaction of 7SK with hnRNP R is shown which results in disinhibition of p-TEFb. (B) Western blotting shows the proteins that are pulled down by CyclinT1 antibody, you can see that CyclinT1 binds HEXIM1, Larp7 but not hnRNP R, hnRNP A1 and Smn and Gapdh. (C) qPCR shows that CyclinT1 interacts efficiently with 7SK.

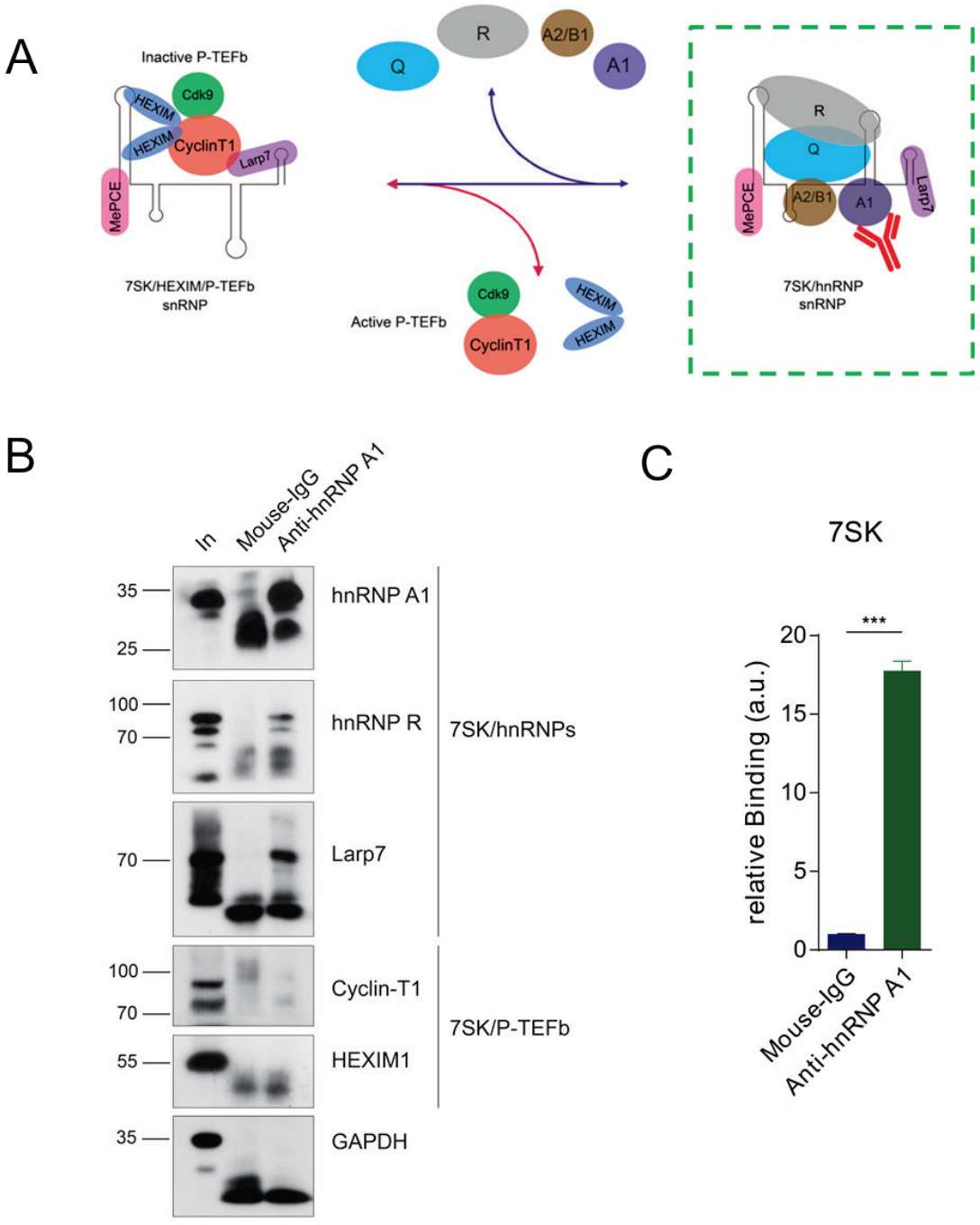

Figure 59: Western blot analysis showing the proteins that are pulled down by hnRNP A1 antibody. (A) Carton illustrates the different interactions the 7SK/hnRNPs in the context of inhibition (left box) and disinhibition (right) of the pTEFb complex. (B) Western blotting shows the proteins that are pulled down by hnRNP A1 antibody. This experiment reveals that hnRNP A1 binds hnRNP R and Larp7 but not CyclinT1, HEXIM1 and Gapdh. (C) qPCR shows that hnRNP A1 interacts efficiently with 7SK.

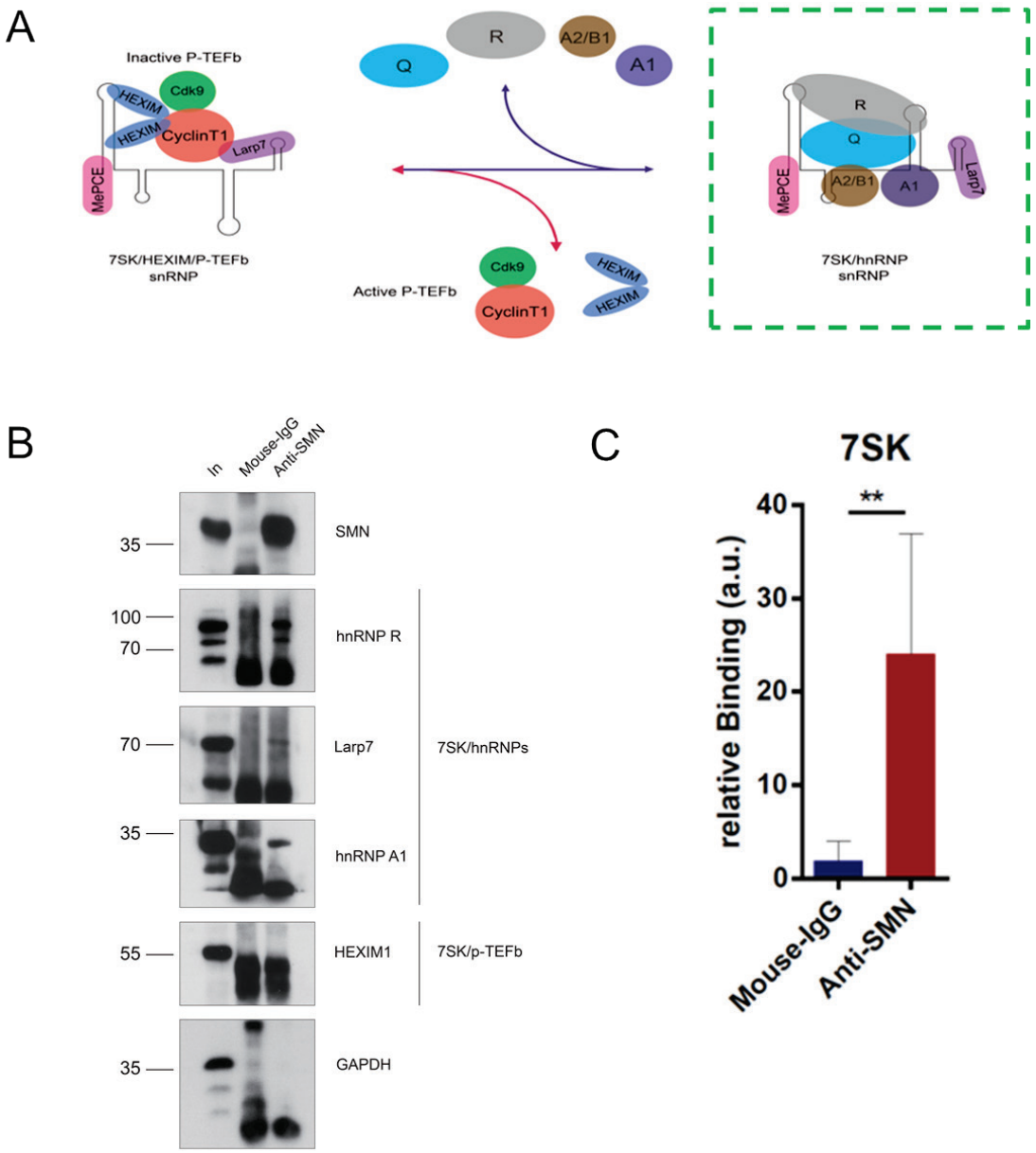

Figure 60：Western blot analysis of the proteins that are pulled down by a Smn antibody. (A) Carton illustrating the different states of the 7SK/hnRNP complexes in the context of pTEFb regulation. The conformation shown in the box shows the classical function as an inhibitor of pTEFb. (B) Western blot analysis of proteins that are co-immunoprecipitated by Smn antibody: Smn can co-immunoprecipitate hnRNP R, Larp7, hnRNP A1 but not HEXIM1 and Gapdh. This means that Smn only associates with the 7SK/hnRNPs complex but not 7SK/pTEFb complex. (C) qPCR shows that Smn binds to a small but significant amount of 7SK.

4.12. Smn interacts with the core 7SK snRNP

As mentioned before, the 5´ end of 7SK is normally bound by MEPCE, the 3´ end by Larp7. In order to completely confirm that the Smn complex interacts with 7SK snRNP, I treated the NSC34 lysate with RNase A as a next step, then did the Co-IP by using MEPCE or Larp7 antibody to check whether Smn binding to 7SK/hnRNP complex depends on the presence of RNA or not. I found that after RNase A treatment Smn, SmB/B´N, Gemin2 still bind with Larp7 or MEPCE, but hnRNP R, hnRNP A1 binding are abolished (**Figure 62**). CyclinT1 and CDK9 binding was reduced after RNase A treatment. This is consistent with published data [11].

In order to make sure that the antibody can target MECPE or Larp7, I did RIP-qPCR to demonstrate that the antibody can also pull down 7SK. The result also proves that MECPE and Larp7 also bind U6 snRNA [12]. Interestingly, both MEPCE and Larp7 can pull down great quantities of beta-actin mRNA (**Figure 63**). This could mean that MECPE and Larp7 associate with other mRNA binding proteins contained in mRNP particles. The mechanism how they regulate the function of these RNA binding proteins needs to be further investigated.

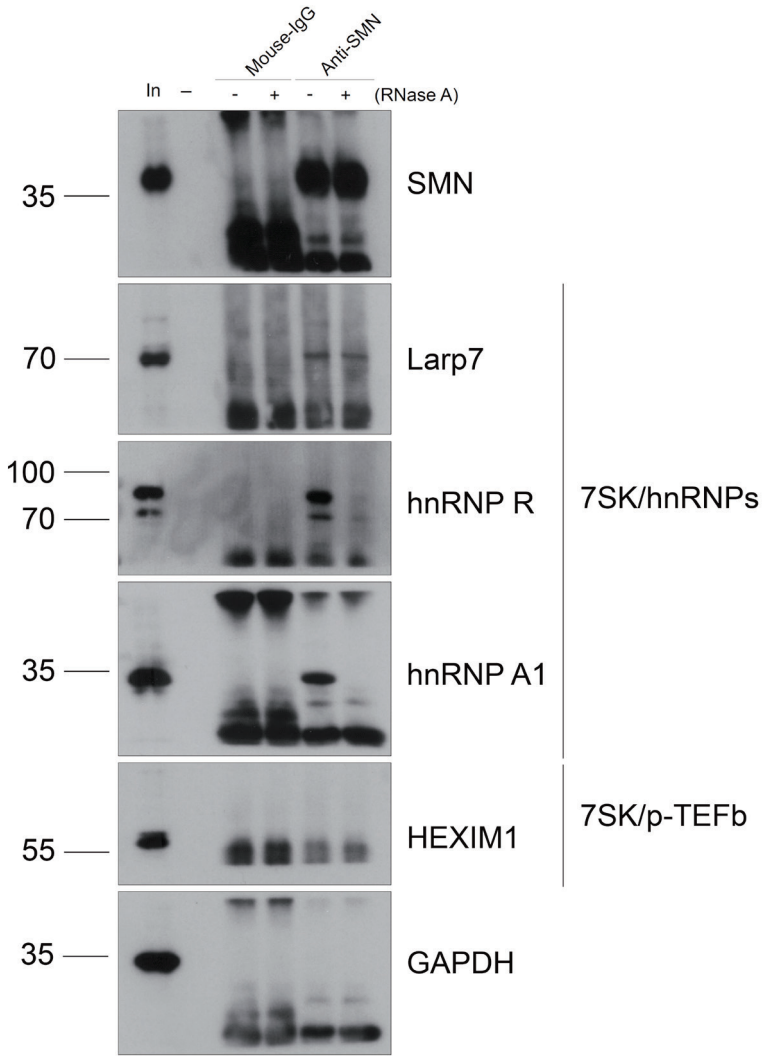

Figure 61: Western blot analysis of proteins that are co-immunoprecipitated by Smn antibody.

Smn can co-immunoprecipitate hnRNP R, Larp7, hnRNP A1 without RNase A treatment. After RNase A treatment, the binding of hnRNP R, hnRNP A1 to Smn is abolished. Larp7 still can bind with Smn after RNase A treatment. This indicates that Smn binds hnRNP R, hnRNP A1 indirectly, but binding to Larp7 is direct.

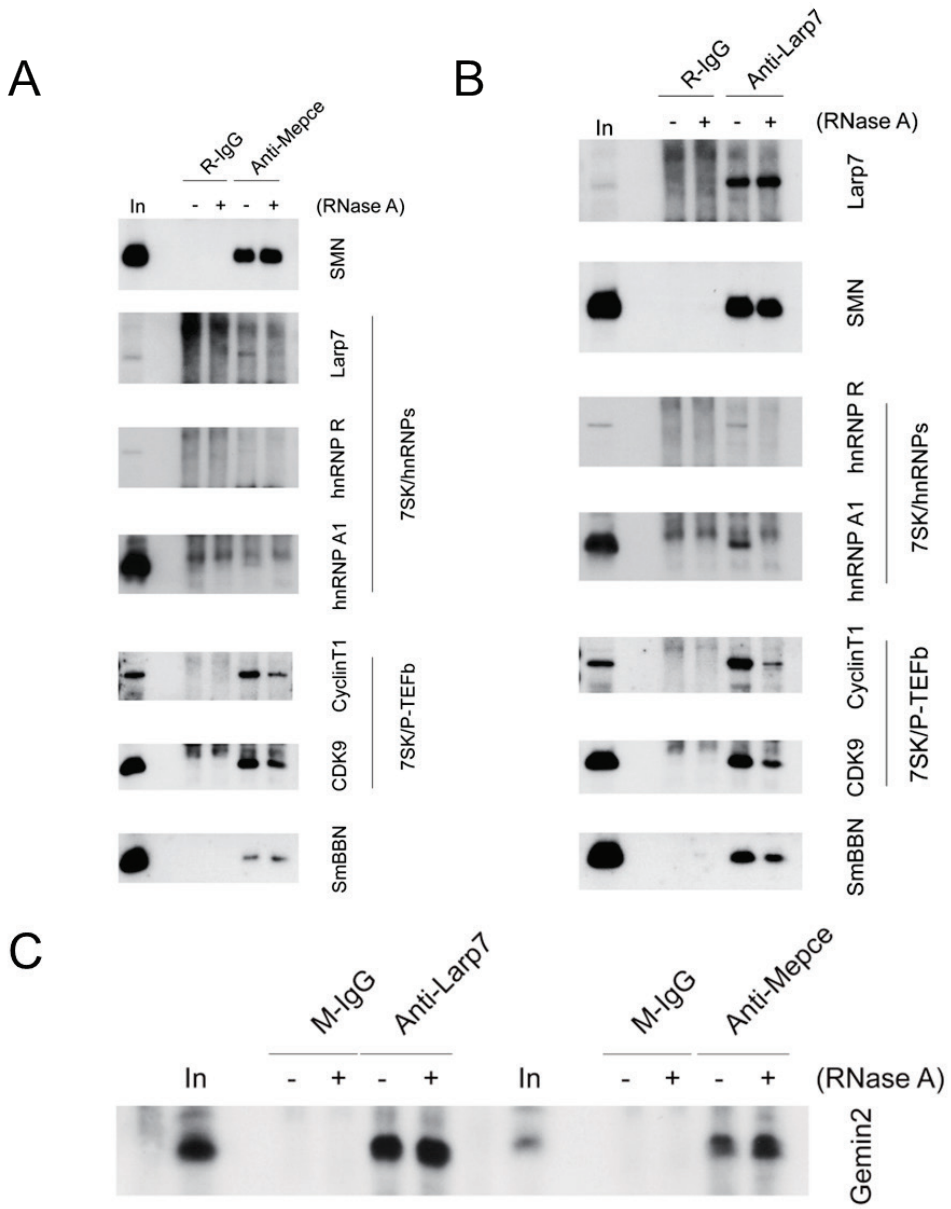

Figure 62: Western blot analysis of proteins that are co-immunoprecipitated by Mecpe2 and Larp7 antibody from total lysate of NSC34 cells without or with RNase A treatment.

Mepce can co-immunoprecipitate hnRNP R, hnRNP A1, Larp7, CyclinT1, CDK9, Smn, SmBBN without RNase A treatment. After RNase A treatment, the binding of hnRNP R, hnRNPA1, Larp7 binding to MEPCE is abolished. CyclinT1, CDK9, Smn, SmBBN still can bind with MEPCE after RNase A treatment. Larp7 can co-immunoprecipitate hnRNP R, hnRNP A1, Larp7, CyclinT1, CDK9, Smn, SmBBN and Gemin2 without RNase A treatment. After RNase A treatment binding of hnRNP R, hnRNP A1 to Larp7 is abolished, CyclinT1, CDK9, Smn, SmBBN still can bind with

Larp7 after RNase A treatment, indicating that Mecpe2 binds hnRNP R, hnRNP A1, Larp7 indirectly but binds CyclinT1, CDK9, Smn, SmBBN directly.

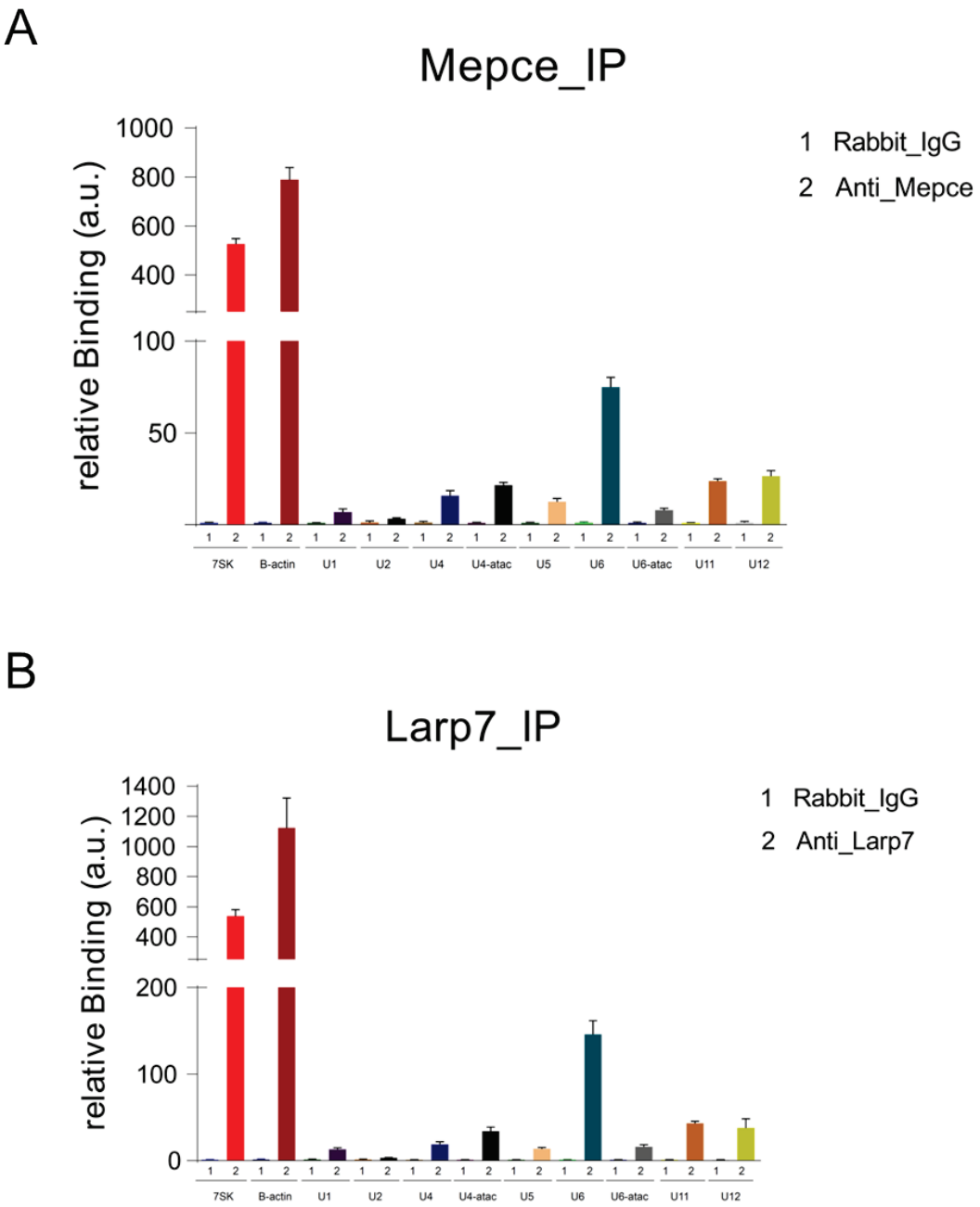

Figure 63: RIP-qPCR using anti-MEPCE and Larp7 antibodies

Fig A shows the qPCR used to check whether 7SK and other RNAs are pulled down by the MEPCE antibody.

Fig B shows the qPCR to check whether 7SK and other RNAs are pulled down by the Larp7 antibody

4.13. RNA determinants of Smn binding to the 7SK snRNP

As an additional approach to investigate the interactions of proteins with 7SK I performed RNA pulldown experiments in which 7SK snRNA generated by *in vitro* transcription is coupled to streptavidin beads through a biotinylated antisense oligonucleotide and incubated with cell lysate. The previous data showed that #6 biotinylated antisense oligonucleotides could efficiently pull down 7SK. The #5 oligo also bound but cannot be used when the region between the SL2 and SL3 is abolished. Therefore, I decided to use oligonucleotide #6 for further experiments. This oligonucleotide binds to the region between SL3 and SL4, predicting to not perturb binding of proteins to SL1, 2, 3 or 4. As an *in vitro* binding assay, all the 7SK mutations can bind on the streptavidin magnetic beads after coupling of biotinylated #6 oligo. Smn can bind with all 7SK mutations except ΔSL123 (**Figure 64**). Putting a GFP spacer sequence between SL1 and SL3 can rescue Smn binding (**Figure 65**). This indicates that besides Larp7 also other proteins are needed to facilitate Smn recruiting to the 7SK/hnRNP complex. Additionally, I found that hnRNP A1 binding occurred in a similarly manner to as hnRNP R binding with 7SK, and this binding could be abolished when SL3 or SL123 are deleted, which is consistent with previous data.

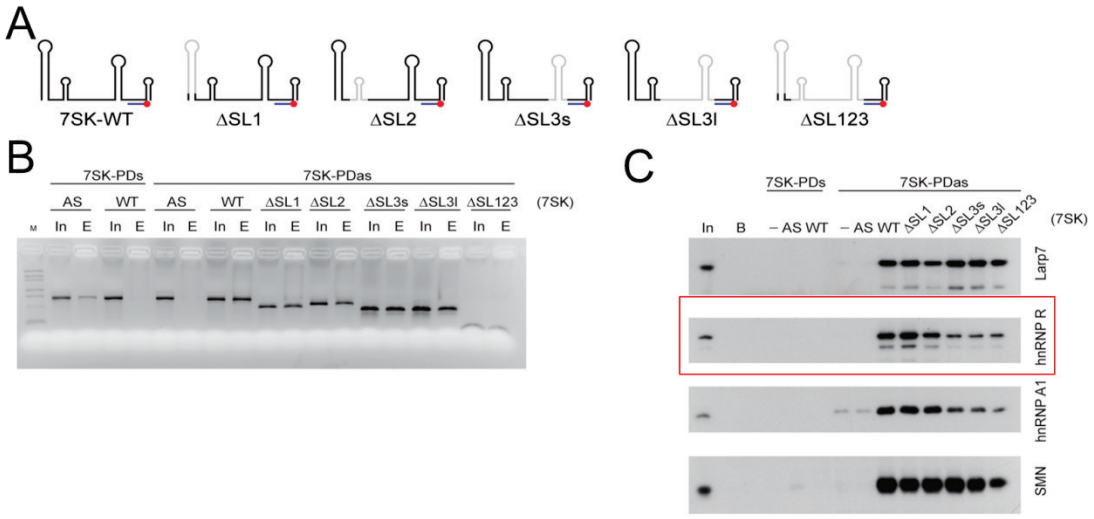

Figure 64: RNA determinants of Smn binding to the 7SK snRNP (A) Diagram of 7SK mutations used for testing with Biotin antisense oligonucleotides for pulldown experiments. (B) Immobilization of *in vitro* transcribed 7SK snRNAs on streptavidin beads using a biotinylated antisense oligonucleotide. Agarose gel electrophoresis of the eluted RNA (E, 100% loading) and the RNA Input (In 1ug each). Lane M, RiboRuler Low Range RNA Ladder from Thermo Fisher Scientific. (C) Western blot analysis of proteins bound to 7SK snRNAs. As a control, 7SK wild-type (WT) and antisense (AS) were purified using either an antisense oligonucleotide that binds to wild-type or a sense oligonucleotide that binds to antisense. In, input.

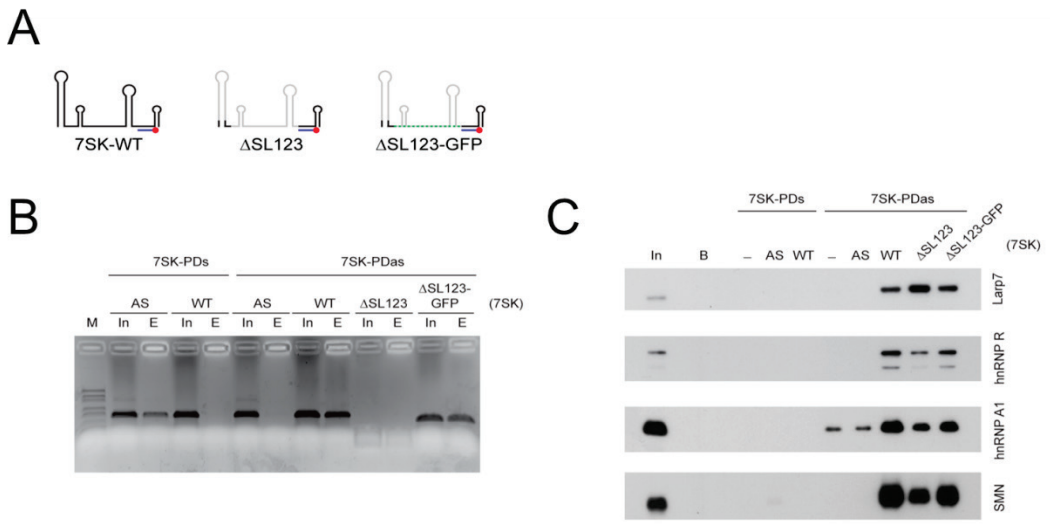

Figure 65: ΔSL123-GFP chimera RNA can rescue Smn binding (A) Diagram of

7SK WT, 7SK-ΔSL123 and ΔSL123-GFP isoforms and their putative binding with Biotin antisense oligonucleotide. (B) Immobilization of *in vitro*-transcribed 7SK snRNAs and 7SK-GFP chimeric RNA on streptavidin beads using a biotinylated antisense oligonucleotide. Agarose gel electrophoresis of the eluted RNA (E, 100% loading) and the RNA Input (In 1 ug each). Lane M, RiboRuler Low Range RNA Ladder from Thermo Fisher Scientific. (C) Western blot analysis of proteins bound to 7SK snRNAs. As a control, 7SK wild-type (WT) and antisense (AS) were purified using either an antisense oligonucleotide that binds to wild-type or a sense oligonucleotide that binds to antisense. In, input.

4.14. SmBBN interacts with the core 7SK snRNP

As a next step, I also investigated another snRNP protein SmBBN which binds with Smn directly and plays a very important role in the U1 snRNP assembly. I did the Co-IP by using SmBBN antibody to check SmBBN binding to 7SK/hnRNP complex and whether this interaction depends on RNA or not. After RNase A treatment, I found that Smn and Larp7 still bind with SmBBN, but hnRNP R, and hnRNP A1 binding are abolished. HEXIM1 does not bind with SmBBN, which is is consistent with previous data [65] (**Figure 66**). Additionally, I also did qPCR to confirm that SmBBN can bind 7SK and U1 (**Figure 67**).

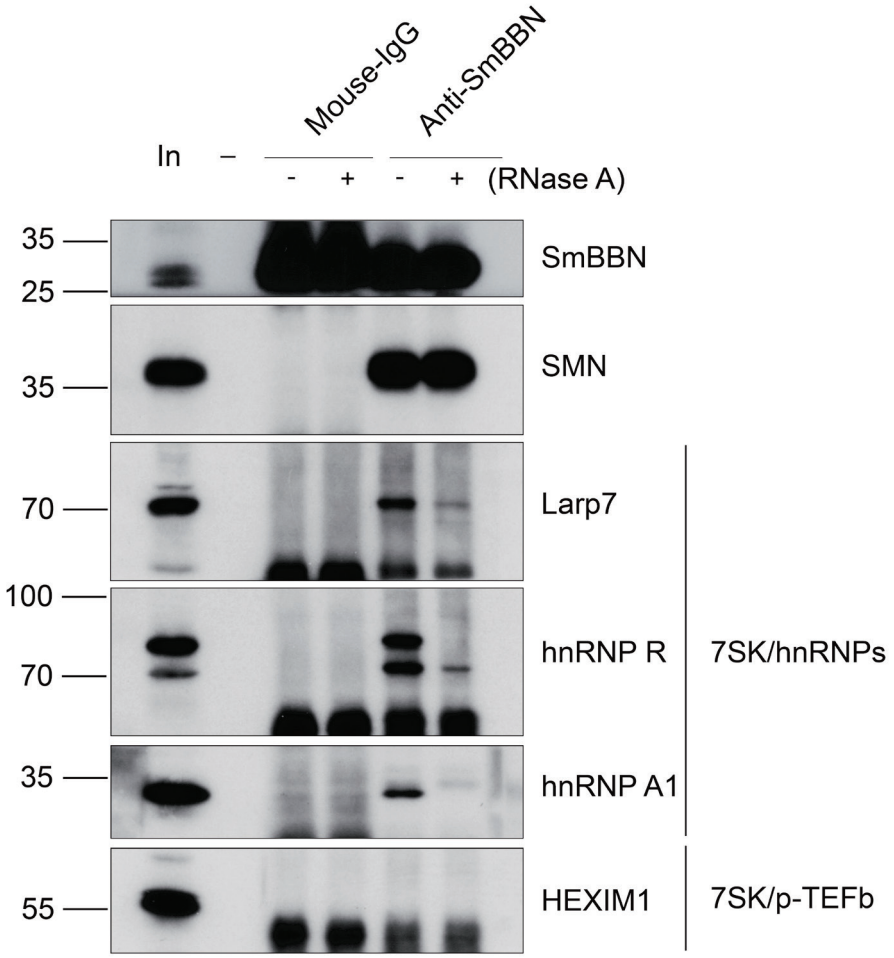

Figure 66: Western blot analysis of proteins that are co-immunoprecipitated by SmBBN antibody in the total lysate of NSC34 cells.

SmBBN can co-immunoprecipitate hnRNP R, hnRNP A1, Larp7, Smn without RNase A treatment. After RNase A treatment, binding of hnRNP R, hnRNPA1, and binding to SmBBN are abolished. In contrast, Smn, Larp7 still can bind with SmBBN after RNase A treatment. This indicates that SmBBN binds hnRNP R, hnRNP A1 indirectly, and binds Smn and Larp7 directly. SmBBN cannot co-immunoprecipitate HEXIM1, with or without RNase A treatment, indicating that SmBBN does not associate with the 7SK/HEXIM1/PTEFb complex.

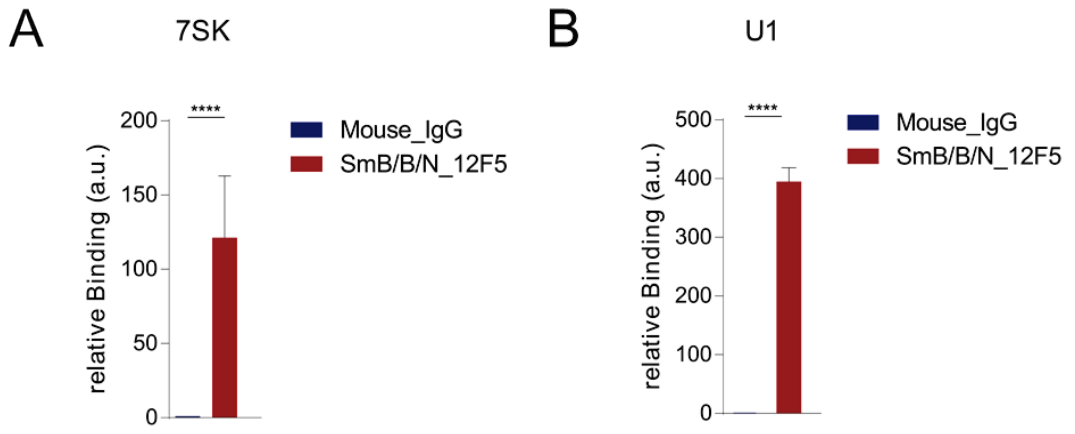

Figure 67: qPCR analysis for testing interaction of 7SK and U1 with SmB/B/N after immunoprecipitation

4.15. Smn interacts with 7SK/hnRNP in the nucleus and cytosol

In order to investigate whether Smn interacts directly or indirectly with 7SK/hnRNP in the cytosol or nucleus, I did the Co-IP by using Smn antibody to check Smn binding to 7SK/hnRNP complex and its dependence on the presence of RNA. I found that Smn still binds Larp7 after RNase A treatment in the nuclear and cytosolic fractions. Smn only binds hnRNP R short isoform after RNase A treatment in the nuclear and cytosolic fractions. Additionally, Smn binding to hnRNP A1 was abolished both in the nucleus and in the cytosol after RNase A treatment (**Figure 68**).

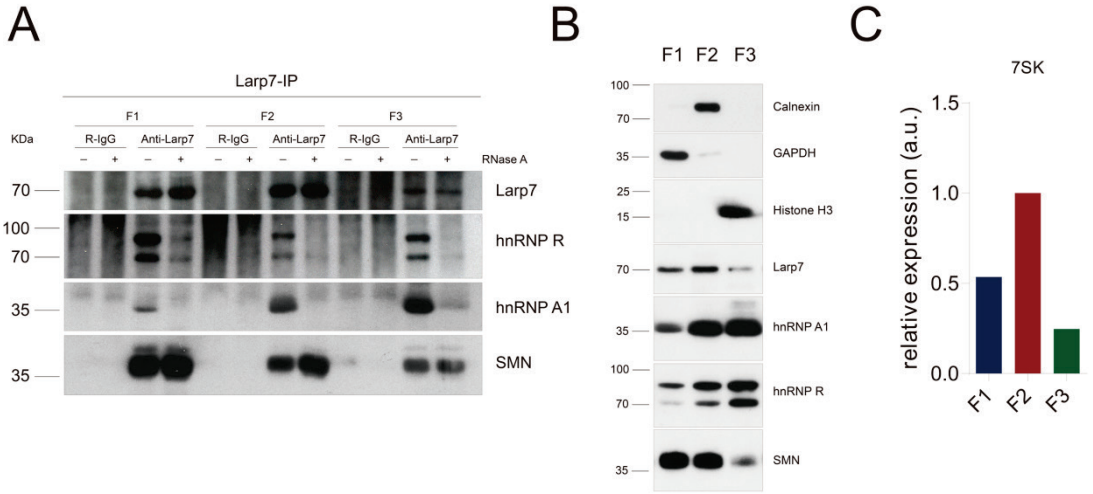

Figure 68: Western blot analysis of proteins that are co-immunoprecipitated by Larp7 antibody in different subcellular fractions of NSC34 cells

Smn can co-immunoprecipitate hnRNP R, hnRNP A1 without RNase A treatment in

F123 fractions. After RNase A treatment, the binding of hnRNP R, hnRNP A1 to Smn is abolished in F123 fractions, In contrast, Larp7 can still can interact with Smn after RNAse A treatment in F123 fractions, indicating that Smn binding to hnRNP R, hnRNP A1 is indirect, but binding to Larp7 is direct in F123 fractions .

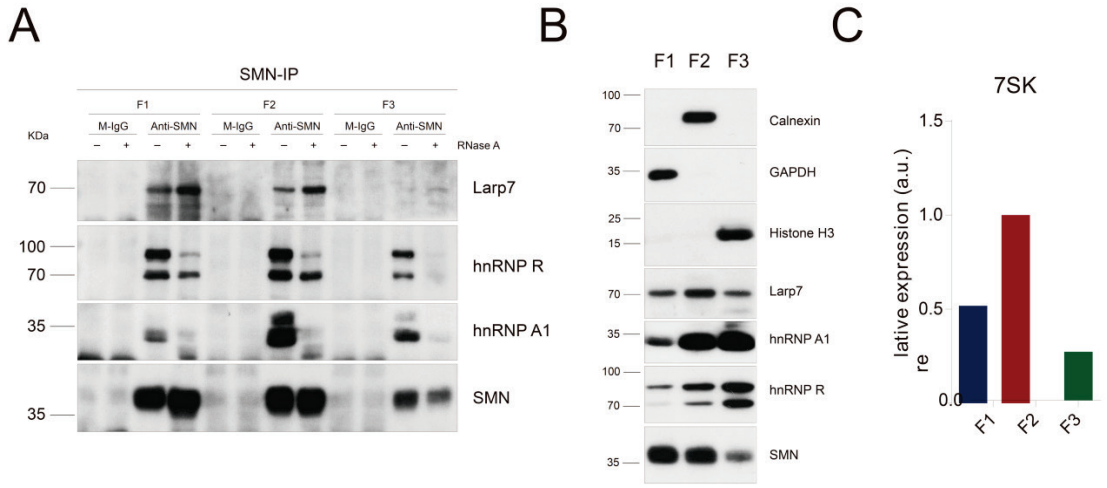

Figure 69: Western blot analysis of proteins that are co-immunoprecipitated by Smn antibody in different subcellular fractions of NSC34 cells

Larp7 can co-immunoprecipitate hnRNP R, hnRNP A1 without RNase A treatment in F123 fractions. After RNase A treatment, binding of hnRNP R, hnRNP A1 to Larp7 is abolished in F123 fractions. In contrast, Larp7 still can interact with Smn after RNase A treatment in F123 fractions, indicating that Larp7 binds hnRNP R, hnRNP A1 indirectly, but binds Smn directly in F123 fractions(**Figure 69**).

4.16. Transcription-dependent balance between 7SK/P-TEFb and 7SK/hnRNP complexes

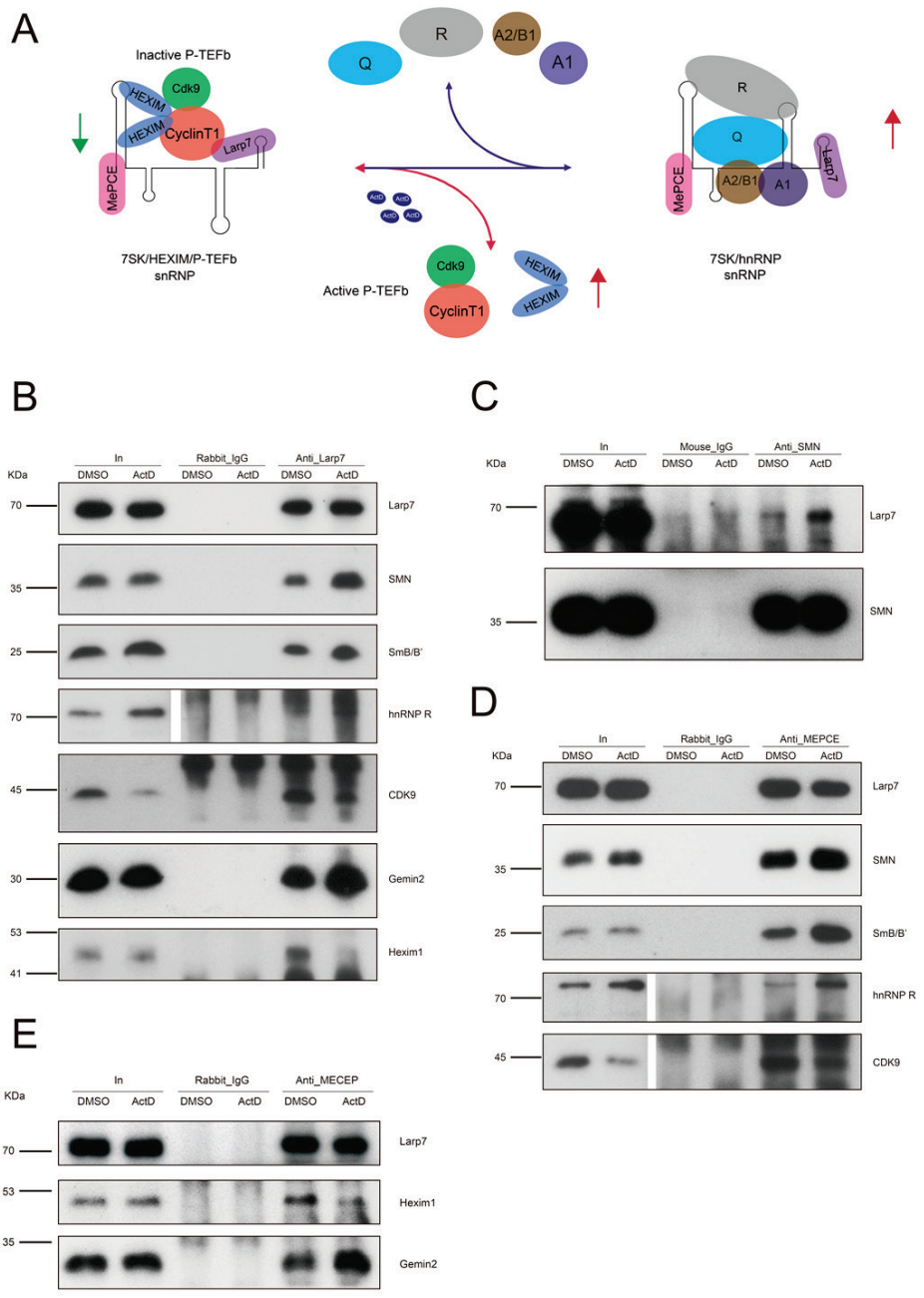

Figure 70: Western blot analysis of proteins that are co-immunoprecipitated by Larp7 antibody in total cellular lysate of NSC34 cells after treatment with Actinomycin D (RNA Pol inhibitor) (control with 20% DMSO).

For all the samples, the same amount of total protein was used after measuring the concentration by BCA kit. I found that Larp7 co-immunoprecipitated hnRNP R, hnRNP A1, Smn. This interaction is increased after Actinomycin D (RNA Pol inhibitor)

or flavopiridol treatment comparing the control. Interaction with CDK9 which is co-immunoprecipitated by Larp7 is reduced. This indicates that the assembly of the 7SK/ hnRNPs complex is increased and assembly of the 7SK/HEXIM1/PTEFb complex is reduced after Actinomycin D treatment (**Figure 70**).

4.17. Co-sedimentation assay

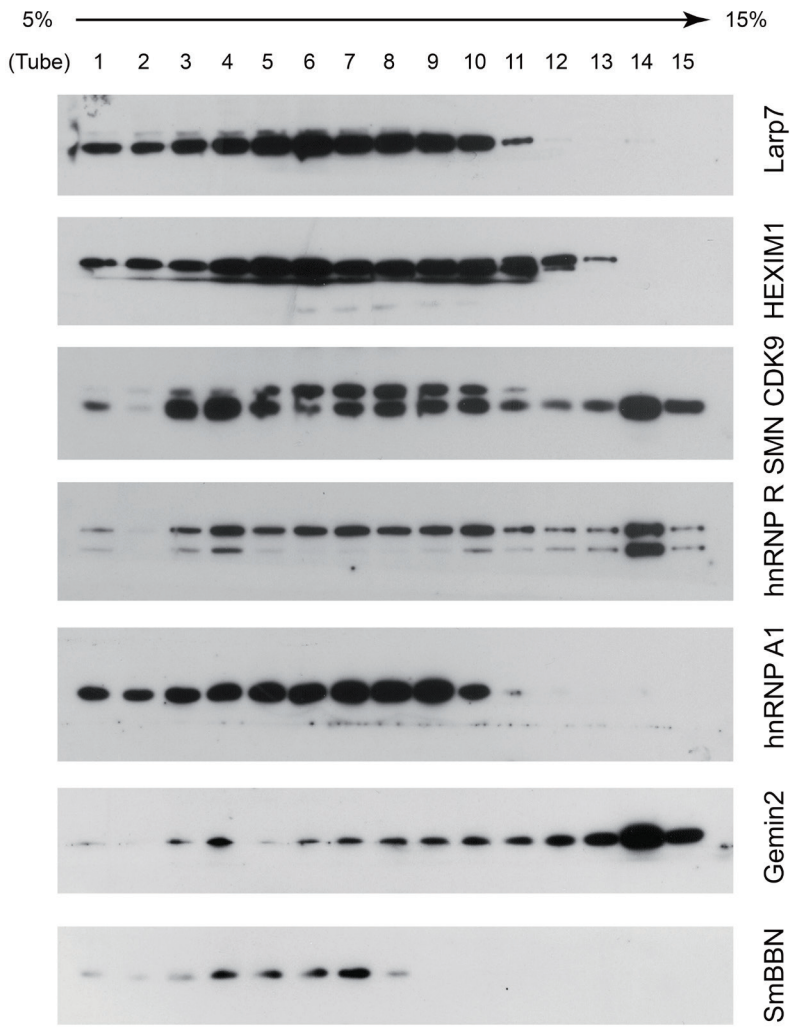

Figure 71: Western blot analysis of the proteins in different fractions of the Sucrose gradient.

Mostly HEXIM1 and CDK9 cosegregate with Larp7, Partly Smn, hnRNPR, hnRNP A1, Gemin2, SmBBN cosegregate with Larp7 (**Figure 71**).

5. Discussion

So far, most previous studies on the pathophysiology of motoneuron diseases such as SMA or ALS have focused on altered microRNA and protein functions, including those of RNA binding proteins, but the role of noncoding RNAs for motoneuron functionality and maintenance is still not clear. In my Ph.D. I have investigated the interaction of hnRNP R with the noncoding RNA 7SK and have identified a novel 7SK subcomplex containing the SMA-determining protein SMN.

Using a number of *in vitro* and *in vivo* experiments I found that hnRNP R binds SL1 and SL3 of 7SK. Rescue experiments have shown that 7SK WT, but not 7SK with deletion of the SL1 or SL3 region, restores axon growth of motoneurons depleted of 7SK [67]. These findings indicate that hnRNP R binding to 7SK is important for axon growth. However, it needs to be taken into account that hnRNP R is only one of several hnRNPs binding proteins for 7SK, and that deletion of SL1 and SL3 will also abolish binding of these hnRNPs to 7SK. For example, in addition to hnRNP R, hnRNP A1, A2 and Q bind to SL3 of 7SK [116]. This indicates that multiple 7SK/hnRNP subcomplexes exist and that 7SK simultaneously regulates the functions of several hnRNPs, each of which is embedded in distinct and overlapping mRNP particles. Nevertheless, the finding that knockdown of hnRNP R affects axon growth of motoneurons in a manner similar to knockdown of 7SK is consistent with the notion that 7SK/hnRNP R complexes contribute to motoneuron development in general and axonogenesis in particular [117].

Like many hnRNPs, hnRNP R is abundant in the nucleus where it regulates pre-mRNA processing. Accordingly, iCLIP tags of nuclear hnRNP R are located predominantly in intronic regions [67]. Outside the nucleus, hnRNP R is also detectable in the cytosol of motoneurons where it has been associated with functions in axonal mRNA transport [74] This observation is in agreement with an enrichment of cytosolic hnRNP R iCLIP tags in 3'UTRs. The surprising finding that 7SK RNA is also detectable in the cytosol led to the hypothesis that 7SK/hnRNP R complexes exert functions in the cytosol that are distinct from their roles in transcriptional regulation in the nucleus [67].

In order to identify novel 7SK protein interactors in an unbiased manner I pulled down endogenous 7SK complexes using an RNA antisense oligonucleotide complementary to a region located in SL1 of 7SK that is normally targeted by HEXIM1. Therefore, the

pulldown oligo enriched for 7SK complexes not containing HEXIM1 and P-TEFb which allowed me to selectively investigate the composition of 7SK/hnRNP complexes. Using this pulldown strategy, mass spectrometry of the bound proteins by Jakob Bader and Felix Meissner (MPI Munich) revealed the SMN complex as interaction partner of 7SK. The SMN complex mediates spliceosomal snRNP biogenesis and is composed of SMN and Gemins2-8. The SMN complex is present in nuclear structures termed gems and in the cytosol where it fulfills its function in spliceosomal snRNP production. Through a series of immunoprecipitation experiments I found that, in addition to SMN itself, also Gemin2 and SmB/B' interact with Larp7 and Mepce. From these data it can be inferred that the SMN complex interacts as a whole with 7SK particles. Additionally, I found that SMN associates with 7SK complexes containing hnRNP R but not with 7SK/HEXIM1/pTEFb complexes. Thus, the interaction between SMN and 7SK complexes seems to be tightly regulated.

SMN has previously been shown to interact with hnRNP R [65, 74, 118]. Using immunoprecipitation in the presence or absence of RNase I could show that the interaction of SMN with hnRNP R was RNase-sensitive. This is in agreement with a study showing that also the interaction of FUS with SMN is mediated through RNA [119]. I observed that knockdown of 7SK abolished binding of SMN to hnRNP R. Thus, the interaction between SMN and hnRNP R is mediated by 7SK. This has important implications given that SMN localizes in close proximity to hnRNP R in axons of motoneurons [66] and that hnRNP R regulates the axonal transport of *β-actin* mRNA in a SMN-dependent manner [74]. It could be envisaged that 7SK is part of such transport mRNPs and acts as a scaffold that brings together RBPs and their target mRNAs. Such a model is supported by the finding that depletion of 7SK or hnRNP R alters the axonal levels of a common set of transcripts in motoneurons [67].

In contrast to its RNA-dependent binding to hnRNP R, SMN interacted with the 7SK core components Mepce and Larp7 in an RNA-independent manner. In agreement with this finding, LARP7 and MePCE have previously been shown to interact with each other independently of 7SK [8]. This suggests a model according to which the SMN complex is recruited to 7SK particles through direct protein contacts. Given that Larp7 and Mepce are part of the core 7SK RNP it was surprising to find an association of SMN with 7SK/hnRNP but not with 7SK/HEXIM1/pTEFb complexes. What could be the molecular basis for this selectivity? It has previously been shown that pTEFb is recruited to 7SK not only by HEXIM1 that interacts with SL1 but also

requires the presence of LARP7 [14]. Furthermore, CDK9 directly interacts with LARP7 [13]. Thus, as part of 7SK/HEXIM1/pTEFb complexes LARP7 might be inaccessible for binding with SMN through steric hindrance or conformational changes induced by CDK9 binding to LARP7.

What could be the functional significance of SMN binding to 7SK? In order to address this question I first investigated the subcellular distribution of 7SK complexes. For this purpose I optimized a fractionation procedure using digitonin which selectively permeabilizes the cholesterol-containing outer membrane. This way, a cytosolic fraction can be obtained that is devoid of organelles and nuclear soluble proteins. Using this fractionation procedure I detected 7SK and Larp7 not only in the nuclear fraction, where they were most abundant as expected, but also in the cytosol. This finding is in agreement with *in situ* hybridization data revealing cytosolic 7SK in motoneurons [67]. With the help of pulldown experiments I could then show that 7SK complexes in the cytosol contain hnRNP R and SMN, indicating regulatory interactions between 7SK and SMN complexes in this cellular compartment.

The release of P-TEFb from 7SK is governed by transcription and can be induced by the transcriptional inhibitor ActD. Following ActD exposure I observed increased interaction of SMN with 7SK complexes. Given that 7SK functions in transcriptional regulation in the nucleus and SMN in snRNP biogenesis in the cytosol it is tempting to speculate that this finding indicates a mechanism whereby cells regulate the production of snRNPs according to their transcriptional demand. This possibility could be investigated further in future experiments by knocking down Mepce or Larp7 or both and then immunoprecipitate SMN to investigate whether the composition of the SMN complex is altered upon removel of 7SK complexes. Furthermore, the effect of transcriptional inhibition or activation on snRNP biogenesis could be measured by immunoprecipitating SmB/B' followed by qPCR analysis of bound snRNAs. Alternatively, an antibody against the 2,2,7-trimethylguanosine (TMG) cap structure, which is an important functional characteristic of snRNAs and required for transport of snRNPs from the cytosol to the nucleus during biogenesis [120], could be used for immunoprecipitation.

In summary, in this Ph.D. thesis I have investigated the interaction of hnRNP R with 7SK RNA and identified SMN as a novel interactor of 7SK complexes. The data presented here suggest that 7SK acts as a scaffold not only for nuclear proteins in response to transcriptional changes but also to the cytosolic machinery implicated in

spliceosome biogenesis. Cells might utilize such a mechanism to fine-tune the production of the splicing machinery according to the levels of nascent pre-mRNA being generated in the nucleus. This way, an overproduction of snRNPs could be avoided which, otherwise, might lead to defects in splicing or even aggregation of proteins and protein-RNA complexes involved in the splicing machinery.

6. Appendix

Primer list

U6+7SKWT-a	GGACTAGTGATCCGACGCCGCCATCT
U6+7SKWT-b	CAGCCAGATCGCCCTCACATCCAAACAAGGCTTTTCT CCAAGG
U6+7SKWT-c	GGAGAAAAGCCTTGTTTGGATGTGAGGGCGATCTGG
U6+7SKWT-d	GGACTAGTCAAAAGAAAGGCAGACTGCCA
U6+7SKWT-a1	CCATCGATGATCCGACGCCGCCATCTCT
U6+7SKWTd1	CCATCGATCAAAAGAAAGGCAGACTGCCA
ClaIFor(forsequen	GACAGGCCCGAAGGAATAGAAGAAG
ClaIRev(forsequen	TTACGACATTTTGGAAAGTCCCGTTGA
U6+7SKWT-a2	TTTTTTCCATCGATGATCCGACGCCGCCATCTCT
U6+7SKWT-d2	TATAATCCATCGATCAAAAGAAAGGCAGACTGCC
U6+7SKMM3-c	GCTAGAACCAGGACACTAGCTCTCCCGGTCCATAGT ACCTGAACGTAGG
U6+7SKMM3-b	CCTACGTTCAGGTACTATGGACCGGGAGAGCTAGTG TCCTGGTTCTAGC
pJET1.2forward	CGACTCACTATAGGGAGAGCGGC
pJET1.2reverse	AAGAACATCGATTTTCCATGGCAG
EGFP-qPCRup	ACGTAAACGGCCACAAGTTC
EGFP--qPCRdown	AAGTCGTGCTGCTTCATGTG
M13/pUCforward	GTAAAACGACGGCCAGT
M13/pUCreverse	CAGGAAACAGCTATGAC
7SK_elute_3	GCCAGGGTTGATTCGGC
7SK_pulldown_3neg	GCCGAATCAACCCTGGC
T7up	CAGGAAACAGCTATGACCAT
T7down	TTTCTACAGATCCTCTAGA
HIUP	GTGAAATGTCTTTGGATTTGGGAATCTT
HIDOWN	GATCTGGTCTAACCAGAGAGACCCAGTA
7SK_elute	TGGCTGCGACATCTGTC
7SK_neg_elute	TGGCTGCTTGATCTGTC
7SK_pulldown_2	GACAGATGTCGCAGCCAGATCGCCCTCACATCCB
7SK_elute_2	GGATGTGAGGGCGATCTGGCTGCGACATCTGTC
7SK_elute_3	GCCAGGGTTGATTCGGC
pJET1.2forward	CGACTCACTATAGGGAGAGCGGC
pJET1.2reverse	AAGAACATCGATTTTCCATGGCAG
mGapdhfor	GCAAATTCAACGGCACA
mGapdhrev	CACCAGTAGACTCCACGAC
hGapdhfor	GCAAATTCCATGGCACC
hGapdhrev	CGCCAGTGGACTCCACGAC
RT	GTCGTATCCAGTGCAGGGTCCGAGGTATTCGCACTG GATACGACAAACCTC
T7-7SKUP	TAATACGACTCACTATAGGGATGTGAGGGCGATCTG GCTGCGA

T7-7SKDN	AAAAGAAAGGCAGACTGCCACATGC
T7-7SKUPAS	TAATACGACTCACTATAGGGAAAAGAAAGGCAGACTGCCACATG
T7-7SKDNAS	GGATGTGAGGGCGATCTGGCTGCGA
7SKDN	GGTTCTAGCAGGGGAGCGCAG
7SKUP	GGATGTGAGGGCGATCTGGCT
7SK_F3	GCTGGCTAGGCGGGTGTCCC
7SK_R3	CTTGACCGAAGACCGGTCCTC
7SK_R4	GGAAGCTTGACTACCCTACGT
7SK_UP4	GGATGTGAGGGCGATCTGGCTG
7SK_DN4	AATTGATTACTATTAATAACTA
7SK_F5forSL13	GCTGCGACATCTGTCACCCGCT
7SKSL3F_R	AAAAGAAAGGCAGACTGCCACATGCAGCGCCTCATTTGGATGTGTCTCCTTGACCGAAGACCGGTCCTCCTCTAT
T7-SL1UP	TAATACGACTCACTATAGGGATGTGAGGGCGATCTGGCTGCGACATCTGTCACCCGCTGGCTAGGCGGGTGTCCCCTT
7SK_FforSL1	CTGTCACCCGCTGGCTAGGCGGGTGTCCCCTT
7SK_F5forSL13	GCTGCGACATCTGTCACCCGCT
SL1_For	GCTGGCTAGGCGGGTGTCCCCTT
SL1_Rev	GGGTGACAGATGTCGCAGCCAGA
SL3F_For	AGACACATCCAAATGAGGCGCTG
SL3F_Rev	CCTTGACCGAAGACCGGTCCTCCT
SL1_FF	CTGTCACCCCATTGATCGCCAGGGTTGATTCGGCTGATCTGGCTGGCTAGGCGGGTGTCCCCTTCCTCCCTCACCGCTCCATGTGCGTCCCTCCCGAAGCTGCGCGCTCGGTCGAAGAGGACGACCTTCCCCGAATAGAGGAGGACCG
SL1_F	CTGTCACCCCATTGATCGCCAG
SL3F_DN	GAGATGCTCTAGAAAGATTATAATCCATCGATCAAAAGAAAGGCAGACTGCCACATGCAGCGCCTCATTTGGATGTGTCTGGAGTCTTGGAAGCTTGACTACCCTACGTTCTCCTACAATGGACCTTGAGAGCTTGTTTGGAGGTTCTAGCAGGGGAGCGCAGCTACTCGTATACCCTTGACCGAAGACCGGTCCTCCTCTATTCGGGGAAGGT
DN	GAGATGCTCTAGAAAGATTATAA
SL3_FULLDN	GCTCTAGAAAGATTATAATCCATCGATCAAAAGAAAGGCAGACTGCCACATGCAGCGCCTCATTTGGATGTGTCTGGAGTCTTGGAAGCTTGACTACCCTACGTTCTCCTACAATGGACCTTGAGAGCTTGTTTGGAGGTTCTAGCAGGGGAGCGCAGCTACTCGTATACCCTTGACCGAAGACCGGTCCTCCTCTATTCGGGGAAG
SL1_FULLUP	CTGTCACCCCATTGATCGCCAGGGTTGATTCGGCTGATCTGGCTGGCTAGGCGGGTGTCCCCTTCCTCCCTCACCGCTCCATGTGCGTCCCTCCCGAAGCTGCGCGCTCGGTCGAAGAGGACGACCTTCCCCGAATAGAGGAGGACCG
7SK_F5forSL13	GCTGCGACATCTGTCACCCGCT
7SK_R5forSL1	ATGGACCTTGAGAGCTTGTTTG

7SK_FforSL3F	ATTGATCGCCAGGGTTGATTCG
7SK_RforSL3F	GCCTCATTTGGATGTGTCTCCT
SL3F_Rev1	CCCCTTGACCGAAGACCGGTCCTCCT
SL1_F	GGGCGATCTGGCTGCGACATCTGTCACCCGCTGGCTAG
SL1_R	AGAATATTGTAGGAGATCTTCTAGAAAGATTATAATCCATCGATCAAAAGAAAGGC
SL3F_F	GGGCGATCTGGCTGCGACATCTGTCACCCCATTGATCG
Primer_F	TGTCCCCTTCCTCCCTCAC
Primer_R	CGAAGACCGGTCCTCCTCTA
Primer_2_F	GGTGTCCCCTTCCTCCCT
Primer_2_R	CTATTCGGGGAAGGTCGTCC
7SL_F	CCTGTAGTCCCAGCTACTCG
7SL_R	CTGCTCCGTTTCCGACCTGG
Malat1_F2	TGCAGTGTGCCAATGTTTCG
Malat1_R2	AGTCTGCTGTTTCCTGCTCC
7SK_pull_down_5_AS_Elute	CTCGTATACCCTTGACCGAAGACC
7SK_pu_wn_5_Elute	GGTCTTCGGTCAAGGGTATACGAG
EGFP-For	CTACCCCGACCACATGAAGC
EGFP-Rev	GTAGTTGCCGTCGTCCTTGA
Biot_7SK_PD_RNA_4_Scrambl	B-CAAUCAUACUGCUCACU
Bio_TEG_7SK_PD_5_sho	BIOTIN-TEG-CCTTGACCGAAGACCGG
7SK_PD_5_Elute_short	CCGGTCTTCGGTCAAGG
7SK_PD_RNA_4_Scrambl	BIOTIN-CAAUCAUACUGCUCACU
Bi_TEG_SK_PD_5_sh_AS	BIOTIN-TEG-CCGGTCTTCGGTCAAGG
7SK_F5forSL13	GCTGCGACATCTGTCACCCGCT
7SK_R5forSL1	ATGGACCTTGAGAGCTTGTTTG
7SK_FforSL3F	ATTGATCGCCAGGGTTGATTCG
7SK_RforSL3F	GCCTCATTTGGATGTGTCTCCT
tRNA_F	GTCAGGATGGCCGAGCGGTCTAAG
tRNA_52R	AGGGGAGACTGCGACCTGAA
mNEAT1_F	ACCCTTTTTCATGGGGGTAG
mNEAT1_R	GCTGGATGGAGGCTTGTTTA
T7_7SK_SL1P_F	TAATACGACTCACTATAGGGATGTGAGGGCGATCTGGCTGCGCCCCTTCCTCCCTCACCGCTCCATGTG
T7_7SK_SL1F_F	TAATACGACTCACTATAGGGATGCCGCTCCATGTGCGTCCCTCCCGAAGCT
T7_7SK_SL123F_F	TAATACGACTCACTATAGGGATGCCGCTCCATGTCCAAGACTCCAGACACATCCAAATGAGGCGCTGCATGTGGCAGTCTGCCTTTCTTT
T7_SL2F_F	TAATACGACTCACTATAGGGATGTGAGGGCGATCTG

	GCTGCGACATCTGTCACCCCATTGATCGCCAGGGTT GATTCGGCTGATCTGGCTGGCTAGGCGGGTGTCCCC TTCCTCCCTCACCGCTCCATGTGCCCGGTCTTCGGTC AAGGGTATA
T7_SL3F+ST_R	AAAAGAAAGGCAGACTGCCACATGCAGCGCCTCATTT GGATGTGTCTGGAGTCTTGGAATCCTCCTCTATTCGG GGAAGGTC
T7_SL3F-ST_R	AAAAGAAAGGCAGACTGCCACATGCAGCGCCTCATTT GGATGTGTCTGGAGTCTTGGAAGGTCCTCCTCTATTC GGGGAAGGT
Lap7_F2_for_sh2	GAAGAGGGAGAGGTGCAGC
Lap7_R2_for_sh2	TGCTTCCTCTTCACCTTTGAGA
7SK_pulldown_neg	Biotin-5-GACAGATCAAGCAGCCA-3
7SK_pulldown	Biotin-5-GACAGATGTCGCAGCCA-3
7SK_pulldown_2	5-GACAGATGTCGCAGCCAGATCGCCCTCACATCC-3-Biotin
7SK_pulldown_3	Biotin-5-GCCGAATCAACCCTGGC-3
7SK_pulldown_4	Biotin-5-GACAGAUGUCGCAGCCA-3
7SK_pull_down_5	Biotin-5-CTCGTATACCCTTGACCGAAGACC-3
7SK_pull_down_6	Biotin-5-GATGTGTCTGGAGTCTTGGA-3
7SK_pull_down_7	Biotin-5-CTTGACCGAAGACCGGTCCT-3
7SK_pull_down_8	5-CGCAGCTACTCGTATACCCTTGA-3-Biotin
7SK_pull_down_9	5-ATTTGGATGTGTCTGGAGTCTTG-3-Biotin
7SK_pull_down_10	Biotin-5-GTCTGGAGTCTTGGAAGCTTGA-3

Primary antibody antibody list

Primary antibody	Function	Dilution	Company and Order number
Mouse anti-Gapdh(6C5)	WB	1:5000	Calbiochem CB1001
Rabbit anti-hnRNP R	WB and IP	1:5000	Abcam ab30930
Rabbit anti-Larp7	WB	1:1000	MyBioSource MBS2530149
Mouse anti-hnRNP A1(4B10)	WB and IP	1:2000	Santa Cruz sc-32301
Mouse anti-hnRNP A2/B1 (C-3)	WB	1:2000	Santa Cruz sc-393674
Mouse anti-Cyclin T1 (C-6)	WB and IP	1:1000	Santa Cruz sc-271575
Rabbit anti-CDK9 (D-7)	WB and IP	1:1000	Santa Cruz sc-13130
Rabbit anti-HEXIM1	WB	1:1000	Bethyl A303-113A-M
Goat anti-calnexin	WB	1:5000	Sicgen AB0041-200
Rabbit anti-Histone H3	WB	1:5000	Abcam ab18521
Mouse Anti-Smn	WB and IP	1:3000	BD 610646
Mouse Anti-Gemin2 (3F8)	WB	1:2000	Santa Cruz sc-32806
Mouse Anti-Gemin2	WB	1:2000	Merck 05-1540
Mouse anti-SmBBN(12F5)	WB and IP	1:1000	Santa Cruz sc-130670
Rabbit anti-LARP7 antibody - C-terminal region	IP		Biozol ASB-ARP40847_P050
Rabbit anti-LARP7 antibody	IP		Proteintech Group 17067-1-AP
Rabbit anti-MEPCE	IP		Proteintech Group 14917-1-AP
normal Mouse IgG	IP		Santa Cruz sc-2025
normal Rabbit IgG	IP		PeproTech 500-P00-500ug

Secondary antibody list

Secondary Antibodies	Dilution for WB	Company and Order number
Donkey Anti-Rabbit IgG (H+L)	1:5000	Jackson 711-005-152
Goat anti-mouse IgG affiniPure(H+L)	1:5000	Jackson 115-035-003
Donkey Anti-Goat IgG (H+L)	1:5000	Jackson 705-005-003

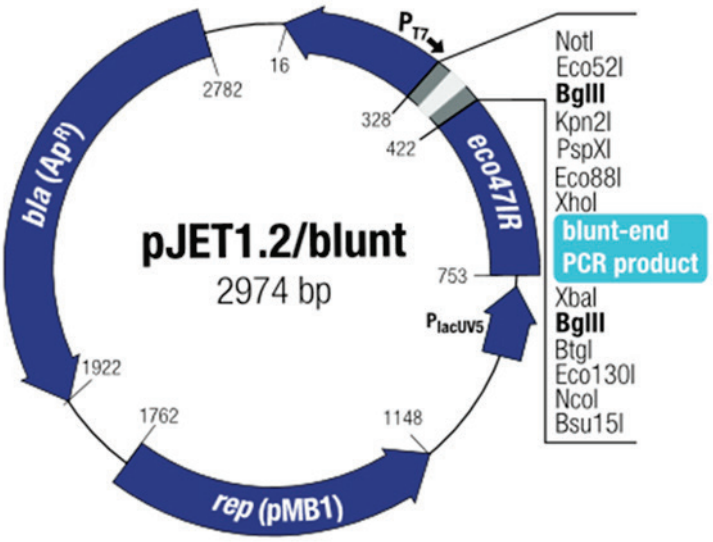

Map of pJET1.2 plasmid

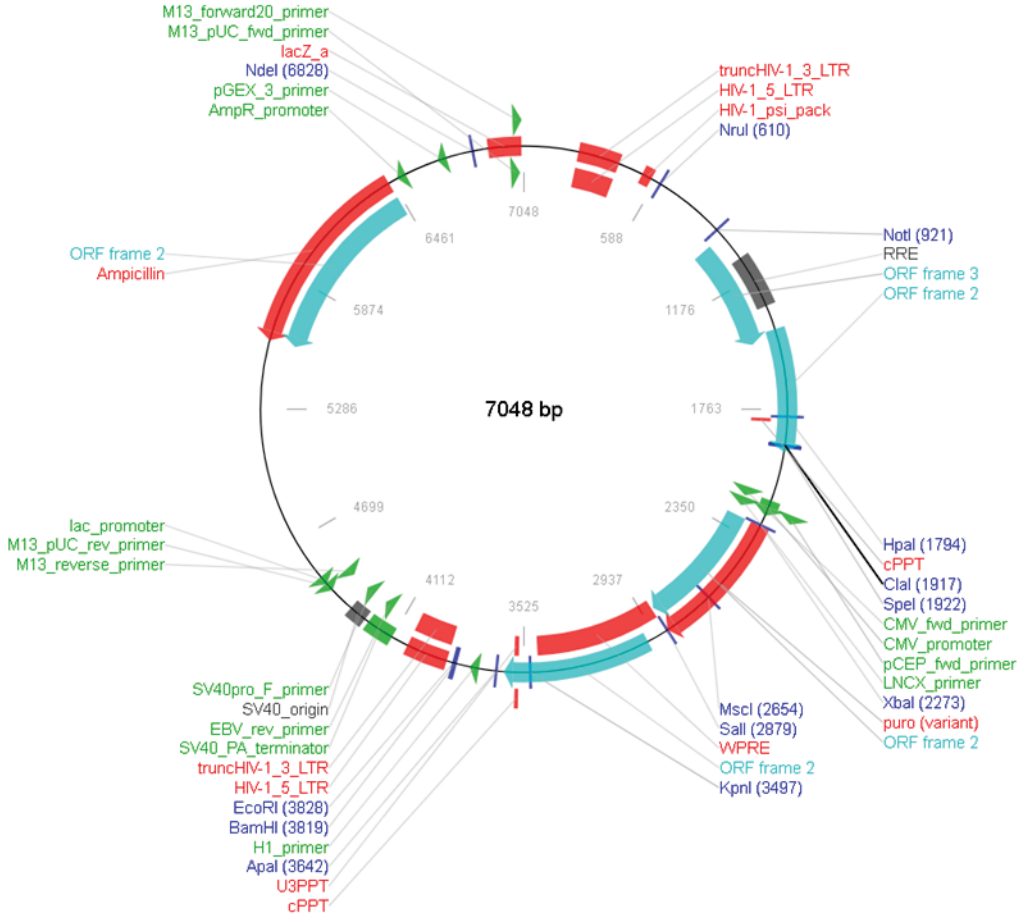

Map of pSIH plasmid

Abbreviation index

A	adenine
aa	amino acid
Amp	ampicillin
APS	ammonium persµLfate
asRNA	antisense RNA
ATP	adenosine triphosphate
BSA	bovine serum albumin
C	cytosine
cDNA	complementary DNA
CDS	coding sequence
CFU	colony forming units
Cm	chloramphenicol
CO_2	carbon dioxide
DNA	deoxyribonucleic acid
DNase	deoxyribonuclease
dNTP	deoxyribonucleotide
ds	double - stranded
DTT	dithiothreitol
EDTA	ethylenediamine tetraacetate
EtOH	ethanol
gDNA	genomic DNA
GFP	green fluorescent protein
H_2O	water (distilled)
HCl	hydrochloric acid
mRNA	messenger RNA
NaCl	sodium chloride
NaOH	sodium hydroxide
OD_{550}	optical density at a wavelength of 550 nm
OE	overexpression
ORF	open reading frame
PAA	polyacrylamide
PAGE	polyacrylamide gel electrophoresis
PBS	phosphate buffered saline
P:C:I	phenol:chloroform:isoamyl alcohol

PCR	polymerase chain reaction
RBP	RNAbinding protein
RBS	ribosome binding site
RNA	ribonucleic acid
RNase	ribonuclease
RNA-seq	RNA sequencing
RT	reverse transcription
rRNA	ribosomal RNA
siRNA	short interfering RNA
SDS	sodiumdodecylsµLfate
ss	single-standed
TAE	Tris/Acetate/EDTA
TBE	Tris/Borate/EDTA
TEMED	tetramethylethylendiamin
Tm	melting temperature
mRNA	messanger RNA
Tris	tris-(hydroxymethyl) aminomethan
tRNA	transfer RNA
TSS	transcriptional start site
UTP	uridine triphosphate
UTR	untranslated region
UV	ultraviolet
vol	volume
v/v	volume/volume
w/v	weight/volume in g/ml
WT	wild-type
SL	stem loop

Units

%	percent
°C	degree Celsius
A	ampere
Bp	base pair(s)
Ci	Curie
Da	Dalton
g	gram
L	liter
M	molar
min	minute(s)
molar	gram molecµLe
N	normality (volumetic)
nt	nucleotide(s)
pH	minus the decimal logarithm of the hydrogen concentration
rpm	rounds per minute
s/sec	second(s)
u	unit V Volt W Watt

Multiples

M	mega (10^{6})
k	kilo (10^{3})
c	centi (10^{-2})
m	milli (10^{-3})
µ	micro(10^{-6})
n	nano (10^{-9})
p	pico (10^{-12})

Reference

1. Wassarman, D.A. and J.A. Steitz, *Structural analyses of the 7SK ribonucleoprotein (RNP), the most abundant human small RNP of unknown function.* Mol Cell Biol, 1991. 11(7): p. 3432-45.
2. Gursoy, H.C., D. Koper, and B.J. Benecke, *The vertebrate 7S K RNA separates hagfish (Myxine glutinosa) and lamprey (Lampetra fluviatilis).* J Mol Evol, 2000. 50(5): p. 456-64.
3. Egloff, S., E. Van Herreweghe, and T. Kiss, *Regulation of Polymerase II Transcription by 7SK snRNA: Two Distinct RNA Elements Direct P-TEFb and HEXIM1 Binding.* Molecular and Cellular Biology, 2006. 26: p. 630-642.
4. Muniz, L., S. Egloff, and T. Kiss, *RNA elements directing in vivo assembly of the 7SK/MePCE/Larp7 transcriptional regulatory snRNP.* Nucleic Acids Research, 2013. 41(8): p. 4686-4698.
5. Jeronimo, C., et al., *Systematic analysis of the protein interaction network for the human transcription machinery reveals the identity of the 7SK capping enzyme.* Mol Cell, 2007. 27(2): p. 262-74.
6. Shumyatsky, G.P., S.V. Tillib, and D.A. Kramerov, *B2 RNA and 7SK RNA, RNA polymerase III transcripts, have a cap-like structure at their 5' end.* Nucleic Acids Res, 1990. 18(21): p. 6347-51.
7. Shumyatsky, G., D. Wright, and R. Reddy, *Methylphosphate cap structure increases the stability of 7SK, B2 and U6 small RNAs in Xenopus oocytes.* Nucleic Acids Res, 1993. 21(20): p. 4756-61.
8. Xue, Y., et al., *A capping-independent function of MePCE in stabilizing 7SK snRNA and facilitating the assembly of 7SK snRNP.* Nucleic Acids Res, 2010. 38(2): p. 360-9.
9. Schneeberger, P.E., et al., *de novo MEPCE nonsense variant associated with a neurodevelopmental disorder causes disintegration of 7SK snRNP and enhanced RNA polymerase II activation.* Scientific reports, 2019. 9(1): p. 12516-12516.
10. He, N., et al., *A La-related protein modulates 7SK snRNP integrity to suppress P-TEFb-dependent transcriptional elongation and tumorigenesis.* Molecular cell, 2008. 29(5): p. 588-599.
11. Barboric, M., et al., *7SK snRNP/P-TEFb couples transcription elongation with alternative splicing and is essential for vertebrate development.* Proceedings of the National Academy of Sciences, 2009. 106: p. 7798-7803.
12. Krueger, B.J., et al., *LARP7 is a stable component of the 7SK snRNP while P-TEFb, HEXIM1 and hnRNP A1 are reversibly associated.* Nucleic acids research, 2008. 36(7): p. 2219-2229.
13. Markert, A., et al., *The La-related protein LARP7 is a component of the 7SK ribonucleoprotein and affects transcription of cellular and viral polymerase II genes.* EMBO reports, 2008. 9: p. 569-75.
14. Muniz, L., S. Egloff, and T. Kiss, *RNA elements directing in vivo assembly of the 7SK/MePCE/Larp7 transcriptional regulatory snRNP.* Nucleic Acids Res, 2013. 41(8): p. 4686-98.
15. Alazami, A.M., et al., *Loss of function mutation in LARP7, chaperone of 7SK ncRNA, causes a syndrome of facial dysmorphism, intellectual disability, and primordial dwarfism.* Human mutation, 2012. 33(10): p. 1429-1434.
16. Ling, T.T. and S. Sorrentino, *Compound heterozygous variants in the LARP7 gene as a cause of Alazami syndrome in a Caucasian female with significant failure to thrive, short stature, and developmental disability.* American journal of medical genetics. Part A, 2016. 170A(1): p. 217-219.

17. Imbert-Bouteille, M., et al., *LARP7 variants and further delineation of the Alazami syndrome phenotypic spectrum among primordial dwarfisms: 2 sisters.* European journal of medical genetics, 2019. 62(3): p. 161-166.
18. Hasler, D., et al., *The Alazami Syndrome-Associated Protein LARP7 Guides U6 Small Nuclear RNA Modification and Contributes to Splicing Robustness.* Mol Cell, 2020. 77(5): p. 1014-1031.e13.
19. C. Quaresma, A.J., A. Bugai, and M. Barboric, *Cracking the control of RNA polymerase II elongation by 7SK snRNP and P-TEFb.* Nucleic Acids Research, 2016. 44(16): p. 7527-7539.
20. Peterlin, B.M., J.E. Brogie, and D.H. Price, *7SK snRNA: a noncoding RNA that plays a major role in regulating eukaryotic transcription.* Wiley Interdisciplinary Reviews: RNA, 2012. 3(1): p. 92-103.
21. Peterlin, B.M. and D.H. Price, *Controlling the Elongation Phase of Transcription with P-TEFb.* Molecular Cell, 2006. 23(3): p. 297-305.
22. Liu, W., et al., *Brd4 and JMJD6-Associated Anti-Pause Enhancers in Regulation of Transcriptional Pause Release.* Cell, 2013. 155(7): p. 1581-1595.
23. McNamara, R.P., et al., *KAP1 Recruitment of the 7SK snRNP Complex to Promoters Enables Transcription Elongation by RNA Polymerase II.* Molecular Cell, 2016. 61(1): p. 39-53.
24. Eilebrecht, S., et al., *7SK small nuclear RNA directly affects HMGA1 function in transcription regulation.* Nucleic Acids Research, 2011. 39(6): p. 2057-2072.
25. Fujinaga, K., et al., *PKC phosphorylates HEXIM1 and regulates P-TEFb activity.* Nucleic Acids Research, 2012. 40(18): p. 9160-9170.
26. Amente, S., et al., *Camptothecin releases P-TEFb from the inactive 7SK snRNP complex.* Cell Cycle, 2009. 8(8): p. 1249-1255.
27. Contreras, X., et al., *HMBA releases P-TEFb from HEXIM1 and 7SK snRNA via PI3K/Akt and activates HIV transcription.* PLoS pathogens, 2007. 3(10): p. e146.
28. Chen, R., et al., *PP2B and PP1α cooperatively disrupt 7SK snRNP to release P-TEFb for transcription in response to Ca2+ signaling.* Genes & development, 2008. 22(10): p. 1356-1368.
29. Elagib, K., et al., *Calpain Drives Megakaryopoiesis by Targeting the 7SK snRNP Complex: A Connection to Down Syndrome Megakaryocytic Neoplasia.* Blood, 2011. 118: p. 552-552.
30. McNamara, Ryan P., et al., *Transcription Factors Mediate the Enzymatic Disassembly of Promoter-Bound 7SK snRNP to Locally Recruit P-TEFb for Transcription Elongation.* Cell Reports, 2013. 5(5): p. 1256-1268.
31. Cho, W.-K., et al., *Modulation of the Brd4/P-TEFb Interaction by the Human T-Lymphotropic Virus Type 1 Tax Protein.* Journal of Virology, 2007. 81: p. 11179-11186.
32. Ji, X., et al., *SR Proteins Collaborate with 7SK and Promoter-Associated Nascent RNA to Release Paused Polymerase.* Cell, 2013. 153(4): p. 855-868.
33. Calo, E., et al., *RNA helicase DDX21 coordinates transcription and ribosomal RNA processing.* Nature, 2015. 518(7538): p. 249.
34. Bugai, A., et al., *P-TEFb Activation by RBM7 Shapes a Pro-survival Transcriptional Response to Genotoxic Stress.* Molecular Cell.
35. Yang, Z., et al., *The 7SK small nuclear RNA inhibits the CDK9/cyclin T1 kinase to control transcription.* Nature, 2001. 414: p. 317.
36. Nguyen, V.T., et al., *7SK small nuclear RNA binds to and inhibits the activity of CDK9/cyclin T complexes.* Nature, 2001. 414(6861): p. 322-5.
37. Prasanth, K.V., et al., *Nuclear organization and dynamics of 7SK RNA in regulating gene expression.* Molecular biology of the cell, 2010. 21(23): p. 4184-4196.
38. Yik, J.H., et al., *Inhibition of P-TEFb (CDK9/Cyclin T) kinase and RNA polymerase II*

transcription by the coordinated actions of HEXIM1 and 7SK snRNA. Mol Cell, 2003. 12(4): p. 971-82.
39. Egloff, S., E. Van Herreweghe, and T. Kiss, *Regulation of Polymerase II Transcription by 7SK snRNA: Two Distinct RNA Elements Direct P-TEFb and HEXIM1 Binding.* Molecular and Cellular Biology, 2006. 26(2): p. 630.
40. Michels, A.A., et al., *MAQ1 and 7SK RNA Interact with CDK9/Cyclin T Complexes in a Transcription-Dependent Manner.* Molecular and Cellular Biology, 2003. 23(14): p. 4859-4869.
41. Kobbi, L., et al., *An evolutionary conserved Hexim1 peptide binds to the Cdk9 catalytic site to inhibit P-TEFb.* Proceedings of the National Academy of Sciences, 2016. 113: p. 12721-12726.
42. Van Herreweghe, E., et al., *Dynamic remodelling of human 7SK snRNP controls the nuclear level of active P-TEFb.* The EMBO Journal, 2007. 26: p. 3570-3580.
43. Geuens, T., D. Bouhy, and V. Timmerman, *The hnRNP family: insights into their role in health and disease.* Human genetics, 2016. 135(8): p. 851-867.
44. Dreyfuss, G., et al., *hnRNP Proteins and the Biogenesis of mRNA.* Annual Review of Biochemistry, 1993. 62(1): p. 289-321.
45. Jean-Philippe, J., S. Paz, and M. Caputi, *hnRNP A1: The Swiss Army Knife of Gene Expression.* International Journal of Molecular Sciences, 2013. 14(9): p. 18999-19024.
46. Pinol-Roma, S., et al., *Immunopurification of heterogeneous nuclear ribonucleoprotein particles reveals an assortment of RNA-binding proteins.* Genes Dev, 1988. 2(2): p. 215-27.
47. Pinol-Roma, S. and G. Dreyfuss, *Shuttling of pre-mRNA binding proteins between nucleus and cytoplasm.* Nature, 1992. 355(6362): p. 730-2.
48. Siomi, H. and G. Dreyfuss, *A nuclear localization domain in the hnRNP A1 protein.* J Cell Biol, 1995. 129(3): p. 551-60.
49. Han, K., et al., *A Combinatorial Code for Splicing Silencing: UAGG and GGGG Motifs.* PLOS Biology, 2005. 3(5): p. e158.
50. Huelga, S.C., et al., *Integrative genome-wide analysis reveals cooperative regulation of alternative splicing by hnRNP proteins.* Cell Rep, 2012. 1(2): p. 167-78.
51. Huelga, Stephanie C., et al., *Integrative Genome-wide Analysis Reveals Cooperative Regulation of Alternative Splicing by hnRNP Proteins.* Cell Reports, 2012. 1(2): p. 167-178.
52. Henics, T., et al., *Enhanced stability of interleukin-2 mRNA in MLA 144 cells. Possible role of cytoplasmic AU-rich sequence-binding proteins.* J Biol Chem, 1994. 269(7): p. 5377-83.
53. Hamilton, B.J., et al., *Modulation of AUUUA response element binding by heterogeneous nuclear ribonucleoprotein A1 in human T lymphocytes. The roles of cytoplasmic location, transcription, and phosphorylation.* J Biol Chem, 1997. 272(45): p. 28732-41.
54. Kim, H.J., et al., *Mutations in prion-like domains in hnRNPA2B1 and hnRNPA1 cause multisystem proteinopathy and ALS.* Nature, 2013. 495(7442): p. 467-73.
55. Siomi, M.C., et al., *Transportin-mediated nuclear import of heterogeneous nuclear RNP proteins.* J Cell Biol, 1997. 138(6): p. 1181-92.
56. Pollard, V.W., et al., *A novel receptor-mediated nuclear protein import pathway.* Cell, 1996. 86(6): p. 985-94.
57. Clower, C.V., et al., *The alternative splicing repressors hnRNP A1/A2 and PTB influence pyruvate kinase isoform expression and cell metabolism.* Proc Natl Acad Sci U S A, 2010. 107(5): p. 1894-9.
58. Hutchison, S., et al., *Distinct sets of adjacent heterogeneous nuclear ribonucleoprotein (hnRNP) A1/A2 binding sites control 5' splice site selection in the*

hnRNP A1 mRNA precursor. J Biol Chem, 2002. 277(33): p. 29745-52.
59. Gao, Y., et al., *Multiplexed Dendritic Targeting of α Calcium Calmodulin-dependent Protein Kinase II, Neurogranin, and Activity-regulated Cytoskeleton-associated Protein RNAs by the A2 Pathway.* Molecular Biology of the Cell, 2008. 19(5): p. 2311-2327.
60. Shan, J., et al., *Binding of an RNA trafficking response element to heterogeneous nuclear ribonucleoproteins A1 and A2.* J Biol Chem, 2000. 275(49): p. 38286-95.
61. Goodarzi, H., et al., *Systematic discovery of structural elements governing stability of mammalian messenger RNAs.* Nature, 2012. 485: p. 264.
62. Kosturko, L.D., et al., *Heterogeneous Nuclear Ribonucleoprotein (hnRNP) E1 Binds to hnRNP A2 and Inhibits Translation of A2 Response Element mRNAs.* Molecular Biology of the Cell, 2006. 17(8): p. 3521-3533.
63. Munro, T.P., et al., *Mutational analysis of a heterogeneous nuclear ribonucleoprotein A2 response element for RNA trafficking.* J Biol Chem, 1999. 274(48): p. 34389-95.
64. Shan, J., et al., *A molecular mechanism for mRNA trafficking in neuronal dendrites.* J Neurosci, 2003. 23(26): p. 8859-66.
65. Rossoll, W., et al., *Specific interaction of Smn, the spinal muscular atrophy determining gene product, with hnRNP-R and gry-rbp/hnRNP-Q: a role for Smn in RNA processing in motor axons?* Hum Mol Genet, 2002. 11(1): p. 93-105.
66. Dombert, B., et al., *Presynaptic localization of Smn and hnRNP R in axon terminals of embryonic and postnatal mouse motoneurons.* PloS one, 2014. 9(10): p. e110846-e110846.
67. Briese, M., et al., *hnRNP R and its main interactor, the noncoding RNA 7SK, coregulate the axonal transcriptome of motoneurons.* Proc Natl Acad Sci U S A, 2018. 115(12): p. E2859-e2868.
68. Briese, M., et al., *hnRNP R and its main interactor, the noncoding RNA 7SK, coregulate the axonal transcriptome of motoneurons.* Proceedings of the National Academy of Sciences, 2018: p. 201721670.
69. Glinka, M., et al., *The heterogeneous nuclear ribonucleoprotein-R is necessary for axonal β-actin mRNA translocation in spinal motor neurons.* Human Molecular Genetics, 2010. 19(10): p. 1951-1966.
70. Rossoll, W., et al., *Specific interaction of Smn, the spinal muscular atrophy determining gene product, with hnRNP-R and gry-rbp/hnRNP-Q: a role for Smn in RNA processing in motor axons?* Human Molecular Genetics, 2002. 11(1): p. 93-105.
71. Ling, S.-C., et al., *ALS-associated mutations in TDP-43 increase its stability and promote TDP-43 complexes with FUS/TLS.* Proceedings of the National Academy of Sciences, 2010. 107(30): p. 13318-13323.
72. Hein, Marco Y., et al., *A Human Interactome in Three Quantitative Dimensions Organized by Stoichiometries and Abundances.* Cell, 2015. 163(3): p. 712-723.
73. Kamelgarn, M., et al., *Proteomic analysis of FUS interacting proteins provides insights into FUS function and its role in ALS.* Biochimica et Biophysica Acta (BBA)-Molecular Basis of Disease, 2016. 1862(10): p. 2004-2014.
74. Rossoll, W., et al., *Smn, the spinal muscular atrophy-determining gene product, modulates axon growth and localization of beta-actin mRNA in growth cones of motoneurons.* J Cell Biol, 2003. 163(4): p. 801-12.
75. Saal, L., et al., *Subcellular transcriptome alterations in a cell culture model of spinal muscular atrophy point to widespread defects in axonal growth and presynaptic differentiation.* Rna, 2014. 20(11): p. 1789-802.
76. Gittings, L.M., et al., *Heterogeneous nuclear ribonucleoproteins R and Q accumulate in pathological inclusions in FTLD-FUS.* Acta Neuropathol Commun, 2019. 7(1): p. 18.
77. Duijkers, F.A., et al., *HNRNPR Variants that Impair Homeobox Gene Expression Drive*

Developmental Disorders in Humans. Am J Hum Genet, 2019. 104(6): p. 1040-1059.
78. Barrandon, C., et al., *The Transcription-Dependent Dissociation of P-TEFb-HEXIM1-7SK RNA Relies upon Formation of hnRNP-7SK RNA Complexes.* Molecular and Cellular Biology, 2007. 27: p. 6996-7006.
79. Barrandon, C., et al., *The transcription-dependent dissociation of P-TEFb-HEXIM1-7SK RNA relies upon formation of hnRNP-7SK RNA complexes.* Mol Cell Biol, 2007. 27(20): p. 6996-7006.
80. Luo, Y., et al., *C-myc deregulation during transformation induction: involvement of 7SK RNA.* Journal of Cellular Biochemistry, 1997. 64(2): p. 313-327.
81. He, W.J., et al., *Regulation of two key nuclear enzymatic activities by the 7SK small nuclear RNA.* Cold Spring Harb Symp Quant Biol, 2006. 71: p. 301-11.
82. Faust, T.B., et al., *The HIV-1 Tat protein recruits a ubiquitin ligase to reorganize the 7SK snRNP for transcriptional activation.* Elife, 2018. 7.
83. Gagnon, K.T., et al., *Analysis of nuclear RNA interference in human cells by subcellular fractionation and Argonaute loading.* Nature Protocols, 2014. 9: p. 2045.
84. Egloff, S., et al., *The 7SK snRNP associates with the little elongation complex to promote snRNA gene expression.* The EMBO Journal, 2017.
85. Rogell, B., et al., *Specific RNP capture with antisense LNA/DNA mixmers.* RNA (New York, N.Y.), 2017. 23(8): p. 1290-1302.
86. Ivanyi-Nagy, R., et al., *The RNA interactome of human telomerase RNA reveals a coding-independent role for a histone mRNA in telomere homeostasis.* eLife, 2018. 7: p. e40037.
87. Briese, M., et al., *Whole transcriptome profiling reveals the RNA content of motor axons.* Nucleic acids research, 2016. 44(4): p. e33-e33.
88. Prasanth, K.V., et al., *Nuclear organization and dynamics of 7SK RNA in regulating gene expression.* Mol Biol Cell, 2010. 21(23): p. 4184-96.
89. Tripathi, V., et al., *SRSF1 regulates the assembly of pre-mRNA processing factors in nuclear speckles.* Molecular biology of the cell, 2012. 23(18): p. 3694-3706.
90. Barrandon, C., B. Spiluttini, and O. Bensaude, *Non-coding RNAs regulating the transcriptional machinery.* Biol Cell, 2008. 100(2): p. 83-95.
91. Kaida, D., et al., *U1 snRNP protects pre-mRNAs from premature cleavage and polyadenylation.* Nature, 2010. 468: p. 664.
92. Roithová, A., et al., *The Sm-core mediates the retention of partially-assembled spliceosomal snRNPs in Cajal bodies until their full maturation.* Nucleic Acids Research, 2018. 46(7): p. 3774-3790.
93. Lorković, Z.J. and A. Barta, *Role of Cajal Bodies and Nucleolus in the Maturation of the U1 snRNP in Arabidopsis.* PLOS ONE, 2008. 3(12): p. e3989.
94. Gutschner, T., M. Hammerle, and S. Diederichs, *MALAT1 -- a paradigm for long noncoding RNA function in cancer.* J Mol Med (Berl), 2013. 91(7): p. 791-801.
95. Sun, Q., Q. Hao, and K.V. Prasanth, *Nuclear Long Noncoding RNAs: Key Regulators of Gene Expression.* Trends in genetics : TIG, 2018. 34(2): p. 142-157.
96. Liu, P., et al., *The lncRNA MALAT1 acts as a competing endogenous RNA to regulate KRAS expression by sponging miR-217 in pancreatic ductal adenocarcinoma.* Scientific Reports, 2017. 7(1): p. 5186.
97. Bowerman, M., et al., *Therapeutic strategies for spinal muscular atrophy: SMN and beyond.* Disease Models & Mechanisms, 2017. 10: p. 943-954.
98. Passini, M.A., et al., *CNS-targeted gene therapy improves survival and motor function in a mouse model of spinal muscular atrophy.* The Journal of Clinical Investigation, 2010. 120(4): p. 1253-1264.
99. Singh, N.K., et al., *Splicing of a critical exon of human Survival Motor Neuron is regulated by a unique silencer element located in the last intron.* Mol Cell Biol, 2006.

26(4): p. 1333-46.
100. Ottesen, E., *ISS-N1 makes the First FDA-approved Drug for Spinal Muscular Atrophy*. Vol. 8. 2017. 1-6.
101. Gubitz, A.K., W. Feng, and G. Dreyfuss, *The SMN complex.* Experimental Cell Research, 2004. 296(1): p. 51-56.
102. Omer Javed, A., et al., *Microcephaly Modeling of Kinetochore Mutation Reveals a Brain-Specific Phenotype.* Cell Rep, 2018. 25(2): p. 368-382.e5.
103. Chabot, B., et al., *An intron element modulating 5' splice site selection in the hnRNP A1 pre-mRNA interacts with hnRNP A1.* Mol Cell Biol, 1997. 17(4): p. 1776-86.
104. Yang, X., et al., *The A1 and A1B proteins of heterogeneous nuclear ribonucleoparticles modulate 5' splice site selection in vivo.* Proc Natl Acad Sci U S A, 1994. 91(15): p. 6924-8.
105. Mayeda, A. and A.R. Krainer, *Regulation of alternative pre-mRNA splicing by hnRNP A1 and splicing factor SF2.* Cell, 1992. 68(2): p. 365-75.
106. Mohagheghi, F., et al., *TDP-43 functions within a network of hnRNP proteins to inhibit the production of a truncated human SORT1 receptor.* Hum Mol Genet, 2016. 25(3): p. 534-45.
107. Cammas, A., et al., *Cytoplasmic relocalization of heterogeneous nuclear ribonucleoprotein A1 controls translation initiation of specific mRNAs.* Mol Biol Cell, 2007. 18(12): p. 5048-59.
108. Dreyfuss, G., V.N. Kim, and N. Kataoka, *Messenger-RNA-binding proteins and the messages they carry.* Nat Rev Mol Cell Biol, 2002. 3(3): p. 195-205.
109. Guil, S. and J.F. Caceres, *The multifunctional RNA-binding protein hnRNP A1 is required for processing of miR-18a.* Nat Struct Mol Biol, 2007. 14(7): p. 591-6.
110. Guil, S., J.C. Long, and J.F. Caceres, *hnRNP A1 relocalization to the stress granules reflects a role in the stress response.* Mol Cell Biol, 2006. 26(15): p. 5744-58.
111. Taylor, J.P., R.H. Brown, Jr., and D.W. Cleveland, *Decoding ALS: from genes to mechanism.* Nature, 2016. 539(7628): p. 197-206.
112. Honda, H., et al., *Loss of hnRNPA1 in ALS spinal cord motor neurons with TDP-43-positive inclusions.* Neuropathology, 2015. 35(1): p. 37-43.
113. Molliex, A., et al., *Phase separation by low complexity domains promotes stress granule assembly and drives pathological fibrillization.* Cell, 2015. 163(1): p. 123-33.
114. Couthouis, J., et al., *Targeted exon capture and sequencing in sporadic amyotrophic lateral sclerosis.* PLoS Genet, 2014. 10(10): p. e1004704.
115. Liu, T.Y., et al., *Muscle developmental defects in heterogeneous nuclear Ribonucleoprotein A1 knockout mice.* Open Biol, 2017. 7(1).
116. Van Herreweghe, E., et al., *Dynamic remodelling of human 7SK snRNP controls the nuclear level of active P-TEFb.* The EMBO journal, 2007. 26(15): p. 3570-3580.
117. Glinka, M., et al., *The heterogeneous nuclear ribonucleoprotein-R is necessary for axonal beta-actin mRNA translocation in spinal motor neurons.* Hum Mol Genet, 2010. 19(10): p. 1951-66.
118. Mourelatos, Z., et al., *SMN interacts with a novel family of hnRNP and spliceosomal proteins.* The EMBO journal, 2001. 20(19): p. 5443-5452.
119. Yamazaki, T., et al., *FUS-SMN protein interactions link the motor neuron diseases ALS and SMA.* Cell reports, 2012. 2.
120. Jia, D., et al., *Systematic identification of non-coding RNA 2,2,7-trimethylguanosine cap structures in Caenorhabditis elegans.* BMC molecular biology, 2007. 8: p. 86-86.